Université de Montréal

Exploring TERRA (TElomeric Repeat-containing RNA) Expression and Regulation During Cell Growth in *Saccharomyces cerevisiae*

Par
Carmina Angélica Pérez Romero

Département de biochimie
Faculté de médecine

Mémoire présenté à la Faculté de médecine
en vue de l'obtention du grade de M.Sc.
en Biochimie
option Cellular Dynamics of Macromolecular Complexes (CDMC)

Avril, 2013

Université de Montréal
Faculté des études supérieures et postdoctorales

Ce mémoire intitulé :

Exploring TERRA (TElomeric Repeat-containing RNA) Expression and Regulation During Cell Growth in Saccharomyces cerevisiae

Présentée par:
Carmina Angélica Pérez Romero

a été évalué par un jury composé des personnes suivantes :

Daniel Zenklusen, président-rapporteur
Pascal Chartrand, directeur de recherche
Stephen Michnick, membre du jury

Résumé

Les télomères à l'extrémité des chromosomes constituent une structure d'ADN et de protéines essentielle à l'intégrité de ces chromosomes. La télomérase est l'enzyme responsable du maintien des répétitions télomériques à l'extrémité des chromosomes. Cette enzyme est constituée d'une sous-unité catalytique, qui possède une activité de transcriptase réverse, et d'une sous-unité d'ARN, qui fourni la matrice nécessaire à la synthèse des répétitions télomériques. Les ARN contenant des répétions télomériques (ou Telomeric repeats-containing RNA; TERRA) constitue une nouvelle classe d'ARN non-codants transcrits à partir des télomères et conservée chez la plupart des eucaryotes. TERRA a été proposé d'agir comme un régulateur de l'homéostasie des télomères et comme inhibiteur de la télomérase, mais sa fonction spécifique reste inconnue. De plus, chez la levure *Saccharomyces cerevisiae*, TERRA est rapidement dégradé par l'exonucléase 5'-3' Rat1, ce qui complique l'étude de cet ARN par les méthodes biochimiques classiques.

Dans cette thèse, nous rapportons l'utilisation d'une approche cytologique pour étudier TERRA dans les cellules de levures. Deux approches sont utilisées : l'hybridation in situ en fluorescence (FISH) et l'étiquetage de TERRA à l'aide du système MS2-GFP, qui nous permet de visualiser l'expression de TERRA transcrit d'un seul télomère dans des cellules vivantes. Avec ces deux approches, nous observons que TERRA exprimé à partir d'un seul télomère s'accumule dans un faible nombre de cellules, sous la forme d'un focus périnucléaire. De plus, nous montrons que TERRA est exprimé lorsque son télomère raccourcit.

Par immunoprécipitation, nous montrons que TERRA interagit *in vivo* avec l'ARN de la télomérase de levure, *TLC1*. L'élongation des télomères dépend de l'action de multiples molécules de télomérase, qui sont visibles sous la forme de clusters de télomérases, qui s'associent en phase S avec les télomères chez la levure et les cellules de mammifère. Nous démontrons que TERRA stimule la nucléation de ces clusters de

télomérase. Par imagerie en temps réel de TERRA et de l'ARN *TLC1*, nous observons que TERRA agit comme molécule d'échafaudage pour générer des clusters de télomérases, qui sont par la suite recrutés, en phase S, au télomère duquel TERRA a été exprimé. Le recrutement d'un focus de TERRA à son télomère d'origine dépend des facteurs contrôlant le recrutement de la télomérase aux télomères : Mre11, Tel1 et le complexe yKu. Nous proposons qu'un télomère court exprime TERRA pour assembler et organiser les molécules de télomérase, afin que celles-ci soit puissent être recrutées au télomère court pour permettre son élongation.

Enfin, nous observons une surexpression de l'ARN de la télomérase *TLC1* et de TERRA, ainsi qu'une accumulation cytoplasmique de ceux-ci sous la forme de foci, lorsque la cellule passe de la phase de croissance exponentiel à la phase diauxique, puis à la phase stationnaire. Dans ces conditions, les foci d'ARN *TLC1* colocalisent avec les foci de TERRA, suggérant que la fonction de TERRA comme molécule d'échafaudage pour générer des foci de télomérase est aussi nécessaire durant ces phases du cycle de croissance des levures.

Mots-clés: TERRA, télomérase, télomère, ARN non-codant, *Saccharomyces cerevisiae*, microscopie, MS2-GFP, imagerie en cellule vivante, localisation cellulaire, croissance exponentielle, phase diauxique, phase stationnaire

Abstract

The physical ends of eukaryotic chromosomes consist of repetitive DNA sequences, which are associated with specialized proteins forming a nucleoprotein structure essential for the integrity of the linear chromosomes, and are known as telomeres. Telomerase is an enzyme responsible for the maintenance of the telomeric repeats at the end of the chromosomes. Telomerase is a ribonucleoprotein, which contains a catalytic subunit that possesses reverse transcriptase activity, and a RNA subunit that acts as a template, since it possess the telomeric repeat sequences necessary to amplify telomere ends. Telomeres are transcribed in most eukaryotes into a non-coding RNA know as TERRA (Telomeric repeats-containing RNA). It has been proposed that TERRA may act as a regulator of telomere homeostasis, and as an inhibitor of telomerase, however, its specific function is still unknown. In *Saccharomyces cerevisiae*, TERRA is rapidly degraded by the 5'-3' Rat1 exonuclease, which has hampered its study by classic biochemical experiments in yeast.

In this thesis, we report the use of cytological approaches to study TERRA in budding yeast. Two different approaches were used for this purpose: the fluorescent in-situ hybridization (FISH) and the labeling of TERRA by the MS2-GFP system, which allow the visualization of TERRA transcripts form a single telomere in living cells. With these two approaches, we observed that TERRA is expressed from a single telomere and accumulates as a single perinuclear foci, in a small percentage of cells population. We also demonstrate that TERRA expression occurs due to telomere shortening.

We demonstrate that TERRA interacts *in vivo* with the telomerase RNA (*TLC1)* in yeast. Telomere elongation depends on the action of several telomerase molecules that are visible as clusters, which associate with telomeres in late S phase in yeast, and mammalian cells. In adidition, we show that TERRA stimulates the nucleation of telomerase clusters. By performing time course experiments of TERRA and *TLC1* RNA in live cells, we observed that TERRA acts as a scaffold for generating telomerase clusters, which are then recruited in late S phase to the telomere from which TERRA molecules originated. The

recruitment of TERRA to its telomere of origin is dependent on factors that control telomerase recruitment at telomeres like: Mre11, Tel1 and the yKu complex. We propose that a short telomere expresses TERRA to assemble and organize telomerase molecules, which later on allows their recruitment at the short telomere, where elongation is needed.

Finally we showed an up-regulation of TERRA, and telomerase RNA *TLC1,* accompanied by a predominant cytoplasmic localization as cell growth progresses from exponential growth to diauxic shift, and stationary phase. In these conditions, TERRA foci co-localize with *TLC1* RNA foci, suggesting that the function of TERRA as a scaffold molecule to generate telomerase cluster is necessary for this yeast cell growth phases.

Keywords: TERRA, telomerase, telomere, non-coding RNA, *Saccharomyces cerevisiae*, microscopy, MS2-GFP, live cell imaging, cellular localization, logarithmic growth, diauxic shift, stationary phase.

Table of Contents

List of Tables

Chapter IV

Chapter VI

List of Figures

List of Movies

Available in annexed CD

Abbreviation

DNA	Deoxyribonucleic acid
RNA	Ribonucleic acid
NHEJ	Non-homologous end joining
TPE	Telomere position effect
TERRA	Telomeric Repeat-containing RNA
RNP	Ribonucleoprotein
TERT	Human telomerase reverse trascriptase
Est2	Budding yeast telomerase reverse trascriptase
TERC	Human telomerase RNA
TLC1	Budding yeast telomerase RNA
TR	Telomerase RNA
TBE	Template boundary element
T-Recs	Telomerase recruitment clusters
Poly(A)	Poly-adenylation
NMD	Nonsense mediated decay
iPSC	Induced pluripotent stem cells
GFP	Green fluorescent protein
NLS	Nuclear localization signal
PKA	Protein kinase A
KAN	Kanamycin

RT-qPCR	Reverse trascriptase quantitative polymerase chain reaction
YPD	Yeast extract/peptone medium
SD	Selection media
OD	Optical density
NA	Numerical apertura
EM	Electron multiplying
qFISH	Quantitative flourescent in situ hybridization
DAPI	4’,6 diamidino-2-phenylindole
IP	Immunoprecipitation
P	P values
WT	Wild type cells
Tel1L	Telomere 1 left arm
Tel6R	Telomere 6 right arm
2D/3D	Two dimension/ three dimension
-RT	Minus reverse transcripase
RFP	Red fluorescent protein
CFP	Cyan fluorescent protein

Acknowledgments

I would like to thank my supervisor Dr. Pascal Chartrand for believing in me and providing me with the opportunity to be part of his laboratory and this amazing project. In addition, for providing me with the experimental guidance, for the critical feed-back on all of my experiments and this thesis, for allowing me to pursue my own hypothesis and for accepting my ideas. Most importantly, I would like to thank Dr. Chartrand for taking part in the achievement of one of my dreams.

A special thank you goes to a postdoctoral fellow in the laboratory Dr. Emilio Cusanelli for all his unconditional support during the long days of encouraging and frustrating experiments; for his direction, and vision of the project; his good ideas, comments that helped in improving and making this project a success. I thank you for being the best project director, for being my friend and especially for being a great scientific role model. Emilio, I don't know what I would have done without you!

It is also important to acknowledge the entire laboratory, who made the long working hours shorter, the bad days good days, and the good days even better. Together with their help, comments and great insightful conversations, I was able to keep a smile in my face no matter how the science might be going. Thank you all, you guys and gals rock my world. Present Members: Dr. Emilio Cusanelli, Dr. Karen Shahbabian, Genevieve Leroux, Dr. Emmanuelle Querido, Maxime Lalonde, Faissal Ouenzar, Dr. David Guerit. Former Members: Catherine Menard, Anik St Denis, Amelie Forget, Anne-Laure Finoux, Ting-Ting Cui, Zhifa Sheng.

I would like to thank Dr. Daniel Zenkluzen for always listening to my scientific issues and and providing me with advice during the times when I most needed. I really appreciated his unbiased point of view; comments and constructive criticism which helped enrich this project. I want to thank his laboratory members for allowing me to use the microscope and aiding me in FISH techniques, and a special thanks to my friend Samir.

I would like to extend my gratitude to Dr. Stephen Michnick for going through the trouble of reading this thesis, for letting me use his laboratory equipment and letting me feel welcome, and for his support in my career choices. I also want to thank his laboratory members for adopting me as a member of their laboratory, for their thoughtful advice on experiments and overall for their great support when I was low and for letting me know that giving up is not an option. Special thanks to Durga, Jacqueline, Emmanuelle, Vince, and Luz for always being there for me and hearing me out, and giving me not only scientific but life advice. I also want to thank Lara although not part of this lab, and whom I wouldn't have met without Durga, thank you to both for being awesome women and for sharing values, thoughts, and our visions of science with me.

In addition, I would like tothank Dr. Christian Baron for allowing me to be part of the exciting CDMC (Cellular Dynamics of Macromolecular Complexes) NSCERC CREATE program.

For all the people in the Department, professors, secretaries and everyone that had to cope with my bad French skills and questions of all kinds of sorts to make this master thesis a success. Merci à tout le Departement de Biochiemie spécialement au Silvie Beauchimin qui a fait mon vie administrative a l'université très simple.

Importantly, I would like to thank my family and friends for their unconditional support even if we are separated by a thousand miles, their words of encouragement and their trust on me go through any frontiers. I dedicate this thesis for you. I want to especially thank my sister for being an example of perseverance through the hard times, and demonstrating to me that no matter how bad life can be, it is worth living it and facing it with a smile in your face.

Finally but not least, I want to thank science for putting me in the same microscopy course and allowing me to meet my boyfriend at the time with whom I have shared lots of life and science experiences and without whom I wouldn't be able to complete this thesis, thank you Mike.

A mi padre por su inspiración
A mi madre por su apoyo incondicional
A mi hermana por su admiración
A mi hermano por su curiosidad
A mis amigos por creer en mí
A mi novio por su amor
A mi sueño por impulsarme

To my father for inspiring me
To my mother for her unconditional support
To my sister for her admiration
To my brother for his curiosity
To my friends for believing
To my boyfriend for his love
To my dream for pushing me forward

Preface

I started writing this thesis more than a year ago when no paper in preparation was in horizon or any results were making much sense. We had tons of observations (where ever we look there was TERRA); however none of these observations seemed to describe a specific function for TERRA. It was quite exciting since it was a blank canvas to draw on, but at the same time very frustrating since it was hard to convince others that the results I was observing may have an important biological role.

I was on the verge of giving up, but as time passed by, finally the jig-saw puzzle started solving itself in front of my own eyes… and now half of the results on this thesis can be found in a manuscript in preparation in the result section.

I decided to keep the structure of the thesis as it was being conceived when I started writing it, since I believe it demonstrates the rough but interesting road of thinking and knowledge, that now led me to see the bright light at the end of the road.

I hope someone who reads this thesis will find the inspiration to continue excavating through the tunnel of my other half of the results so that eventually they would also see the light, and do not perish in darkness. To that person, I wish you success; remember if you need advice I will be there. Let me assure you that no matter how hard the road may be, there will always be a bright light at the end, as long as you don't give up.

So now prepare yourself because this is a long thesis for a Master's degree but I hope you enjoy the reading as much as I enjoyed the ride.

So now let me take you through a journey of mystery, enigmas and questions waiting to be solved…

…The journey begins with a bottle of beer and pizza; as you enjoy them you realize that this delicious food couldn't be in your mouth without the help of a microorganism, which lives in a microcosm that you can't see with your bare eyes. However, if you zoom in a thousand times, a new world of wonder starts to reveal itself, full of knowledge yet to be discovered. Let me take you on a journey to uncover the mystery behind TERRA (TElomeric Repeat-containing RNA).

Chapter I

Introduction

The main dogma in molecular biology is that DNA (deoxyribonucleic acid) is the nucleic acid that contains the information required for an organism to live in the form of genes, which are later transcribed into messages (RNA, ribonucleic acid) and then translated into functional units (proteins). However, biology cannot be described in such an easy way; instead it is a complex universe of interconnecting players, orchestrating life.

For instance, DNA is packed into more compact structures with the help of histone proteins into chromatin. Chromatin can be found in two different states: a relaxed one called euchromatin and a condensed state called heterochromatin. These states are highly controlled by histone modification enzymes. Chromatin is then further compacted into chromosomes.

The physical ends of eukaryotic chromosomes consist of repetitive DNA sequences which are associated with specialized proteins forming a nucleoprotein structure called telomeres. This is the start location of our journey, and where most of our story will develop, so let me introduce you to the world of telomeres...

1.1 Telomeres… the eukaryotic chromosomes ends

Telomeres ensure genome stability by protecting the chromosomes from being recognized as sites of DNA damage, by helping prevent: chromosome end-to-end fusions, homologous recombination, non-homologous end joining (NHEJ), and recognition as double strand breaks (Riethman 2008 a).

Telomeres act as a buffer region enabling cell division to occur without compromising genome integrity and stability. Telomeres are shortened during each cell division until their length reaches a threshold limit, which generates dysfunctional telomeres that compromise genome integrity, thus cells stop dividing and enter replicative cellular senescence (Levy 1992). The number of times that a cell can divide before entering cellular senescence is known as the Hayflick limit and it differs among cell types and organisms. (Campisi 2005). Replicative senescence has been linked to organismal aging and natural aging, and is believed to have an important role as a tumor suppressor mechanism (Campisi 2005).

Telomeres are shortened during each cell cycle division due to the end replication problem. This problem arises due to the uni-directionality (5`→3`) of the DNA polymerase and the need for an RNA primer to start DNA replication. Upon DNA replication the removal of this primer at the 5' end of the lagging strand leaves a gap that cannot be filled by conventional means. On the other hand, the replication of the leading strand terminates with a blunt end that can be recognized as DNA damage (Figure 1.1).

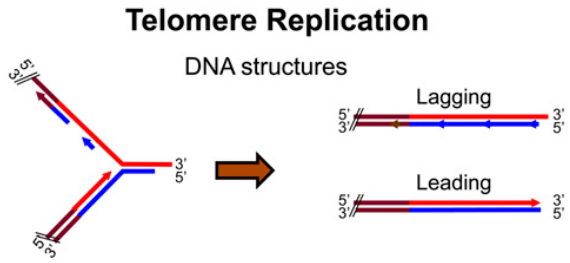

Figure 1.1 The end-replication problem. DNA structures generated during telomere replication when the replication fork is still in the double-stranded telomeric repeats (left) and after having reached the physical end (right). The lagging strand telomere has a 3' overhang formation due to the RNA primer degradation used to start DNA replication. While the leading strand results in a blunt end. Resection of the blunt end in the leading strand and the 3' overhang formation in the lagging strand results in telomere shortening. The red line or 3' end of the telomere is known as the G-rich strand, while the blue line or 5' end is called the C-rich strand. Adapted from (Z. Wellinger 2012).

Therefore, to solve the end replication problem, the leading strand blunt end is first resected by post-replication C-strand degradation which generates a 5' end overhang (E. L. Wellinger 1996). The overhangs are then extend by a specialized enzyme, known as telomerase, a ribonucleoprotein complex which adds telomeric repeats to the 3' end of chromosomes (G-rich strand) by reverse-transcription of its RNA template. The 5' end (C-rich strand) of the telomere can then be synthesized by normal DNA polymerase replication, resulting in the re-lengthening of the telomere (Greider 1985). Since telomerase action regenerates telomeric repeats, the cells can avoid cell death and continue to divide indefinitely; leading to unwanted cell proliferation, which then might result in diseases such as cancer (Shay 1997).

The DNA component of telomeres vary in sequence, length, and composition among species but its structure is conserved, consisting of:

- *The telomeric repeats*: which consist of a double stranded guanine-rich tandem repeats sequence on the G-rich strand that contains the 3` end, which

protrudes forming a single stranded overhang known as the G-tail (Figure 1.2 A) (Geli 2007). Telomeres are bound by a complex array of proteins known as the shelterin, which are double-stranded or single-stranded specific DNA binding proteins, that participate in telomere maintenance and capping (Figure 1.12A, D) (d. Lange 2009). Recruitment of the shelterin complex and the guanine-rich property of the telomeric repeats allow telomeres to adopt complex conformations. For example: they can form loop structures called T-loops, which result from the 3` single-stranded overhang invasion of the double-stranded telomeric DNA (Figure 1.1B) (d. Lange 2009), or they can form G-quadruplexes which are four-stranded structures that consist of non-canonical base pairing between guanines stabilized by hydrogen bonds (Figure 1.12C) (Dai 2007). The protein complexes and 3D structures help capping the telomeres, preventing them to be subjected to DNA repair by homologous recombination or NHEJ.

- *The sub-telomeric regions:* are immediately adjacent to the telomeric repeats and comprise about 25% of the most distal 500kb and 80% of the most distal 100 kb in human DNA. They are composed of a mosaic of repetitive elements that exhibit a high level of polymorphism, such as alternative repetitive sequences with different copy number variation. Although very little is known about these regions, the great variation in sub-terminal DNA is likely to have important consequences on expression/dosage of sub-terminal transcripts, and in chromatin structure mediating telomere function and chromosome stability (H. Riethman 2008 b).

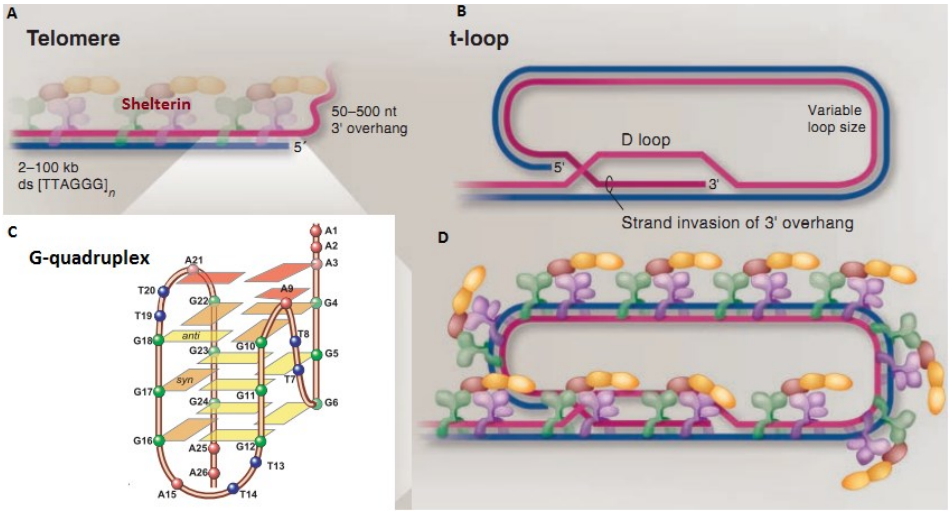

Figure 1.12 The telomeric repeats structures. (A) Human and mouse telomeres are composed of long stretches of the repetitive sequence TTAGGG and a telomere specific protein complex, shelterin which binds single or double-stranded telomeric DNA. **(B)** The T-loop results from the invasion of the 3` single-stranded overhang into the double-stranded telomeric DNA. **(C)** Schematic drawing of the folding topology of the uni-molecular human telomeric G-quadruplex formed of an array of repetitive guanine-rich sequences. Modified from (Dai 2007). **(D)** At the very end of the T-loop, the single-stranded telomere DNA is held onto a region of double-stranded telomeric DNA which disrupts the double-helical structure of the DNA forming a triple-stranded structure referred to as a displacement loop or D-loop, which is stabilized by G-quadruplex formation. This complex structure is recovered by the shelterin capping the telomere and protecting it from being degraded by endonucleases or being recognized by the DNA damage machinery. Modified from (d. Lange 2009)

Telomeres are formed of highly compact DNA known as constitutive heterochromatin, in which histones are hypoacetylated and hypermethylated, enabling the binding of different arrays of proteins involved in promoting gene silencing. The epigenetic heterochromatic state of telomeres prevents transcription of sub-telomeric genes, a phenomenon referred to as telomere position effect (TPE) (Tham 2002). TPE silencing occurs when a normally euchromatic gene is inserted in the telomere of a eukaryotic chromosome and its transcription is diminished. This phenomenon is thought to contribute to the control of telomerase and promote constitutive heterochromatin formation (Doheny 2008). Telomere structure and protein complexes tend to locally associate in transcriptionally silent areas of the genome, which have predominant perinuclear localization (close to the nuclear envelope). This localization is believed to contribute to the TPE (Gasser 2009). Telomeres, due to TPE and their heterochormatic state, were believed to be transcriptionally silent; until recently when a non-coding RNA was discovered to be

transcribed from telomeres (Azzalin 2007) (Schoeftner, Developmentally regulated transcription of mammalian telomeres by DNA-dependent RNA polymerase II 2008). This non-coding RNA was named Telomeric Repeat-containing RNA (TERRA).

1.2 Yeast Telomeres

In *Saccharomyces cerevisiae*, telomeric DNA consists of approximately 300nt irregular $C_{1-2}A/TG_{1-3}$ telomeric repeats, terminating with 15nt single 3' strand overhang referred to as the G tail. Yeast sub-telomeric regions contain two different types of repetitive elements X and Y'. The X core repetitive elements are present in all telomeres and are more heterogeneous in sequence and length. A subset of yeast telomeres contains only X repetitive elements followed by the telomeric repeat tract. The other half of yeast telomeres contains the X elements followed by the Y' repetitive elements. The Y' element comes in short (5.2 kb) or long (6.7 kb) formats containing zero to four tandem copies which are then followed by the telomeric repeat tract (Wellinger and Zakian, 2012). These regions suffer frequent recombination events and have binding sites for multiple transcription factors and proteins, which might confer distinct behaviors to individual telomeres (Figure 1.3).

Yeast telomeres are bound by a wide array of proteins with various functions which help to achieve and maintain telomere capping, to avoid it from being subjected to DNA repair mechanism, as well as to recruit telomerase for telomere lengthening. Several proteins are involved in the homeostasis of yeast telomeres (Figure 1.3) (Z. Wellinger 2012): Rap1, a major transcription factor in yeast which binds sequence-specific telomeric double-stranded DNA. It is important in telomere capping, length regulation and TPE. The CST complex, consisting of three-proteins Cdc13, Stn1, and Ten1 which binds telomeric single-stranded DNA in a sequence-specific manner and are involved in telomere capping and telomerase regulation. Rif1 and Rif2 proteins both interact with Rap1 and act as telomerase regulators; Rif2p is also involved in telomere capping. Sir2/3/4 which interact with each other, with Rap1 and histone tails; together they form part of the shelterin-like complex components which are essential for histone modification, silencing of the telomere

and TPE. The yKu complex consists of two components yKu70 and yKu80 which are involved in non-homologous end joining. They also interact with the RNA component of telomerase to regulate telomere length, capping, and position. Finally, Tbf1 is a transcription factor which recognizes sites in sub-telomeric DNA that, mark telomere boundaries are involved in recruiting telomerase to short telomeres. (Z. Wellinger 2012)

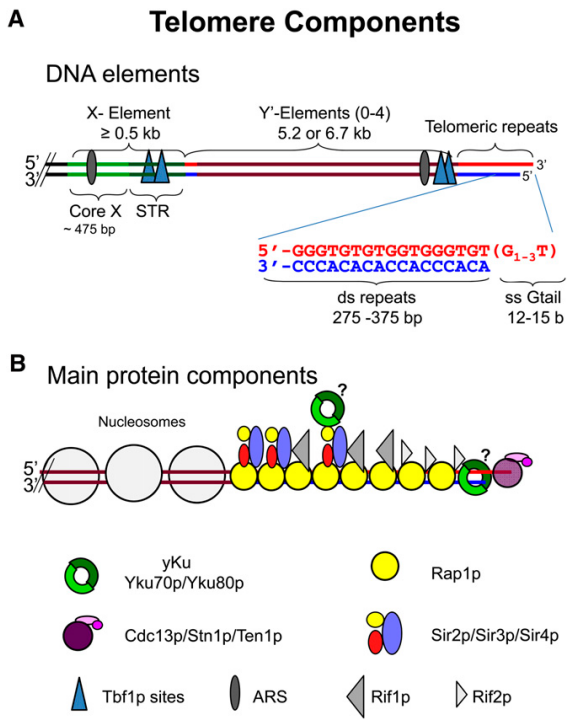

Figure 1.3 DNA structure and major protein components of telomeres. A) DNA arrangement at telomeres indicating the sub-telomeric X and Y' elements as well as the terminal repeat sequences. Red strand, G-rich strand with 3' overhanging end and blue strand, C-rich strand with 5' end. Core X and STR (subtelomeric repeated elements) represent subareas in the X element. **(B)** Proteins are schematically positioned on the telomere drawing and the identity of the symbols explained on the bottom. Open circles represent nucleosomes. Taken from (Z. Wellinger 2012)

1.3 Telomerase… a solution for telomere shortening

Telomerase is a conserved ribonucleoprotein (RNP) enzyme found in most eukaryotes from yeasts to humans. It contains two catalytically essential subunits: the telomerase reverse transcriptase protein (TERT in humans, Est2 in yeast) and the telomerase RNA (TERC in humans, TLC1 in yeast) that acts as a template (Figure 1.4)

Telomerase adds sequence repeats to the 3' ends of linear chromosomes by reverse-transcription of the template region of its RNA, to counteract the lost telomeric DNA due to the end replication problem.

The RNA component of telomerase shows great variations in length among eukaryotes. However, it contains conserved structural elements that are important for the formation and function of an active telomerase RNP. First is the single-stranded template, which is typically complementary to about 1.5 repeat of the telomeric DNA sequence, the 3' region of the template aligns the DNA substrate, while the 5' portion is copied. Adjacent to the template is a unique pseudoknot fold stabilized by triple-helix formation, which is believed to help positioning the template relative to the active site of the reverse transcriptase. The template-pseudoknot domain is typically closed by long-range base-pairing of sequence near the 5' end of the RNA. This sequence provides a 5' template boundary element (TBE) to prevent the copying of non-template RNA sequences. Apart from these structures, the yeast telomerase RNA has terminal and intermediate hairpin structures important for RNA stability, localization as well as RNP folding and catalytic activation. (Figure 1.4) (Egan 2012)

In budding yeast, telomerase is always expressed, and it is the preferred telomere extension pathway. The telomerase RNA *TLC1* is the limiting factor in telomerase activity. Apart from the catalytic activity conferred by the reverse transcriptase Est2, yeast telomerase includes another array of proteins important for its biological role. Key proteins important for yeast telomerase consist of: Est1, which is involved in telomerase recruitment via the interaction with Cdc13 protein, which guides telomerase to the single-stranded telomeric DNA for its extension. Est3 is believed to be involved in the activation of telomerase and is important for telomere maintenance (Z. Wellinger 2012). The yKu complex is involved in telomerase RNP assembly and its accumulation in the nucleolus. Finally, the Sm heptameric complex binds the 3' end of the *TLC1* RNA participating in its stabilization. (Figure 1.4) (Collins 2011)

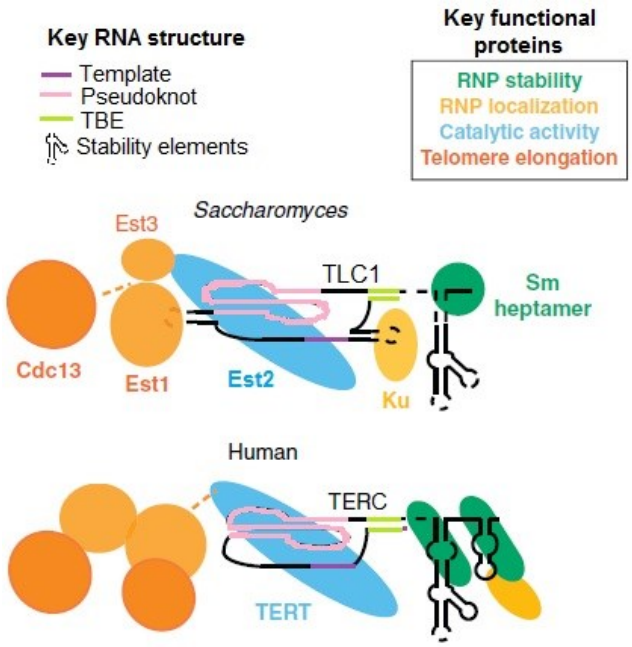

Figure 1.4 Telomerase RNA structure and major protein components in yeast and humans. The key RNA structural elements are highlighted. The key functional proteins are color coded depending on their function. RNP assembly and concentration within the nucleus (green and yellow).Telomerase- and telomere-associated proteins that have high affinity and sequence specificity for telomeric-repeat DNA (dark orange) or that bridge the DNA binding subunits to the reverse transcriptase with lower affinity DNA contacts (light orange) are crucial determinants of telomere elongation in cells. Taken from (Collins 2011) and modified from (Egan 2012).

Human telomeres are maintained almost exclusively by telomerase which is only active in highly proliferative tissues like germ line cells. While in normal somatic cells telomerase activity is low or non-existent, a condition which leads to cellular aging, telomerase is re-experessed in about 90% of all cancer cells. Alterations of telomerase activity in human cells have also been linked to severe diseases such as Dyskeratosis congenita (Beery 2012).

1.4 Telomerase biogenesis, recruitment and localization in yeast

In eukaryotes, small RNP assembly frequently occurs in several sub-cellular compartments and requires the targeting of RNA and protein subunits to specific locations.

Telomerase biogenesis in yeast (Figure 1.5) begins (1) with the transcription of TLC1 by RNA polymerase II, which forms a primarily un-polyadenylated transcript protected by a 5'mono-methylguanosine cap, this is then bound by the Sm proteins which targets its nucleolar accumulation (Egan 2012). (2) In the nucleolus, the cap is hypermethylated by Tgs1p and then TLC1 is exported to the cytoplasm into a Crm1p-dependent manner. (3) In the cytoplasm, TLC1 RNA recruits the protein components of the telomerase complex (4), assembles into a mature RNP (5) and is imported back in the nucleus via a Mtr10p/Kap122p pathway (Gallardo C., 2008). (6) Once in the nucleus active telomerase molecules diffuse, until they are needed to elongate telomeres.

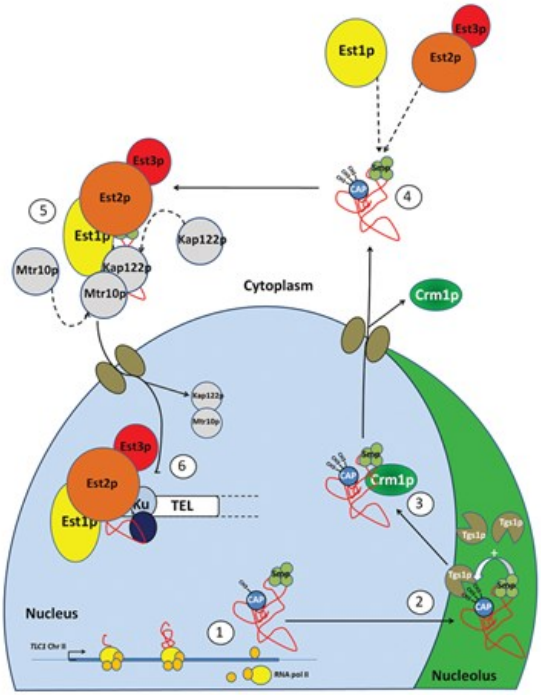

Figure 1.5 Model of telomerase biogenesis in *Saccharomyces cerevisiae*. The numbers represent the steps of telomerase biogenesis as described above. Other than for its assembly, telomerase localization in yeast is strictly nuclear, since its main role is in telomere length maintenance; and only on KO of key proteins involved in telomerase recruitment (yKu, Tel1 and MRX complex) can a cytoplasmic localization of telomerase RNA TLC1 can be seen . Taken from (Gallardo, C., 2008).

The current model of telomerase recruitment to telomeres and telomere extension in budding yeast suggest that until telomerase is required to extend a specific shortened telomeres (around 3 per cell division), its molecules stay diffused in the nucleus throughout the cell cycle. Rif1/2 proteins inhibit the access of telomerase to the telomere throughout

the cell cycle, except after DNA replication in later S phase. It is until then, that several telomerase molecules cluster into T-Recs (telomerase recruitment clusters) that represents active telomerase, which can be visualized by live cell imaging. These clusters then co-localize with the telomeres elongating them in late S phase. Telomere elongation and T-recs localization depend on regulators of telomerase present at telomeres such as MRX, Tel1, Rif1/2, and Cdc13, which suggests that these clusters constitute active and elongating telomerase molecules (Figure 1.6) (L. C. Gallardo 2011).

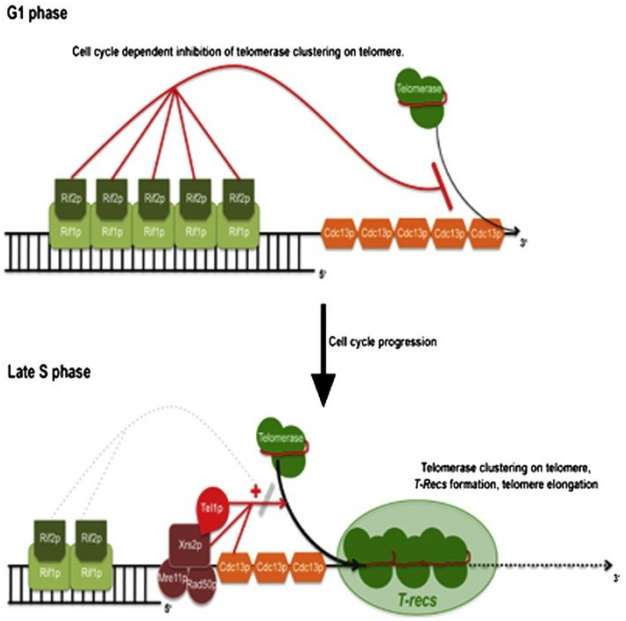

Figure 1.6 Model of telomerase recruitment and telomere extension in *Saccharomyces cerevisiae*. During G1 telomerase molecules are displaced from the telomere by Rif1/2. After DNA replication is completed in late S phase, telomerase molecules cluster into T-recs which represent elongating telomerase molecules which are regulated by MRX, Tel1, Rif1/2, and Cdc13. Taken from (L. C. Gallardo 2011).

Similar to T-recs in yeast, human telomerase RNA (hTR) clusters has been observed in mammalian cells and these clusters have been shown to be important for cancer cell development and tumor progression (Zhao 2011). Therefore, telomerase clustering for telomere elongation seems to be a conserved feature among different species. However, how telomerase cluster formation occurs and which molecules are required for their formation, needs to be discovered.

1.5 TERRA… an unsolved puzzle

Telomeres are maintained in a heterochromatic state that prevents transcription of subtelomeric protein coding genes, a phenomenon referred to as TPE (Buhler and Gasser, 2009). Due to this effect, telomeres were believed to be transcriptionally silent. However, recent evidence has shown that in spite of their heterochromatic state; telomeres are efficiently transcribed, giving rise to a variety of heterogeneous non-coding RNAs known as TElomeric Repeats-containing RNA or TERRA (Azzalin et al., 2007; Bah et al., 2012; Schoeftner and Blasco, 2008).

TERRA expression is highly conserved throughout evolution, from yeasts to humans (Azzalin et al.2007; Schoeftner and Blasco 2008; Luke B et al. 2008; Nergadze SG et al. 2009; Pfeiffer V. and Lingner J, 2012). It is transcribed by the DNA-dependent RNA polymerase II from the telomeric C-rich strand, generating G-rich telomeric transcripts (Azzalin et al., 2007; Schoeftner and Blasco, 2008). The transcription of TERRA, proceeds from the CpG rich islands in the sub-telomeric regions towards the chromosome ends, and terminates within the telomeric-repeat tract, generating long non-coding RNAs which are heterogeneous in length (100 to 9000bp in humans, and 100 to 1200bp in budding yeast).The 5' end of human and yeast TERRA contains a 7-methylguanosine (m7G) cap structure (Feuerhahn 2010). However, human TERRA is mainly non-poly-adenylated, and its poly(A) status plays a role in its stability: the half-life of polyA+ (only in 7% of cells) is 8hs, while the half-life of polyA- TERRA decreases to 3h (Feuerhahn 2010). On the other hand, budding yeast TERRA is poly-adenylated and is degraded by the nuclear 5'-3' exo-nuclease Rat1. Hence, TERRA levels are very low in yeast cells, as the half-life of TERRA is only 30min, while it increases to almost 1h in a *rat1-1* mutant at non-permissive temperature (Figure 1.7) (L. Luke 2009).

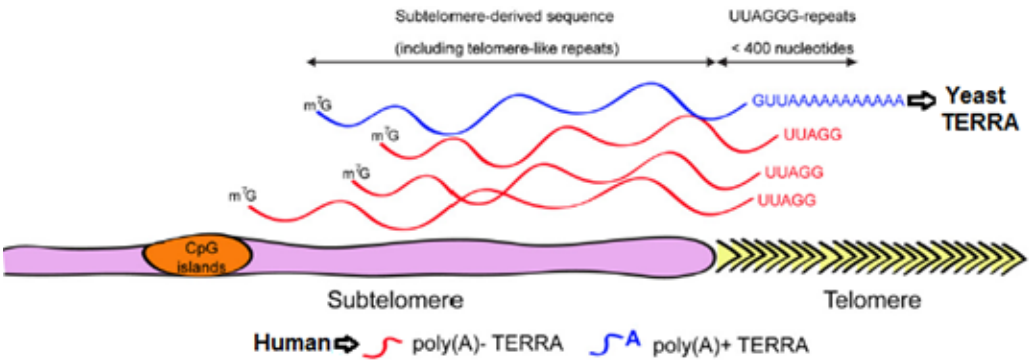

Figure 1.7 TERRA biogenesis in humans and budding yeast. TERRA transcription starts at various locations in the subtelomeric region and proceeds towards chromosome 3' ends up. TERRA 5' ends contain a 7-methylguanosine (m7G) cap structure while its 3' end can be poly-adenylated depending on the species. Modified from (Feuerhahn 2010).

Diverse observations of TERRA had been made by several research groups however its biological function remains largely elusive and the next section will review what is known to date.

Much evidence has shown that in mammalian cells, TERRA is nuclear and co-localizes, to some extent, with telomeres (Azzalin CM et al.2007; Schoeftner S and Blasco MA, 2007). Since not all telomeres show TERRA enrichment (Azzalin CM et al.2007; Lai LT.et al., 2012), it remains to be determined whether only a subpopulation of telomeres expresses TERRA at a given time and if it localizes to the telomere in cis or trans.

Since telomeres consist of G-rich repeats of DNA, they can adopt stable structures called G-quadruplexes. TERRA RNA has similar G-rich repeats to that of telomeric DNA; and RNA/DNA G-quadruplex structure could be formed at the telomeric 3' overhang (Figure 1.8) (Xu 2012). This structure could provide a protective effect on telomere stability, in fact, shelterin proteins responsible for telomere protection and TPE had been found to interact with TERRA in human cells (Arora 2011), and inhibit yeast TERRA in a telomere specific matter (Iglesias 2011). Also evidence shows that TERRA levels increase at dysfunctional telomeres, which might suggest that TERRA could participate in the repair or stabilization of a damaged telomere (N. W. Deng 2009). Nevertheless, this structure could also pose a problem, since it will prevent access to factors needed for DNA replication and telomere lengthening, like telomerase. This problem could be resolved by the displacement of TERRA from the telomere by the Nonsense Mediated Decay (NMD)

factors that are required during DNA replication. This model has not been proven yet, since it has only been shown that when NMD components are depleted from mammalian cells, TERRA is recruited at telomeres (Arora 2011).

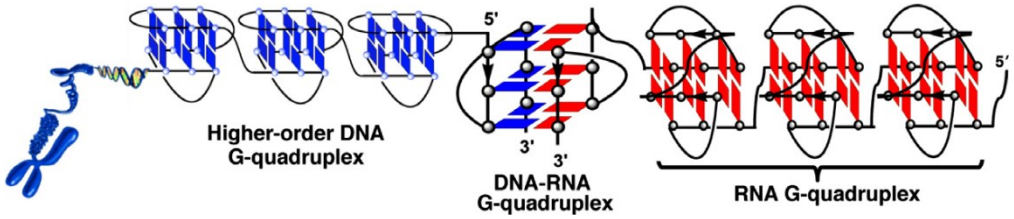

Figure 1.8 DNA/RNA G-quadruplex. Telomeric DNA G-quadruplex, telomeric DNA–RNA G-quadruplex and TERRA RNA G-quadruplex form a superhelix structure at the ends of chromosomes which may provide a protective effect from degradation. Taken from (Xu 2012)

TERRA could also play a role in the regulation of telomere length. Over-expression of TERRA leads to shorter telomeres (Sandell 1994), while its transcriptional repression results in longer telomeres (Arnoult 2012) (P. R. Luke 2008). Contrary to this notion, new evidence shows that telomeres over-elongation does not significantly change TERRA levels (Arora 2011) (Azzalin 2007). So it still remains unclear if telomere shortening or lengthening cause TERRA levels to fluctuate, or if it is the changes in TERRA expression levels that affects telomere length.

Since TERRA is a long non-coding RNA, it has been hypothesized that it may act as a regulator of telomeric heterochromatin, in analogy to other long non-coding RNAs like Xist and HOTAIR. Indeed, alterations in heterochromatin stage of the telomere affect TERRA cellular levels, as its transcription being favored in an open configuration where hypometylation of telomere exist (N. W. Deng 2009). A clear example of the importance of TERRA in heterochromatin regulation has been shown in induced pluripotent stem cells (iPSC) reprograming, where TERRA molecules are needed for heterochromatin remodeling, which leads to higher expression levels of TERRA and telomere elongation (Figure 1.9) (Schoeftner, 2010b). Evidence that TERRA is needed for heterochormatin maintenance has also been shown during X chromosome inactivation during development, where TERRA co-localizes with the non-coding RNA Xist, suggesting it might act as a scaffold to achieve prolonged heterochromatin formation (Shoeftner, 2009) (Lai 2013) (Tattermusch 2011). Interestingly if telomere shortening occurs in these cells, X

chromosome inactivation is relaxed, possibly because TERRA is recruited to the short telomere (Schoeftner, 2010 b).

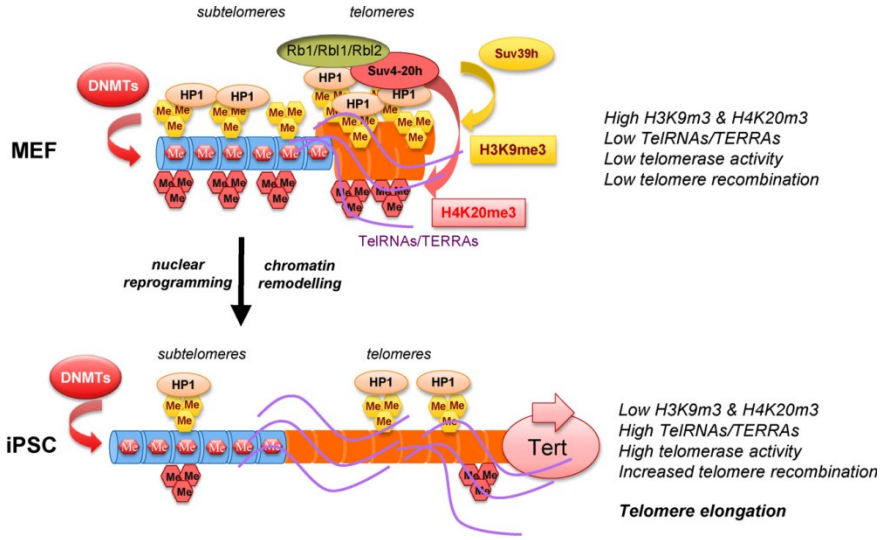

Figure 1.9 Reprogramming of telomeres upon induction of pluripotency in differentiated cell. Telomeres in primary mouse embryonic fibroblasts are shorter than in embryonic stem cells and are organized into a highly compact chromatin structure with low TERRA expression. Induction of pluripotency by many reprogramming factors and TERRA results in an upregulation of telomerase activity and TERRA. Telomerase efficiently elongates these telomeres until the natural limit of telomere length of pluripotent mouse embryonic stem cells. Taken from (Schoeftner, 2010).

The 3' end of the TERRA sequence is complementary to the template region of telomerase RNA and it has been shown that TERRA transcripts can interact with both telomerase RNA (TR) and the telomerase catalytic subunit (TERT) in mammalian cells (Redon 2010). *In vitro* experiments using TERRA mimicking oligonucleotides have suggested that TERRA can inhibit telomerase activity (Redon et al., 2010; Schoeftner and Blasco, 2008). Cell cycle regulation of TERRA has demonstrated that TERRA levels are at their lowest in late S phase and early G2, which corresponds to the time when telomeres are replicated and telomerase is extending chromosome ends (Figure 1.10) (Feuerhahn 2010). However, direct evidence of TERRA telomerase inhibition function *in vivo* remains to be determined. Indeed evidence contradicting this model has been found in iPS cells where high levels of TERRA are required for telomere elongation (Schoeftner, 2010), and evidence in human cancer cells have demonstrated that telomerase efficiently elongates highly

transcribed telomeres (Farnung 2012). Therefore, the relationship between TERRA and telomerase needs to be revisited.

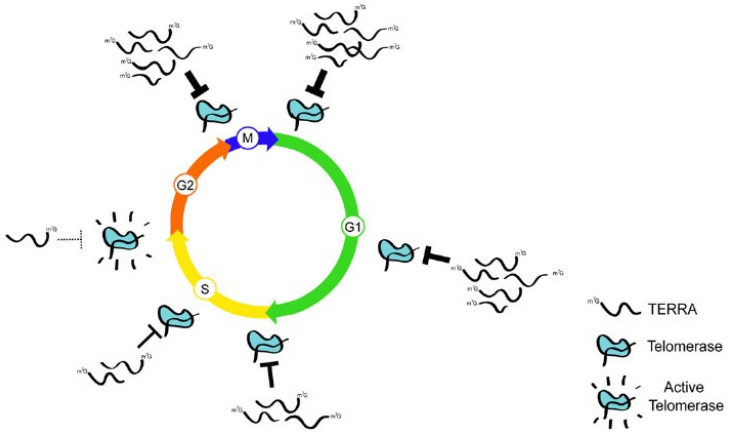

Figure 1.10 Cell cycle regulation of TERRA. TERRA levels are the lowest in late S phase and early G2, when telomerase is active extending chromosome ends. In the model, TERRA represses telomerase outside of late S phase. Taken from (Feuerhahn 2010).

Finally, new evidence has shown that TERRA transcription is induced during different cellular stress (Shoeftner, 2009b), and that TERRA is bound by a wide array of proteins, including heterogeneous nuclear ribonucleoproteins which are needed for telomerase recruitment at the telomeres (de Silanes 2010). Interestingly, TERRA-like small RNAs that are bound by Dicer and PIWI have been found to affect heterochromatin stage at the telomeres (Cao, 2009).

The contradictions in these findings and the difficulty of making the right assumptions to drive conclusions have inspired a new field of regulation of telomeres, fuelled by the mysteries behind TERRA.

1.6 Budding Yeast TERRA: what is known

In *Saccharomyces cerevisiae*, TERRA is transcribed by the RNA polymerase II from the C-rich strand of the telomeres, and is polyadenylated (L. Luke 2009). It is heterogeneous in length and sequence since it can contain X' and Y' element repeats depending of the composition of the telomere it is transcribed from, which results in sizes ranging from 100 to 1200 nt (Z. Wellinger 2012). Yeast TERRA is rapidly degraded in a co- or post-transcriptional manner by the essential RNA 5'-3' exonuclease Rat1p (P. R.

Luke 2008). For these reasons, TERRA levels are very low in wild-type yeast cells and are not easily detectable by biochemical assays. Hence, studies of TERRA in yeast have often required the use of mutant strains or the integration of inducible promoters at telomeres in order to sustain the expression of TERRA. For example, when the thermo-sensitive *rat1KO* strain is shifted to semi-permissive temperatures, cells display an increased level of TERRA, which results in shorter telomeres. This phenotype can be reversed by the overexpression of RNaseH, which removes base-paired DNA/RNA hybrids. This finding suggests that TERRA may be associated with telomeric DNA, where it inhibits telomerase (P. R. Luke 2008). Other experiments, which force telomere transcription by insertion of an artificial promoter, reported shortening of the transcribed telomere in *cis* (Sandell 1994). This shortening comes from a DNA replication-dependent loss of the telomere tract, which leads to premature cellular senescence in the absence of a telomere maintenance mechanism (Maicher 2012). This evidence led researchers to believe that yeast TERRA may act as a telomerase inhibitor, for instance, *in vitro* experiments with human's cells had shown TERRA as a potent telomerase inhibitor. However, no direct *in vivo* evidence has supported this model in yeast or human cells. Therefore, the relationship between TERRA and telomerase is still unclear.

TERRA transcribed from X' or Y' telomeres are subjected to different regulation by the telomere-binding proteins, whose activity represses TERRA expression (Iglesias 2011) (P. R. Luke 2008). Both X' and Y' TERRA are repressed in a telomere specific manner by Rap1, which recruits the Sir2-Sir3-Sir4 complex at X core telomeres and the Rif1-Rif2 complex to all telomeres (Figure 1.11) (Iglesias 2011).

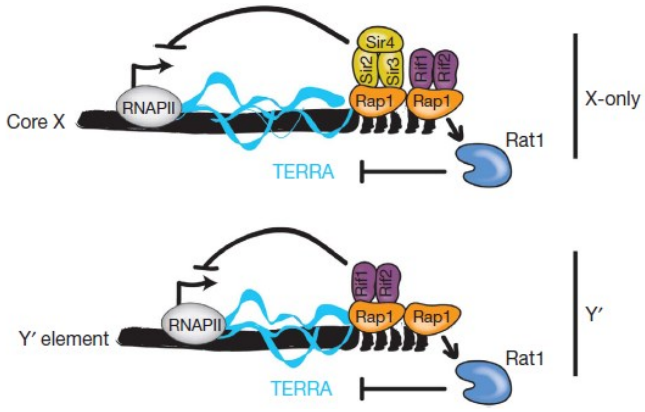

Figure 1.11 A model for Rap1-negative regulation of TERRA at X and Y' telomeres. Rap1 associated at chromosome ends affects TERRA levels at X-core telomeres through both Rat1-mediated degradation and transcriptional silencing through the Sir2/3/4 complex. At Y' elements telomeres, TERRA is regulated by Rap1 through the Rif1 and Rif2 proteins, as well as by the nuclear 5'–3' exonuclease Rat1. Taken from (Iglesias 2011)

It is still unclear whether TERRA is normally expressed in wild type yeast cells, or if these transcripts are constitutively degraded. If TERRA is expressed, then in which conditions and what is their function? So far, most observations of yeast TERRA have been performed using knockouts or mutants of telomeric and RNA degradation pathways, or by using strong inducible promoters, which result in altered levels of TERRA and telomere length. Therefore, a novel approach to study endogenous TERRA in WT cells is essential to understand if TERRA expression is a cause or an effect of telomere shortening. We sought a system that could be used to study TERRA from a single telomere in single WT cells and to study *in vivo*, and for this purpose we decided to use the MS2 system.

1.7 The MS2-GFP assay: a way to label RNAs in living cells

The MS2-GFP system is a method developed to track specific RNAs in real time in living cells, by using the high affinity interaction between sequence-specific RNA stem-loops and the *Escherichia coli* MS2 bacteriophage capsid protein (Bertrand 1998). Incorporation of multiple repeats of the MS2 stem-loops into a target RNA sequence creates an interaction platform capable of binding MS2 proteins fused with a fluorescent protein like GFP, allowing visualization of the RNA (Figure 1.12) (Rodriguez 2007). The RNAs generated from this reporter are transcribed in the nucleus and are properly processed, exported, targeted, and translated, making MS2-GFP a good system to study RNA trafficking (Tyagi 2009).

In order to introduce a reporter into the cell with minimal perturbation to the RNA structure and function, several considerations must be taken: the number of repeats and location of the repeat sequence within the target RNA, reporter protein and RNA stoichiometry, location of the fluorescent protein localization with or without a nuclear

import signal, stability of the fluorescent reporter protein, signal to noise ratio output and phototoxicity during imaging (Querido 2008). This system has successfully been used to label the yeast telomerase RNA by the addition of 10 MS2 stem-loops repeats (C. Gallardo 2011), allowing visualization of *TLC1* RNA in living cells, which has helped understanding telomerase biosynthesis and recruitment to the telomeres (L. C. Gallardo 2011).

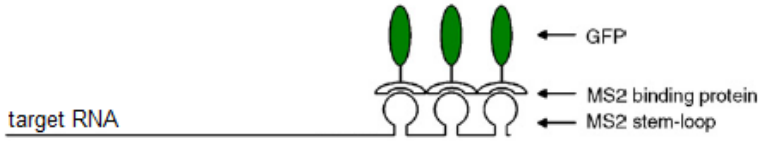

Figure 1.12 The MS2 system. Consisting of a target RNA modified with MS2 stem-loops and being bound by its MS2 binding protein which has been coupled to a fluorophore in this case GFP. Modified from (Rodriguez 2007).

Before the introduction of systems that allowed live cell imaging, the most commonly used assay to study RNA localization in cells was the fluorescent in-situ hybridization (FISH). This assay is highly sensitive, as single molecule RNA species can be visualized, allowing the quantification of different RNAs labeled with different probes and fluorophores (S. Z. Larson 2009). However, this system has its limitations since only snapshots of biologically dynamic processes can be observed. Most importantly, it has been shown that cell fixation and FISH protocols can disrupt RNA clusters visualization, impeding their study; as it has been the case for the visualization and study of telomerase RNA clusters or T-Recs in yeast (L. C. Gallardo 2011) (C. Gallardo 2011).

Therefore, the need to develop live cell imaging system arose. The MS2-GFP was one of the first ones developed, and it has been engineered in different ways to fit with different experimental purposes. Some of these modifications include: changes in MS2 loop sequence to increase affinity to the MS2-GFP protein and changes in the MS2-GFP fusion protein, allowing two GFP molecules to bind, improving the binding and increasing the signal to noise ratio. Also the addition or removal of a nuclear localization signal (NLS) helped reduce the background in the cytoplasm or nucleus (Keryer-Bibens 2008). However, other systems relying on similar setup like the MS2 system have been developed, namely, the lamba-peptide system. This system uses the lambda bacteriophage RNA sequences nutL and nutR, which bind the lambda N protein fused with a GFP protein, to visualize its RNA

(Keryer-Bibens 2008). Another similar assay used to label RNAs in living cells is the U1A-GFP system, which relies on the addition of U1A aptamer sequences to the RNA of interest, which can then be bound by the U1A-GFP fusion protein (Gerst 2011). Recently, the PP7-GFP system has been described, and it relies on the addition of the RNA stem loops of the *Pseudomonas aeruginosa* PP7 bacteriophage to the RNA of interest, and it's binding by the PP7-GFP core fusion protein (Hocine 2013). The MS2 system has been successfully coupled with the PP7 system using two different fluorophores, enabling two-color live cell imaging of two different RNAs (Z. W. Larson 2011).

This system would allow us to do live cell imaging of TERRA during different cell cycle stages and different cell growth conditions. Indeed, we accidentally found a difference in TERRA's expression on different cell growth conditions thanks to this system.

1.8 Yeast cell growth: logarithmic, diauxic and stationary phase

The preferred source of carbon and energy for yeast cells is glucose. When yeast cells are grown in liquid cultures, they ferment glucose predominantly by glycolysis, releasing ethanol in the medium. In this phase, cells go through a short adaptation period known as the lag phase, which then is followed by rapid progression of the cell cycle which increases the cell population exponentially. This phase of yeast cell growth is known as logarithmic growth. Typically, after 1 day of growth, glucose becomes a limiting factor and cells enter the diauxic shift which is characterized by a decreased growth rate and by switching metabolism from glycolysis to aerobic respiration. Here, the cells use the ethanol produced during the fermentation as a carbon source. After the change in metabolism, the cells enter post-diauxic shift were they continue metabolizing ethanol in the medium. When ethanol is depleted from the medium 5 or 7 days after inoculation, yeast cells enter stationary phase or G0. (Figure 1.13) (Lui 2010).

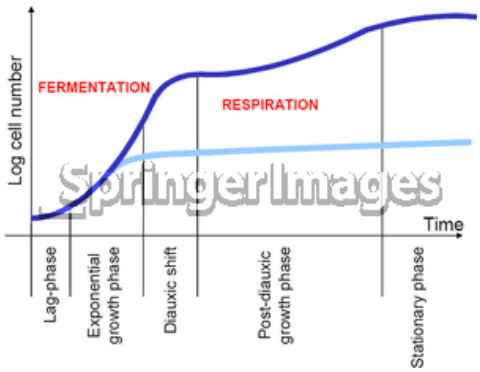

Figure 1.13 Growth curve for yeast grown in rich, glucose-based medium. Glucose is exhausted at the diauxic shift, typically about 1 day after inoculation. During the post-diauxic phase, cells survive with only non-fermentable carbon sources. Cultures reach stationary phase 5–7 days after inoculation. Taken from (Drummond 2011).

The transition of yeast cells from exponential phase to diauxic-shift is regulated by the protein kinase A (PKA), TOR, Snf1p, and Rim15p pathways, which signal changes in the availability of nutrients. These pathways, converge on the transcriptional factors Msn2p, Msn4p, and Gis1p, and elicit extensive reprogramming of the transcription machinery (Galdieri 2010). This way, 30% of yeast genes needed for survival and use of alternative carbon sources become transcriptionally de-repressed but the overall transcription rate is about 3 times lower than in cells growing exponentially, and translation is reduced to about 0.3% (Drummond 2011) (Galdieri 2010). During stationary phase RNA polymerase II is loaded upstream of several hundred genes, poised for transcriptional induction that is required for exit from G0 when nutrients become available (Lui 2010). However, the events in transcriptional regulation during this stage of cell growth are still incompletely understood. Histone acetylation could provide fine-tuning of the transcriptional reprogramming since it decreases during diauxic shift and is induced by the addition of fresh glucose-rich media to stationary phase cells (Galdieri 2010).

Cells in the diauxic shift and stationary phase are stressed by the lack of nutrients and by accumulation of toxic metabolites, primarily from the oxidative metabolism, and are differentiated in ways that maintain their viability for an extended period without nutrients until more favorable conditions arise (Lui 2010). Some of the changes during the diauxic shift and stationary phase resemble the changes observed in cells undergoing stress response, such as induction of heat-shock genes and accumulation of storage molecules.

These cells develop harder cell walls, caused by the depolarization of actin structures (Lui 2010), which makes them more resistant to heat or osmotic shocks, and toxic drugs or enzyme treatment (Galdieri 2010).

Stationary phase yeast cultures are heterogenous and contain at least two different cell types: quiescent and nonquiescent cells. Quiescent cells can be used as a model of aging since they are dense, unbudded, replicatively younger, and are able to synchronously re-enter mitotic cell cycle in fresh media. Nonquiescent cells are less dense, accumulate more reactive oxygen species, and display reduced ability to reenter mitotic cell cycle (Galdieri 2010).

Very little is known about telomeres stage and regulation during diauxic shift. However, during stationary phase, it is known that Rap1 is displaced from the telomeres and occupies the promoter of different genes upon glucose starvation (Buck 2006). It is known that Sir3 and other shelterin-like proteins leave the telomere and localizes in the nucleolus during stationary phase, but this does not result in telomere shortening (Ashrafi 1999). However, it is known that there is a lack of telomere elongation in stationary phase cells (Brevet 1999). Recently, it has been shown that a small percentage of stationary phase cells undergo telomere fusion due to telomere end-joining (Lescasse 2013). However, it is still unclear in what state are the telomeres undergoing diauxic shift, and how telomere regulation is achieved without the binding of Rap1 and sheltering proteins during stationary phases.

Since diauxic shift can be used as a stress model for glucose starvation and oxidative stress, and stationary phase cells can be used as a model of aging, it will be interesting to explore TERRA and telomerase regulation during these stages of cell growth to understand function in cell and telomere biology.

Project Objectives and Hypothesis

Several observations provide insight into the regulation of TERRA. However, up until now, the function of TERRA remains elusive. Previous studies in *Saccharomyces cerevisiae* have shown that endogenous TERRA levels in WT cells are very low, due to their rapid degradation by the exo-nuclease Rat1. Therefore, this limits the possibility to use biochemical approaches to study TERRA in wild-type yeast cells.

The questions we sought to answer in this study are as follows:

- Is it possible to detect the expression of TERRA in a wild-type strain?
- How is TERRA regulated and what is its function?

To answer these questions, our first objective was: **"to use the MS2-GFP system to localize and follow TERRA expressed from a single telomere *in vivo*"**

We hypothesized that by: **"using the MS2-GFP system, we will be able to label, localize and follow TERRA expressed from a single telomere in wild-type yeast cells, allowing us to study its regulation and localization in single cells"**

Once we were able to label TERRA transcripts with the MS2-GFP system, we found that TERRA co-localized preferentially with its telomere of origin, suggesting TERRA as a *cis*-acting regulator of telomeres. A second objective was: **"To dissect the condition of the telomeres expressing TERRA"**

Our hypothesis was that: **"TERRA could act in *cis* at its telomere of origin when this telomere shortens, and this could reveal a role for TERRA and telomerase in telomere elongation"**

Finally, after TERRA was successfully labeled, we found out that TERRA localization changed during cell growth, so our third objective was: **"To assess expression of TERRA and its localization during cell growth"**

Our hypothesis is that by: **"using the MS2-tagged TERRA clones in time courses experiments, we will be able to gain insight on the regulation of TERRA during cell cycle and cell growth"**

And with this… our adventure to uncover the mystery behind TERRA begins…

Chapter II

Materials and Methods

This section describes the diverse tools and methods needed for journey to uncover the mysteries of TERRA.

2.1 Yeast strain generation

All the strains used in this study were generated in a FY23 (MATa leu2 trp1 ura3 flo8-1) haploid background cells. For the MS2-TERRA clones, the integration of 2xMS2 or 6xMS2 at telomere 1L or telomere 6R was performed by integrating a cassette containing the MS2 sequences and a Kanamycin resistance (KAN) gene flanked by lox-p sites (Figure 3.1) (a) The MS2-Kan cassette was PCR amplified from the 6xMS2-pUG6-lox-p-Kan plasmid by using the following primer pairs: HRchr6prS-MS2-6s (AACCAGTGAGGCCA TTTCCGTGTGTAGTGATCCGAACTCAGTTACTATTGATGGAAATGAGGAGGTAC CTAATTGCCTAG) and HRchr6prAS (GGCGTACGCACACGTATGCTAAAGTATATA TTACTTCACTCCATTGCGCCCCATGACCCAGTTAGTGGATCTGATATCACC) for the integration of 2xMS2 at telomere 6R; HRchr6prS-MS2-6sB (AACCAGTGAGGCCAT TTCCGTGTGTAGTGATCCGAACTCAGTTACTATTGATGGAAATGAGGCCAGCTG AAGCTTCGTACG) and HRchr6prAS for the integration of 6xMS2 at telomere 6R; HRchr1LprS-MS2s (GTAGAGGGATGGATGGTGGTTCGGAGTGGTATGGTTGAATG GGACAGGGTAACGAGTGGAGGCAAGGTACCTAATTGCCTAG) and HRchr1LprAS (CTACCCTAACACAGCCCTAATCTAACCCTGGCCAACCTGTCTCTCAACTTACCC TCCATTACCCTAGTGGATCTGATATCACC) for 2xMS2 at telomere 1L; HRchr1LprS-MS2-6s (GTAGAGGGATGGATGGTGGTTCGGAGTGGTATGGTTGAATGGGACAG GGTAACGAGTGGAGGCACCAGCTGAAGCTTCGTACG) and HRchr1LprAS for the integration of 6xMS2 at telomere 1L (b). After integration of the MS2-Kan cassette, Kan resistance gene was eliminated by expressing Cre recombinase from the plasmid pSH47-Gal1-Cre (c). pSH47-Gal1-Cre plasmid carrying the URA selection marker was subsequently eliminated by growing the cells in 5FOA plate. After Kan excision, for each clone the MS2 integration site was PCR amplified and PCR products sequence-verified (d). The specific integration was also confirmed by southern blot using a MS2 specific probe and either telomere 1L or telomere 6R specific probes (Figure 3.1 e). For southern blot analyses genomic DNAs were digested PvuII or EcoRV for the analyses of telomere 6R or telomere 1L, respectively. To express the endogenous Rap1-cherry fusion protein, cells were transformed with a cassette containing a cherry coding sequence and a Kan resistance

gene, as previously described (L. C. Gallardo 2011). Briefly: the cherry-Kan cassette was amplified by PCR, using pFA6-cherry as template, and the following primer pair: Rap1-5'HRcherry (AAACTGGTTAAAAAGCATGGAACTGGTAGAATGGAAATGAGGAAAAGATTTTTTGAGAAGGACTGTTACGGATCCCCGGGTTAATTAA) and Rap1-3'HRcherry (TAGAAAACGTGAATCAGTGAAATAAAGGAGTAAAATAAGTTAAACAATGATGTTACTTAATTCAATTACGAATTCGAGCTCGTTTAAAC). The strain generation work was carried out by PhD Emilio Cusanelli.

The 10xMS2-TLC1 clone was previously prepared in the laboratory in a W303 (trp1 his3-11,15 leu2::LEU2-GAL10-FLP1 adh4::FRT-URA3-TEL270- TEL270-FRT-TEL) background (L. C. Gallardo 2011).

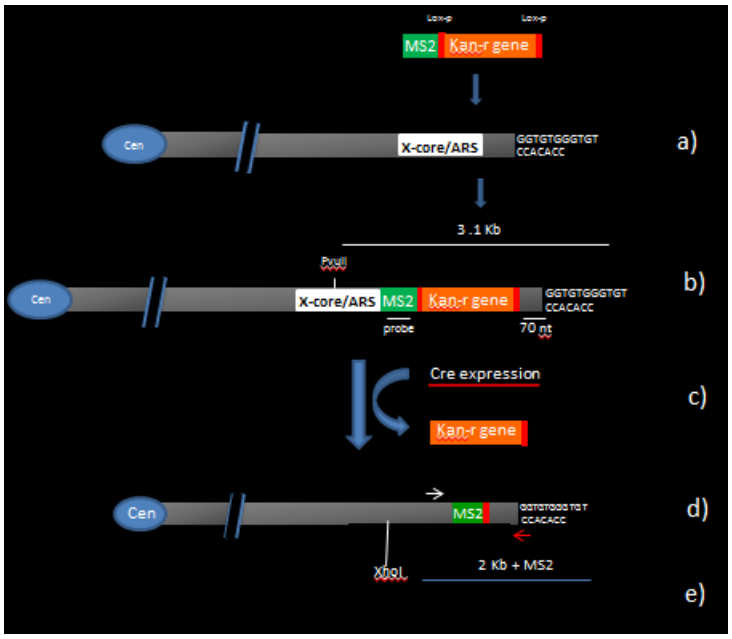

Figure 2.1 TERRA tagged MS2 clone generation. This was performed by Dr. Emilio Cusanelli

2.2 Yeast cell growth conditions

Strains were grown shaking at 30°C in either yeast extract/peptone medium (YPD) with 2% glucose for DNA/RNA extraction purposes or selection media (SD) supplemented with appropriate amino acids and 2% glucose if cells were going to be used for microscopy analysis SD complete media was used to prevent auto florescence.

For logarithmic phase growth conditions a single colony was picked from an agar plate and grown overnight in respective media, next day cells were diluted to 0.15 OD_{600} and grown until desired concentration typically between 0.3–0.5 OD_{600} without exciding 0.8 OD_{600} to ensure logarithmic growth conditions. For fluorescent microscopy study 1 ml sample of culture was taken on an eppendorf tube and slowly centrifuged to concentrate cells, then 8 µl of the pellet were laid on a coverslip for imaging. Note: caution was taken to keep the main culture sterile.

For diauxic shift conditions cells that had been confirmed to be in logarithmic growth condition and their TERRA levels had a normal expression levels (check by fluorescent microscopy) were left to grow for another 16 hour in the same media. The next day after more than 20 hours of initial incubation OD_{600} was checked to be higher than 2 OD_{600} ensuring that the OD_{600} was still slowly going up to ensure diauxic shift conditions and not stationary phase ones. Diauxic shift conditions typically lasted for 24 to 48 hours before stationary phase settling around 7-9 OD_{600} (Drummond 2011). TERRA expression level/localization and TLC1 localization were accessed by fluorescent microscopy checking for over expression.

For glucose replenishment studies cells that had been grown for one week in the same media and had settled in stationary phase were harvested by gentle centrifugation in a falcon tube, and then diluted in fresh 2% glucose media at 0.15 OD_{600} and left to regrow monitoring the OD_{600} and TERRA expression level/localization and TLC1 localization were accessed by fluorescent microscopy checking for over expression. The experiment was continued until TERRA and TLC1 phenotypes were back to normal logarithmic growth conditions.

2.3 DNA extraction and southern blot analyses

Cells were harvested during the right phase of growth (logarithmic or diauxic shift) and washed in ice cold PBS. Pellets were re-suspended in 200µl of lysis buffer (0.01M Tris pH8, 0.1M NaCl, 1mM EDTA pH8, 1% SDS, 2% Triton-X100) and transferred in new tubes containing 200µl of phenol/chloroform and the equivalent of 200ul of glass beads.

Lysis was performed by vortexing samples for 10 minutes at room temperature. After vortexing, 200ul of TE was added to each tube and samples centrifuged for 5 minutes at 13000 Rpm. After one step of chloroform extraction, DNA was precipitated at -20 °C for 1 hour adding 2 volumes of Etanol-100%. DNA was resuspended in 200µl RNAseA-water solution and incubated at least 1 hour at 37 °C. Genomic DNA was subsequently quantified on agarose gel. For southern blot analyses, 10ug of genomic DNA were digested with the appropriate restriction enzyme, and run over-night (30 V voltage) in 1% agarose gel. Gel was subsequently stained and DNA denaturated in 0.5 M NaOH, 1.5M NaCl solution for 1 hour at room temperature. Denaturating solution was then neutralized by incubating the gel 1 hour in 1M Tris pH7.5, 1.5M NaCl solution. DNA was transferred to a nylon membrane (Amersham) by capillarity using 10X SSC transfer buffer, over-night, and subsequently UV-crosslinked to the membrane. Membrane was blocked in hybridization buffer (0.5M NaPO4 pH7.2, 1mM EDTA, 7% SDS, 1% BSA) for at least 4h at the appropriate temperature. 300ng of probe were labeled at the 5'-end by using T4-Polynucleotide kinase (New England Biolabs) and P32-gamma ATP. Hybridization was performed over-night at the appropriate temperature. After hybridization, membranes were washed three times for 30 minutes at the hybridization temperatures in wash buffer (0.5% SDS, 02xSSC). Signal was impressed on film. Note the probes used in this study were: Gprobe (GTGGGTGTGG TGTGTGGGTGTGGTG), Gprobe-Tel6R (TGTGTAGTGATCCGAACTCAGT), MS2probeS (ACATGAGGATCACCCATGTCTG), and Sir4KOAS (TTGGTATTTGATG GGTTGCTC).

2.4 Live cell imaging

Clones used for these studies were the following clones: 6xMS2-Tel6R/Tel1L TERRA, 10xMS2-TLC1 and WT expressing the MS2-GFP and Rap1-cherry. Cells were grown (as explained in the 3.2 section above) and once they reached the desired growth stage a 1 ml sample of culture was taken in an eppendorf tube and slowly centrifuged to concentrate cells, then 8 µl of the pellet (for log phase culture) or of the supernatant (for diauxic shift culture) were laid on a coverslip for imaging. Note: caution was taken to keep the main culture sterile.

Live cell imaging was carried out using a Nikon E8000 upright microscope equipped with an objective 100x/1.46NA and a EM-CCD camera Evolve512 (from Photometrics). TERRA foci were detected by using a FITC fluorescence filter with the following camera setting: 100 ms exposure time, binning 1 x 1, 200 EM gain. TLC1 T-recs foci were detected using a FITC fluorescent filter with the following camera setting: 100 ms exposure time, binning 1 x 1, 200 EM gain. Rap1-cherry signal was detected using a texas-red fluorescent filter with the following camera setting: exposition time 200 ms exposure time, binning 1 x 1, 200 EM gain. DIC images were taken at 50ms Acquisitions were done and analyzed using Metamorph software.

2.5 Fluorescent In Situ Hibridization (FISH)

Probe design: FISH assay was performed as described previously (Gallardo and Chartrand, 2011) with minor modifications. The FISH probes used in this study to target TERRA are the following: MS2-TERRA (5-AGT'CGACCTGCAGACAT'GG GTGATCCTCAT'G TTTTCTAGGCAATT'A-3), endougenous Tel1L-TERRA (5-CCAT'CCCTCTACTT'ACT ACCACT'CACCCACCGT'TACCCTCCAAT'TACCCATATC-3), endougenous Tel6R-TERRA (5-ACGCACACGT'ATGCTAAAGT'ATATATTACT'TCACTCCATT'GCGCC CCAT'GACCC-3), 5 TLC1 probes were used as described in (O. D. Gallardo 2008) and a control probe targeting a small nucelolar RNA U3 (5-TT' CTATAGAAATGATCCT'ATG AAGTACGTCGACTT'A-3) was used as described in (Verheggen 2001) to perform quantitation were synthesised with an amino-allyl modified T residue were stated (') by Biocorp.

Probe labelling: The TERRA probes were labelled in Cy3 dye while the control RNA U3 probe was labelled in Cy5 dye as follows: 10µg of probe were concentrated by speedvac, and resuspened in 35µl of sodium carbonate buffer pH 8.8, followed by the addition of 15µL of monoreactive Cy3 or Cy5 dye pack from GE Health (previously resuspeded in 30 µL of DEPC water). The mixture was incubated for 24 hours at room temperature in the dark with occasional vortexing. The probes were then purified using an RNAse free Sephadex G-25 column (Roche Applied Bioscience) following manufacturer recomedation. Probe concentration was measured at OD 260nm and fluorophore incorporation efficiency

was calculated and verified to be higher than 70% as quality control for our labelling. The labelled probes were then diluted to a final concentration of 1ng/µL in DEPC water for use in FISH.

Coverslips preparation: 22 x 22 x 0.15 mm coverlips (Fisher Scientific) were stripped by boiling them in 0.1N HCl (Sigma) for 30 min, then washed 10 times with distilled water and autoclaved. Then individual covership were put in six-well tissue culture plate (Fisher Scientific) and let to dry. Once dried 200µL of 0.01% poly-L-lysine DEPC (Sigma) was dropped on each coverslip and incubated for 2 min at room temperature, after excess solution was aspirated and let to dry for 2 hours. Then they were washed 3 times for 10 min in DEPC water and let to dry vertically overnight after aspirating excess liquid. Finally the coated surface was left facing up and kept for further use at room temperature.

Fixation and spheroplasting of yeast cells: Overnight yeast cultures were diluted in 50 ml of appropriate media until they reach early log phase (OD_{600} between 0.2-0.4) or late diauxic shift phase (OD_{600} 4-6) the culture was then centrifugated, washed and resuspended in 1xPBS buffer (10mM KH2PO4, 1.4M NaCl, 40mM KCl, 100mM Na2HPO4, pH 7.5). The cells were then fixed for 45 min at room temperature by adding 6.25 mL of 32% paraformaldehyde (Electron Microscope Sciences), after the cells were pelleted and washed 3 times in 1x ice-cold Buffer B (1.2M Sorbitol, 0.1M potassium phosphate, pH 7.5). The cells were then gently resuspened in 1mL of buffer B containing 20mM vanadyl ribonucleoside complex (VRC), 28mM β-mercaptoethanol, 0.06 mg/mL phenylmethylsulfonyl fluoride, 5µg/mL pepstatin, 5µg/mL leupeptin, 5µg/mL aprotinin, and 120U/mL of RNAse inhibitor. The cells were then transferred into a tube containing oxalyticase (for log phase culture) or into a tube containing 2x oxalyticase and 60 µl of zyomales 5 µg/mL (for diauxic shift culture) or into a tube containing 2x oxalyticase and 70µl of zyomales 5 µg/mL. They were incubated for 15 min (for log phase), 20 min (for diauxic shift), and 25 min (for stationary phase) at 30ºC for spheroplasting, and then washed in 1ml 1x ice-cold buffer B. They were then resuspeded in 750µL of 1x ice-cold buffer B and 100 µL of spheroplast solution was dropped on each poly-L-lysine coated coverslip and let adhere to coverslips for 30 min at 4°C. The coverslips were then washed

with 3 mL of ice-cold buffer B and excess aspirated, followed by adding 5ml of 70% DEPC ethanol to dehydrate the spheroplasts which were kept at -20°C for later use.

In situ hybridization: 10µL of a TERRA probe solution were mixed with 4 µL of E.coli tRNA and 2µL RNA U3 probe, and lyophilize in a speed vacuum kept in the dark. They were resuspened in 12µL of 80% formamide, 10mM sodium phosphate, pH 7. Meanwhile the coverslips containing spheroplasted cells were rehydrated by washing them with 8 ml in 2xSSC buffer for 5 min at room temperature in a Columbia jar. After the cells were incubated in 8ml 2xSSC with the required formamide % (35% for MS2 TERRA probe 40% for TLC1 probe and 50% for endogenous Tel1L and Tel6R TERRA probes). During this incubation the probe solution was heated for 3 min at 95°C, after the probe solution was diluted with 12µL of 4xSSC, 20 mM VRC, 4µg/mL RNAse free BSA and 50U of RNAse inhibitor. For hybridization, a glass plate was covered with a parafilm layer, the probe solution was dropped on the parafilm and the coverslip with surface containing the spheroplasts was laid on the drop. A humidified hybridization chamber was created by covering the coverslips with another parafilm layer and the plate was incubated overnight in the dark at 37°C wrapped in aluminum foil. After hybridization, the coverslips were put back in a Columbia jar and washed twice with 8 ml of pre-heated 2xSSC with the required formamide % at 37°C for 15 min. Then it was washed with 8mL of 2xSSC 0,1% Triton X-100 for 15 min at room temperature (for the endogenous Tel1L TERRA probe this was repeated 2 times). After it was washed twice with 8 ml of 1xSSC at room temperature for 15 min (for the endogenous Tel1L TERRA probe this was repeated 4 times). For DNA staining the cells were incubated with 8 ml of 1xPBS containing 1ng/ml of 4',6 diamidino-2-phenylindole (DAPI) (Invitrogen) for 2 min at room temperature. The coverslips were then mounted on a glass slide with the surface containing the spheroplasts on a 10µl drop of mounting medium. The slides were sealed by applying nail polish, and then were imaged.

Image Adquisition and Analysis: The prepared slides were imaged in an epi-fluorescence microscope Nikon Eclipse TE2000U equipped with Cy3.0, Cy5.0, FITC, DAPI filters, a 100x/1.46NA objective, and a CoolSNAP HQ2 camera from Photmetrics. Images were acquired using NIS Elements software ND acquisition (from Nikon) with at least 15 z-stack images with a 0.20 µm step size, endogenous TERRA and TLC1 foci were detected

using a Cy3.0 filter with 1s exposure time, while MS2-GFP tagged TERRA foci were detected using a FITC filter with 1.5s exposure time, RNA U3 control probe used to check FISH quality and nucleolar labeling was detected using a Cy5.0 filter with 700ms exposure time, DAPI was used as a nuclear label and was detected with a DAPI filter at 50ms exposure time, DIC images were taken at 100ms. All the images were then processed equally using a self-made macro on ImageJ software to perform: maximum intensity projection, adjust brightness/contrast of each channel using the same levels for all the FISH experiments and modifying channel LUTs to desired colors (endogenous TERRA foci in red, MS2-TERRA tagged foci in green, DAPI in blue and DIC in gray scale) to allow us to visualize the final merged images. TERRA foci were then quantified taking in account number of cells with foci and its localization, as control only cells that had been labeled with the RNA U3 control probe were quantified.

2.6 RNA extraction and RT-qPCR analyses

Cells were harvested during the right growth conditions, washed in ice cold PBS and pellets re-suspended in 400µl of ice cold TES solution (10 mM Tris pH7.5, 10 mM EDTA, 0.5% SDS). 400ul of acid phenol were added to each sample and tubes were incubated for 1 hour at 65^{o}C, vortexing 5s every 10 minutes. Samples were then chilled in ice for 5 minutes and centrifuged 13000 Rpm for 5 minutes at room temperature. After chloroform extraction, RNA was precipitated by addition of 1/10 volumes of 3M NaAc pH5.2 and 2 volumes 100% ET-OH. RNA were subsequently collected by centrifugation and washed with 500µl of ethanol 70%. Pellets were re-suspended in DEPC water run on 1xMOPS agarose gel for quantification and quality control. 3µg of RNA were treated with DNase I (from Fermentas) for 1 hour at 37 ^{o}, and 200ng of DNase I treated RNA were retrotranscribed by using H-MULV –H enzyme (from Fermentas) at 42^{o} for 1 hour. 3µl of the RT reaction were used for the qPCR experiments. qPCR were performed in triplicates, using the needed primers (See note below) and the qPCR master mix “SsoFAST EVAGreen Super MIX” from Biorad. qPCR was carried out on a Roche LightCyler 480 sequence-detection system. Analyses were performed by calculating the averages and standard deviations of the actin normalized 2^-Dct values of each triplicate. Note the primers used for RT reaction in this

study were: For TERRA RT we used a Cprobe oligo (ACTGAGTTCGGATCACTACA CA), for TLC1 RT we used (GATCATCACGGTGCCGGATCCTTGTGTGTGGGTGTGG TGA), and for housekeeping gene RT we used Oligo dT. The pair of primers used for the qPCR in this study were: for Y'elements TERRA S (CTCGCTGTCACTCCTTACCCG) and AS (GGCTTGGAGGAGACGTACATG), for Tel6R TERRA S (TGTGTAGTGATCCGAACTCAGT) and AS (AAAACCATGGTAGC ATATTGATATGGCGTACG), for Tel1L TERRA S (AAGTGGTAGGGTAAGCACGT) and AS (CAGCCCTAATCTAACCCTGG) , for TLC1 RNA S (TGTGCGCAATTTGTGG TTTTTTAT) and AS (GTGATCTGCAGATCATCACGGTGCCGGATCC) for housekeeping gene *ALG9* S (CACGGATAGTGGCTTTGGTGAACAATTAC) and AS (TATGATTATCTGGCAGCAGGAAAGAACTTGGG), and for housekeeping gene Actin S (TTCCAGCCTTCTACGTTTCC) and AS (ACGACGTGAGTAACACCATC). It is important to notice that actin was used as housekeeping gene for IP and logarithmic growth qPCR experiments, while ALG9 was used as housekeeping gene for diauxic and stationary phase experiments since the actin gene is down-regulated during these stages (Teste 2009).

2.7 Co-immunoprecipitation assay

For co-immune precipitation (IP) 50 ml culture of logarithmic phase growing cells were pelleted and washed in ice cold PBS. Cells were lysated in 400ul lysis buffer (20mM Hepes pH7.9, 20% glycerol, 0.2mM EDTA, 150 mM NaCl, 0.05% NP40) containing 10mM beta-mercaptoethanol, 1mM PMSF, EDTA free protease inhibitor mix, VRC 2mM, RNAse inhibitor "RNAse OUT" from INVITROGEN, 3ul/ml. Cells were lysated using glass beads by vortexing. Lysates were precleared as described above, and ~200ug of protein lysate were used for the immunoprecipitation experiment over-night, using 2ug of anti-GFP antibody (mouse monoclonal from Roche) or 3/5 ug anti-Myc mouse or rabbit (from abcam) per sample, while ~40ug of protein lysate used for the INPUT. Complexes associated with anti-GFP antibody were collected using protein-G sepharose (Millipore, GE heathcare), and binding allowed by incubation for 1 hour at 4^{o}C. Samples were then washed four times in lysis buffer and RNA was extracted by adding 500ul of TRIZOL reagent to the IP and INPUT samples. RNA extraction was performed according to manufacturer

instruction and isopropanol precipitation allowed for 2 hours at room temperature in the presence of glycogen (20ug per sample). INPUT and IP samples were resuspended in 30ul and 20ul of H_2O mq, respectively, and 2ul were used for RT reaction. RT and qPCR reactions were performed as described above.

2.8 Western Blot analysis

After IP with anti-myc antibodies 40ug of INPUT and protein-G sepharose bids IP samples were loaded with 10ul of protein loading gel and were put at 95°C for 3 minutes and then they were loaded in an 8% SDS-PAGE gel. Proteins were transferred to Immobilon PVDF (0.45 μM) membranes (Millipore), probed with a 1μg rabbit/mouse α-Myc primary antibody and 1/5000 α-rabbit HRP or 1/10000 α-mouse HRP as secondary antibody. Then the membrane was exposed with ECL Plus (Pierce) according to manufacturer protocol and results were visualized by exposing with a film.

2.9 Statistical analysis

The P values were computed for the experiments where significance levels were important or relevant for the study results. The P value was calculated using an unpaired *t* test from GraphPad free calculator that can be find on www.graphpad.com/quickcalcs/ttest1. The results were interpreted as suggested by GraphPad software: $P < 0.05$ * statistically significant difference, $P < 0.01$ ** very significant, $P < 0.001$*** extremely significant.

Results

In this section you will find the description of the journey from tagging TERRA to understanding TERRA function at short telomeres, having an insight on TERRA regulation during yeast cell growth.

Chapter III

Live cell visualization of Telomeric Repeat containing RNA (TERRA) from a single telomere in single WT yeast cells: MS2 repeats integration, and validation

Authors' contribution:

Unless otherwise stated all other figures and analysis were made by Carmina Angélica Pérez Romero

Emilio Cusanelli: MS2-TERRA clone tagging and their genetic validation (Figure 3.1, 3.2), and live cell characterization (Figure 3.3a)

The first step of our adventure started by trying to find a system that could enable the visualization of TERRA in WT yeast cells; therefore we sought the possibility of tagging TERRA from a single telomere with the MS2-system, to allow its study in WT cells. But before trying to study or understand TERRA we first had to integrate the system and validate that what we saw and tagged was indeed TERRA and nothing else… so this is how it all started…

3.1 TERRA from a single telomere in single wild type cells can be visualized *in vivo* by using the MS2-GFP system

TERRA endogenous levels are low in *Saccharomyces cerevisiae* and it is degraded by the 5`-3` exonuclease Rat1 (P. R. Luke 2008), making its study in WT cells challenging. Due to this limitation, early studies used a *rat1-1* mutant background to explore the function of TERRA.

In order to be able to study TERRA transcribed form a single telomere *in vivo,* in single wild-type cells (WT), we decided to use the MS2-GFP system since it has been successfully used in our laboratory to label and study the trafficking of other RNA's, like ASH1 (Bertrand 1998), and the telomerase RNA *TLC1* (L. C. Gallardo 2011).

For this study, we decided to tag TERRA transcribed from different telomeres in order to control for chromosomal differences, as well as for being able to study the effect of TERRA coming from one telomere on another telomere. Unfortunately, telomeric repeats in yeast are highly conserved, making it difficult to target a single telomere during cloning. However, the number and position of subtelomeric X' (short) and Y' (large repeats contained in half of yeast telomeres) repeat elements vary and are transcribed into TERRA (Zhu 2009). So for cloning and study purposes we integrated 2 or 6 MS2 stem-loop in the 3` end of the X' core subtelomeric region of telomere 1 left arm (Tel1L) and telomere 6 right arm (Tel6R) in the FY23 yeast strain, as explained in the material and methods section. The resulting clones were checked for:

- Single integration of MS2 stem-loops: Southern blot analysis using the MS2 probe shows a single integration with the expected size following PvuII digestion of genomic DNA from Tel6R MS2 tagged clones (Figure 3.1a). NcoI digestion of genomic DNA from Tel1L MS2 tagged clones also confirmed a single integration of the MS2 stem-loops, with an expected size of 3 Kb (Figure 3.2a).

- Specific integration of MS2 stem-loops in the subtelomeric region: Sequencing and sequence alignment analysis shows integration of the MS2 repeats in the 3` end of the subtelomeric region of Tel6R and Tel1L. No mutation in the sequence was detected and the correct number of stem-loop 2xMS2 (190 nt) or 6xMS2 (450 nt) was observed (Figure 3.1b and 3.2b).

- Telomere length after the MS2 sequence integration: XhoI digestion of genomic DNA revealed telomere length by Southern blot using telomere 6R or telomere 1L specific probes. This confirmed that no unexpected lengthening or shortening of the telomeric (TG) repeats occurred upon integration of the MS2 repeats (Figure 3.1c and 3.2c).

Once the TERRA MS2 clones 2xMS2 Tel1L and Tel6R or 6xMS2 Tel1L and Tel6R were created, they were transformed with a plasmid containing the MS2-GFP fusion protein. Once the MS2 stem-loops get transcribed into TERRA, the MS2-TERRA transcripts can be labeled by the MS2-GFP protein, allowing their detection.

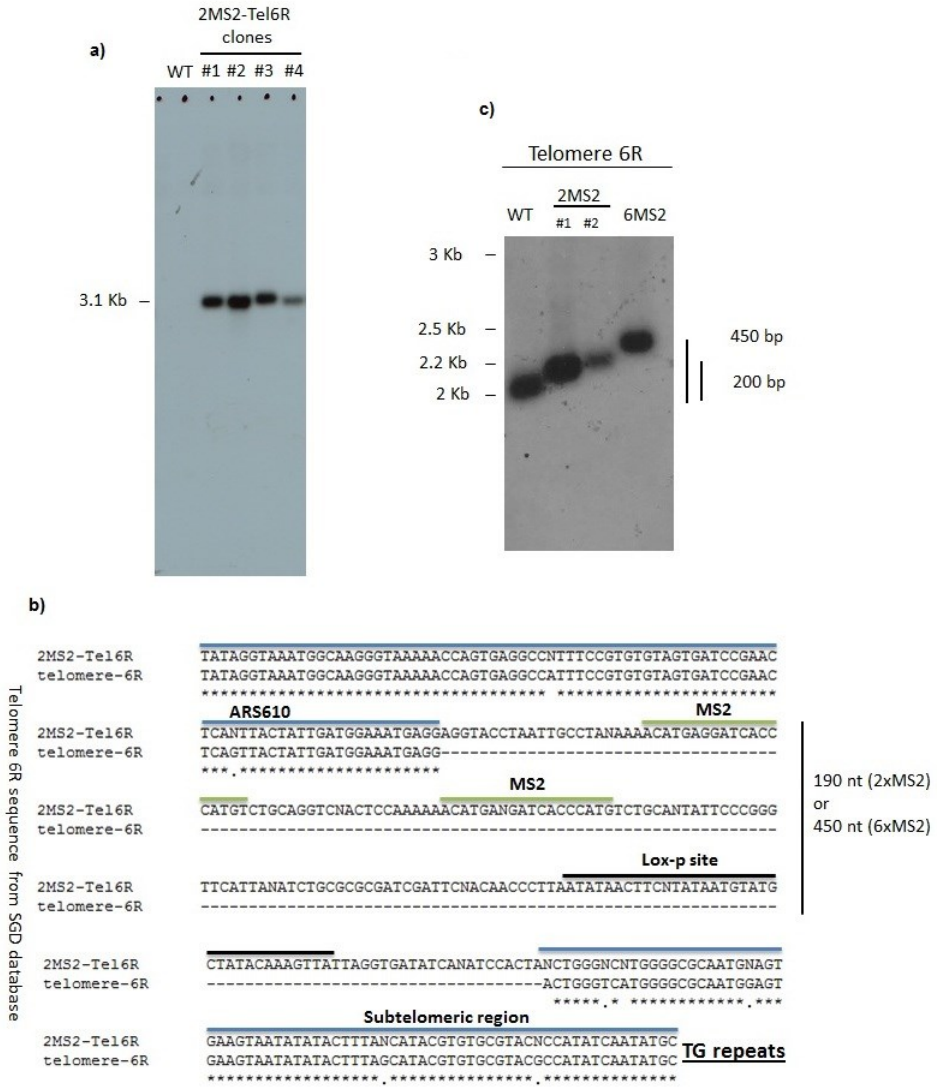

Figure 3.1 Creation and validation of the Tel6R-MS2 yeast clone. a) Southern blot analysis with MS2 probe of PvuII digested genomic DNA reveal single integration at 3.1 Kb of the MS2 repeats in 2xMS2-Tel6R clones as compared with WT cells, which do not contain any MS2 repeats. **b)** Sequence alignment of 2xMS2-Tel6R and WT telomere 6R show same subtelomeric sequence with the integrated sequence of the MS2 repeats, and Lox-p site resulting from the excision of KAN marker by Cre recombination. Note: the 2xMS2 sequences add 190 nt to the subtelomerie, while 6xMS2 repeats add 450 nt to it. ARS: Autonomously Replicating Sequence. **c)** Southern blot analysis with a Tel6R specific probe of XhoI digested genomic DNA to assess telomere length confirm that telomere length do not change more than the 190 nt expected in the 2xMS2 clones (lane 2 and 3) and 450 nt of 6xMS2 clone (lane 4), compared to the WT (lane 1) size of 2 Kb. The clone creation and genetic validation was mostly done by the postdoc fellow in the laboratory Dr. Emilio Cusanelli.

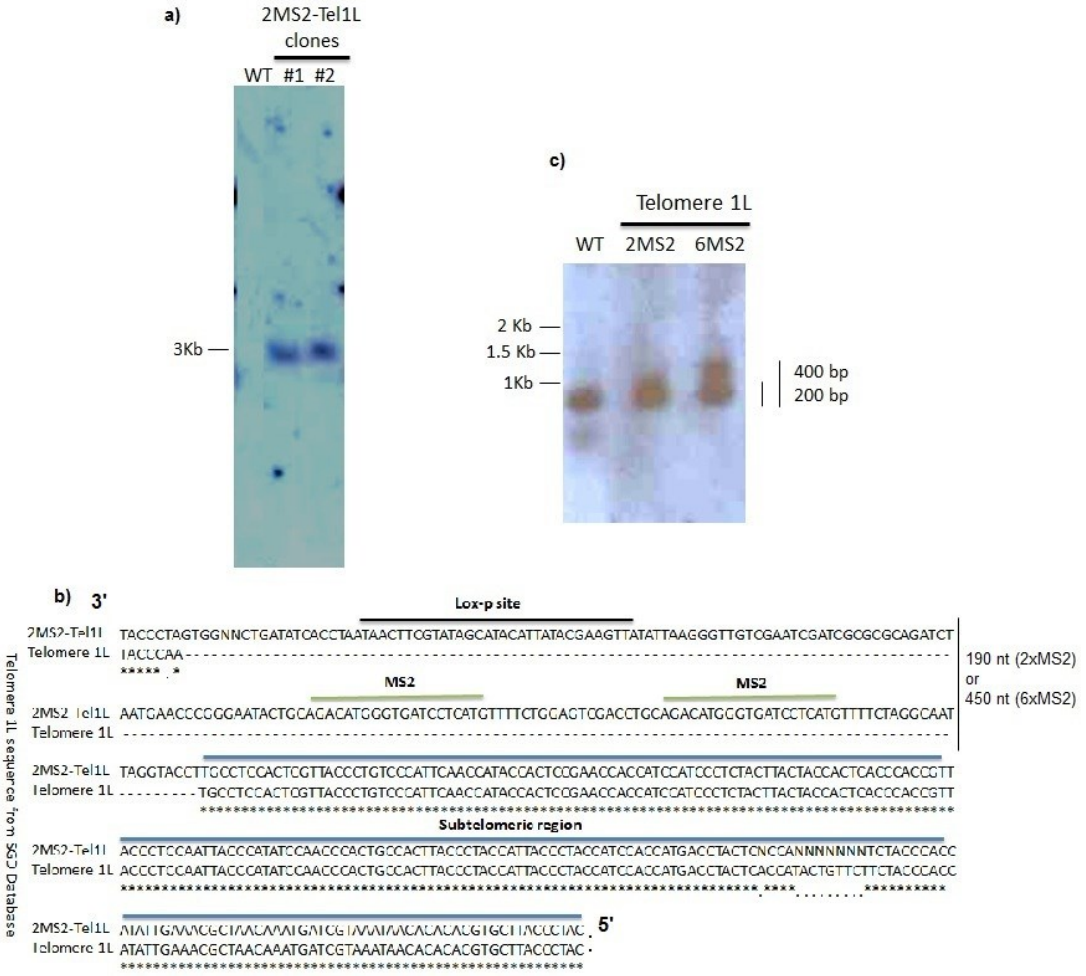

Figure 3.2 Creation and validation of the Tel1L-MS2 yeast clones. a) Southern blot analysis with MS2 probe of NcoI digested genomic DNA reveals a single integration at 3 Kb of the MS2 repeats in 2MS2-Tel1L clones, compared with WT cells. **b)** Sequence alignment of 2xMS2-Tel1L and WT telomere 1L show same subtelomeric sequence, with the integration of the MS2 sequences. **c)** Southern blot analysis with a Tel1L specific probe of XhoI digested genomic DNA to assess telomere length confirm that telomere length do not change more than 190 nt, as expected in the 2xMS2 clones (lane 2) and 450 nt of 6xMS2 clone (lane 3), compared to the WT (lane 1) size of 800bp. Note: Band at the same size as the WT telomere 1L is still visible in the Tel1L-MS2 clones due to the non-specific annealing of the probe to other telomeres. The clone creation and genetic validation was mostly done by the postdoc fellow in the laboratory Dr. Emilio Cusanelli.

To determine the localization of TERRA *in vivo* and to compare it with telomeres distribution, we labeled all the telomeres using the telomere-binding protein Rap1 fused to the mCherry fluorescent protein. This technique has previously been used by our laboratory and has been show to work well for telomere labeling purposes (L. C. Gallardo 2011).

Integration by homologous recombination of a mCherry tag at the C-terminus of Rap1 was carried out in the TERRA-MS2 clones; transformed colonies were confirmed by PCR to assess Rap1-mCherry insertion. Positive clones were then visualized by epifluorescent microscopy to confirm the expression of Rap1-mCherry, as well as to assess the localization of TERRA-MS2 trascripts by co-expression of MS2-GFP protein. A FY23 WT strain expressing both MS2-GFP and Rap1-mCherry fusion proteins was used as negative control. During this analysis, at least 300 cells were individually scored and characterized analyzing foci accumulation (with/without), foci localization in regard to the nucleus (perinuclear, cytoplasmic), and cell cycle stage (G1, early S, late S, G2, or M).

Microscopy analysis shows that TERRA-MS2 transcripts accumulate into a single perinuclear focus in all the clones tested. This perinuclear localization coincides with the already known perinuclear localization of individual telomeres (Doheny 2008). This pattern, characteristic of telomeres, can be appreciated in some of the small foci located at the nuclear periphery using Rap1-mCherry (yellow arrow, Figure 3.3a). No significant difference was observed among the clones from either telomere 1L or 6R. While the foci localization was not changed between 2x and 6xMS2 clones, a slight increase in the size and intensity of the foci was observed. This phenomenon was expected and is due to the higher number of MS2-GFP protein binding to the 6xMS2 stem-loops, which results in an increased sensitivity (Figure 3.3a). Cell counting revealed that only 10% of the cells in normal logarithmic growth conditions express TERRA, from either telomere 1L or 6R. In the control strain, only background fluorescence was observed, excluding the possibility of non-specific foci formation (Figure 3.3b). Although the majority of the foci shows a perinuclear localization, a small cytoplasmic fraction (~16%) was also observed. Cell-cycle analysis of the cells containing a focus shows that the majority of these cells are in G1, with the number of cells with a focus diminishing as cell cycle progresses (Figure 3.3c).

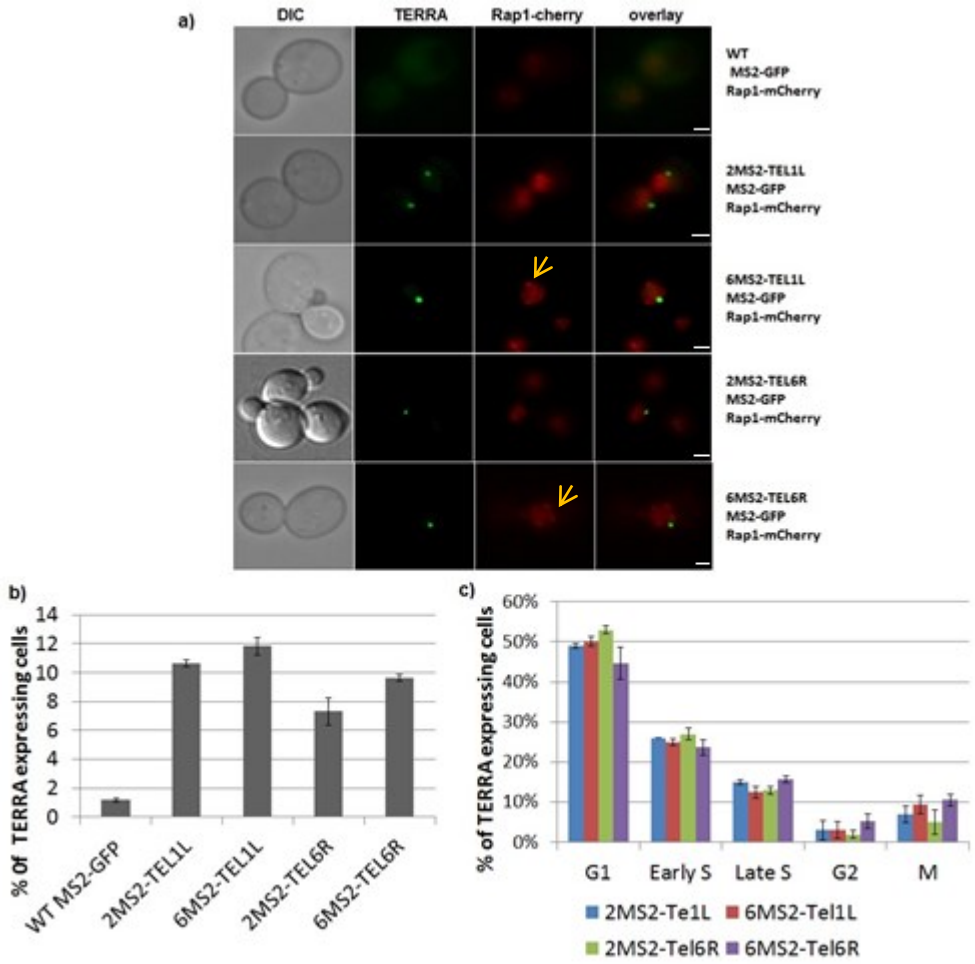

Figure 3.13 Characterization of TERRA-MS2-GFP foci. a) Microscopy analysis of the TERRA MS2-tagged clones reveals TERRA accumulating as a single perinuclear focus. TERRA-MS2-GFP foci are in green, mCherry-labeled telomeres are in red. Telomere clusters at the nuclear periphery are marked with a yellow arrow. In WT cells few or no foci formation was observed. Scale bar: 1 μm. **b)** Percentage of cells expressing TERRA foci in the various clones tested, a minimum of 300 cells were counted in each independent experiment (N=4). **c)** Cell-cycle distribution of cells expressing TERRA foci in the various clones tested, a minimum of 300 cells were counted in each independent experiment (N=4).

Although the reason why most of the cells containing a TERRA focus are in G1 is still unclear, we can see a very significant ($p < 0.0001$) decrease of cells with TERRA foci in late S and G2 phase compared to cells in G1. Late S and early G2 phase coincides with the end of DNA replication and telomeres elongation by telomerase in yeast cells (Dionne 1996) (L. C. Gallardo 2011). In human cells, TERRA has also been shown to be a natural ligand of human telomerase (Redon 2010), and TERRA levels accumulate in early G1, drop in late S phase and reach their lowest expression as cell progress from late S to G2

(Porro 2010), (Feuerhahn 2010). Our results show a very similar pattern as the one observed in human cells, therefore it could be possible that TERRA represses telomerase in yeast at early cell cycle stages and this may then explain the decrease of TERRA foci in late S and G phase of the cell cycle.

3.2 MS2-GFP labeling of TERRA does not affect TERRA foci expression, formation, localization, and stability

Before being able to use the MS2-GFP system as a tool to study TERRA expression in yeast cells, the system has to be validated. For this reason, we first determined if the addition of MS2 stem-loops and MS2-GFP into TERRA do not affect its expression, localization, foci formation and stability (Querido 2008).

First, we determined if TERRA-MS2-GFP foci that we observe by live cell imaging correspond to endogenous TERRA foci, and are not a cloning or microscopy artifact. For these purpose, we performed a co-localization study by using Fluorescent In-Situ Hybridization (FISH) to detect endogenous TERRA in the TERRA-MS2 clones. This technique has already been successfully used in the laboratory to validate the use of MS2-GFP system for tagging yeast telomerase RNA *TLC1* in fixed cells (C. Gallardo 2011). This will allow us to confirm if the MS2-GFP labeled foci we observe (in green) at the microscope correspond to real TERRA foci that can be seen by FISH (in red). If this is the case, we should observe the co-localization of both foci in the cell resulting in a yellow signal.

The study was performed in exponential growth conditions, using the Tel6R- and Tel1L-TERRA MS2-tagged clones expressing MS2-GFP, but without the mCherry-tagged Rap1, since FISH analysis with Rap1-mCherry expressing clones were found to cause microscopy artifacts such as higher background due to the overlapping spectra of the Red (Texas red and cy3) filters. The co-localization study was carried out in the MS2-TERRA clones expressing MS2-GFP fusion protein (in green), using an Cy3-labeled-MS2 specific

FISH probe (in red), and the DNA was labeled with DAPI (4',6-diamidino-2-phenylindole) a DNA binding fluorescent dye (in blue). WT cells expressing MS2-GFP fusion protein but with no MS2 loops in the TERRA sequence was used as control.

When FISH was performed using TERRA clones containing only 2 MS2 stem-loops, very low signal was observed, making the signal/noise ratio too low to appreciate a good TERRA foci signal. This might be due to the annealing of a single MS2 probe to the 2xMS2 sequence, making its detection more difficult. Nevertheless, when FISH was performed on TERRA clones containing 6 MS2 stem-loops, a brighter fluorescent signal was observed for the TERRA-MS2 foci, making their detection easier to visualize from the background noise. This experiment revealed co-localization between MS2-GFP (yellow arrows) and TERRA-MS2 FISH foci (white arrows), confirming that the MS2-GFP foci seen in live cells studies correspond to genuine TERRA RNA foci. As observed in live cell studies, TERRA localization under normal growth conditions is perinuclear for both 6xMS2-Tel1L and 6xMS2-Tel6R clones (Figure 3.4). Note that the FISH protocol was modified to allow the preservation of the MS2-GFP signal to allow the possibility for co-localization studies (for detailed modifications see chapter II).

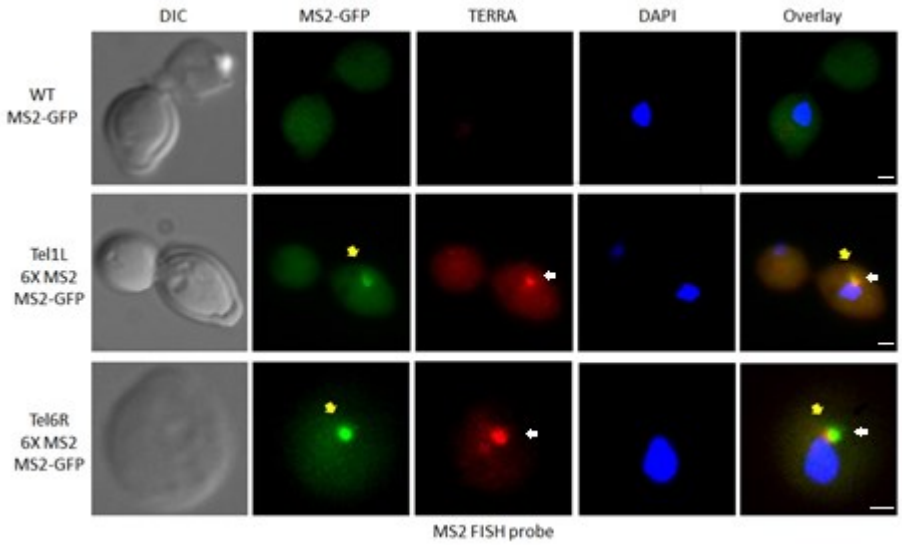

Figure 3.24 MS2-GFP and TERRA-MS2 foci co-localize. FISH analysis demonstrates that MS2-GFP foci (yellow arrows) co-localize with TERRA-MS2 FISH foci (white arrows), in both Tel1L and Tel6R 6xMS2 TERRA clones. WT+MS2-GFP: control strain. MS2-GFP: TERRA-MS2-GFP foci (green); TERRA: MS2 FISH probe (red); DAPI: nuclear DNA (blue). Scale bar: 1 μm.

To confirm that the TERRA-MS2 foci observed by FISH is able to form in the absence of the MS2-GFP fusion protein, and is not the result of unspecific aggregation of the MS2-GFP fusion protein instead of an interaction with genuine TERRA RNA, we performed FISH analysis with the MS2 FISH probe (in red) on the MS2-TERRA tagged clones without the expression of MS2-GFP fusion protein. Nuclear DNA was labeled with DAPI (in blue). At least 500 cells were counted to quantify the expression of TERRA foci for each independent experiment (N=3). The experiment shows that the TERRA-MS2 foci (white arrows) are also formed in the absence of the MS2-GFP protein in both 6xMS2-Tel1L and 6xMS2-Tel6R clones. Moreover, the perinuclear localization and expression levels of TERRA foci are not affected by the MS2-GFP protein. No foci were observed in WT cells using the MS2 FISH probe (Figure 3.5).

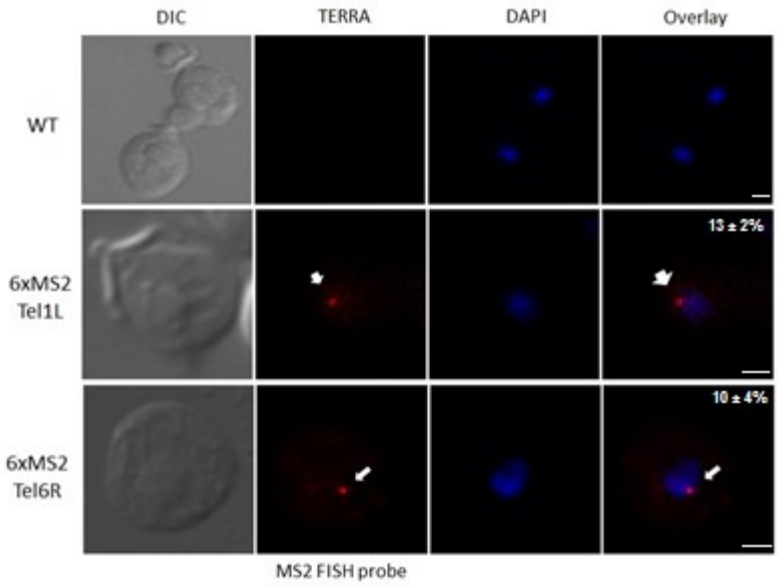

Figure 3.25 TERRA-MS2 foci formation occurs independently of the MS2-GFP fusion protein. TERRA foci (white arrows) display perinuclear localization in the MS2-TERRA tagged clones lacking MS2-GFP expression as shown by the MS2 FISH probe. Quantification of the number of foci observed with the MS2 FISH probe (superior-right corner of the overlay) indicates a similar level of TERRA expression as the one measured using live cell analysis. TERRA is in red by MS2 FISH probe, DNA in blue by DAPI. Scale bar: 1 μm. A minimum of 500 cells were counted in each independent experiment (N=3).

To further validate our observation of the TERRA-MS2 foci and their localization, and determine that they are not artifacts of the MS2 stem-loops integrated in the endogenous TERRA, we performed FISH analysis using Cy3-labeled probes to detect

endogenous TERRA from telomere 1L (green arrows) and telomere 6R (yellow arrows) (Figure 3.6). This experiment was performed in FY23 WT cells, with no modifications. As control, and to ensure that TERRA foci formation is RNA-dependent, an RNAse treatment was performed before probe hybridization. This experiment confirms the expression of endogenous TERRA from telomeres 1L and 6R in a small population of cells. It also confirmed that TERRA foci formation is RNA-dependent, and that it has perinuclear localization, as observed with the MS2-GFP system (Figure 3.6).

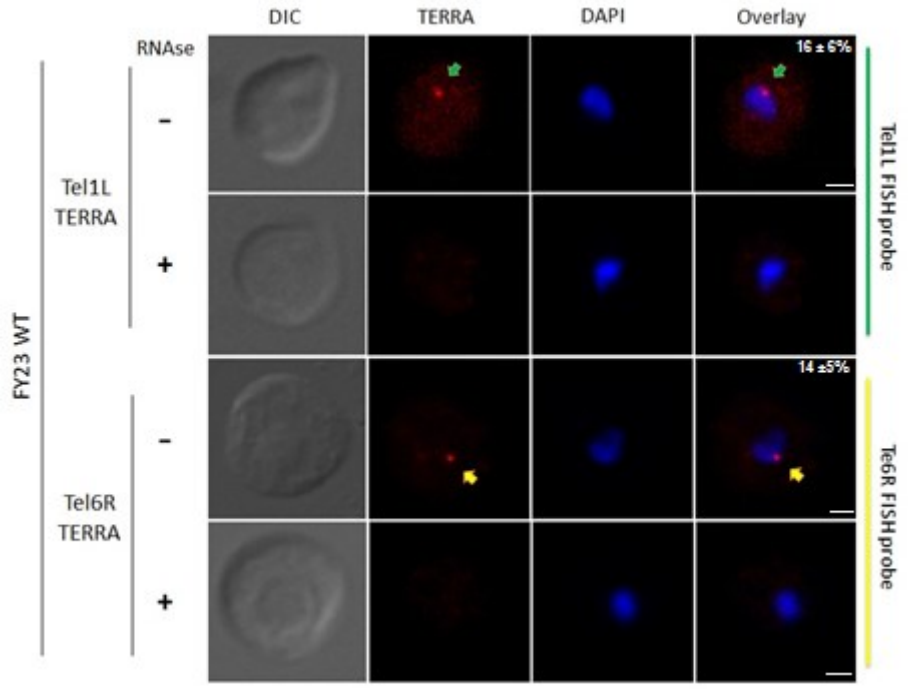

Figure 3.6 Detection of endogenous Tel1L- and Tel6R-TERRA in WT cells. FISH analysis on endogenous Tel1L- and Tel6R-TERRA using TERRA specific FISH probes confirmed the perinuclear localization of TERRA foci. RNAse treatment analysis demonstrates that Tel1L-TERRA foci (green arrows) and Tel6R-TERRA foci (yellow arrows) can only be formed on the presence of integral RNA. Quantification of the number of foci observed (superior-right corner of the overlay) indicates a number of TERRA foci very similar to the number measured with the MS2 FISH probe or the MS2-GFP labeled TERRA. TERRA foci are in red by Tel1L or Tel6R FISH probe, DNA in blue by DAPI. Scale bar: 1 μm. A minimum of 500 cells were counted in each independent experiment (N=4).

FISH is a useful technique since it also allows the quantification of single RNA if probes labeled with different dyes are used to control for the quality of the FISH procedure and clonal differences (S. Z. Larson 2009), (Trcek 2012). To confirm the low expression levels of TERRA foci as observed in our FISH studies and by live cell imaging, we

performed a quantitative FISH (qFISH) analysis using probes with different dyes to control for FISH quality. The probe used for this purpose was a Cy5-labeled U3 probe, which detect the small nucleolar RNA U3 present in the nucleolus of all yeast cells. This probe will allow us to perform a more accurate quantification analysis of TERRA foci in the yeast population. The U3 probe was used in combination with the endogenous Cy3-labeled Tel1L and Tel6R FISH probes in WT cells, and the Cy3-labeled MS2 FISH probe in the 6xMS2-TERRA tagged clones to quantify the number of TERRA foci and account for possible cell-to-cell variation in the spheroplasting of the yeast during FISH procedure. The nuclear DNA was labeled with DAPI. After image acquisition and analysis, a minimum of 1000 cells were scored for: number of cells with TERRA foci, localization of the foci (perinuclear, cytoplasmic, nucleoplasmic and nucleolar), as well as its cell cycle stage (G1, early S, late S, G2, or M).

Quantitative FISH analysis confirmed the small number of cells expressing a TERRA focus which account for only 13% of the cell population. Interestingly, no significant difference (p 0.7606) was observed between the number of cells containing a TERRA focus quantified in previous FISH analysis versus the quantitative FISH analysis. Most importantly, the quantification of TERRA foci between the live cell imagining assay (based on the MS2-GFP system) and the quantitative FISH analysis did not show any significant difference (p 0.0984), validating the use of the MS2-GFP system as a quantitative method for studying TERRA expression (Figure 3.7).

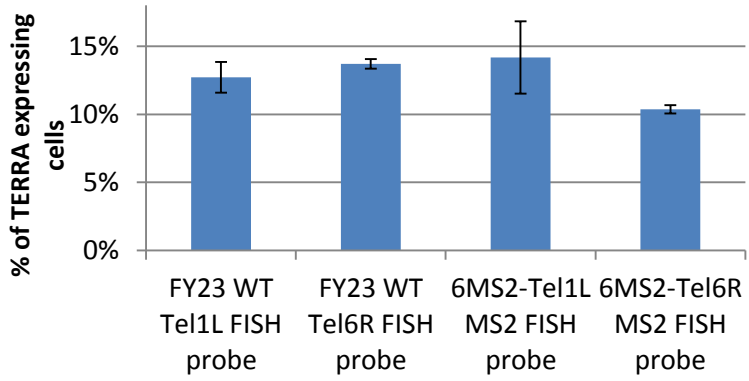

Figure 3.7 Quantification of TERRA foci by qFISH. Quantitative FISH analysis demonstrates that only about 13% of the cell population expresses a TERRA focus regardless of the FISH probe used for the analysis. A minimum of 300 cells were counted in each independent experiment (N=2).

Cell cycle analysis of these FISH results confirmed a very similar pattern ($p > 0.05$) as the one seen by live cell imaging, showing that the majority of the cells expressing TERRA foci are in G1 (56%) and early S (27%), with their number progressively decreasing during G2 and M phases (Figure 3.8). Additional experiments performed in synchronized cells will allow to validate these results, providing further information on the regulation of TERRA foci formation during cell cycle. (L. C. Gallardo 2011).

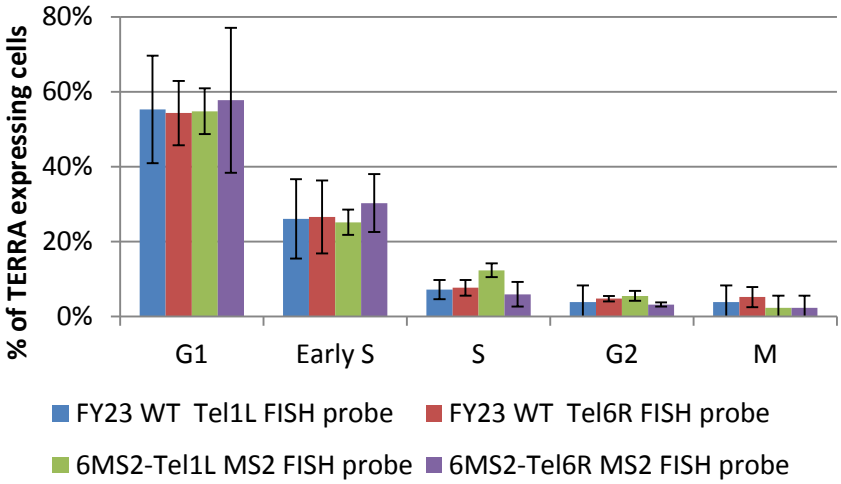

Figure 3.8 Cell cycle distribution of cells expression TERRA foci by qFISH. Quantitative FISH analysis demonstrates that TERRA foci are present in higher percentage in G1 and early S phase cells, and that their presence diminishes as the cell cycle progress, reaching its lower levels in G2 and M phases. A minimum of 300 cells were counted in each independent experiment (N=2).

A more accurate characterization of TERRA foci localization was performed by 2D (two-dimensional) image analysis (maximum intensity projection) of the qFISH images. This analysis confirmed that the majority of TERRA foci are perinuclear (Figure 3.9a), with a small but significant ($p < 0.001$) fraction, 18% of the cells, presenting a cytoplasmic TERRA focus, as was also seen by live cell imaging. Interestingly, a significant ($p < 0.05$) but small (~ 8%) percentage of TERRA foci was found in the nucleolus and the nucleoplasm (Figure 3.9b). It is important to note that there was no significant difference ($p > 0.45$) in the quantification of the foci between the different FISH probes used to detect TERRA (Tel1L, Tel6R and MS2 FISH probes) or clones used for the study (WT, 6xMS2-Tel1L, 6xMS2-Tel6R).

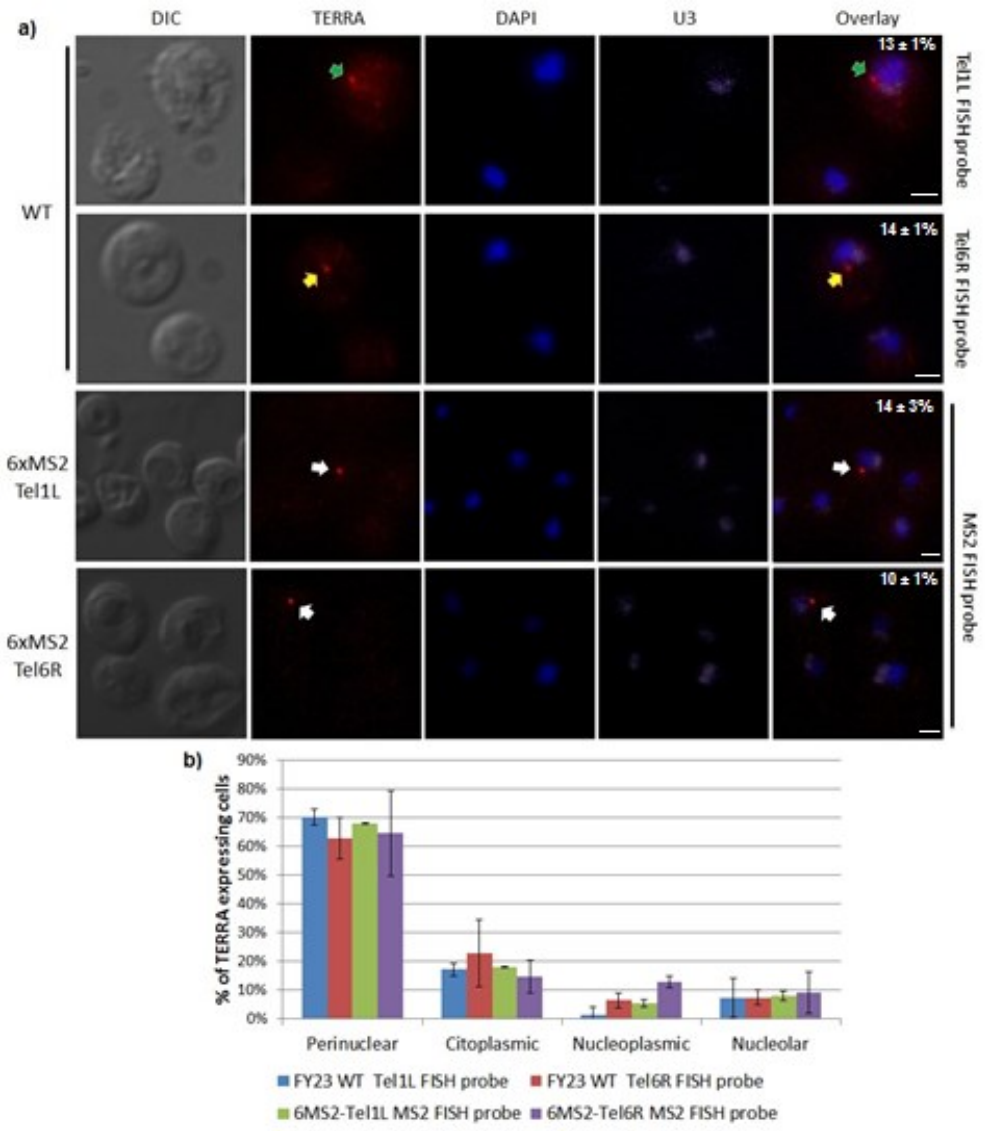

Figure 3.9 Characterization of qFISH on TERRA by 2D image analysis. a) Quantitative FISH analysis shows low percentage of TERRA foci on cell population (superior-right corner of the overlay). TERRA foci are in red by Tel1L- or Tel6R-TERRA FISH probe in FY23 WT yeast cells, or by MS2 FISH probe in Tel1L or Tel6R 6xMS2-TERRA-tagged clones. Nuclear DNA in blue, by DAPI. Nucleolus is in light purple, labeled by U3 RNA FISH probe. Scale bar: 1 μm. **b)** Characterization of TERRA foci localization with the different FISH probes used to label TERRA on this study. A minimum of 300 cells were counted in each independent experiment (N=2).

To find out if the small percentage of TERRA foci in the nucleolus and nucleoplasm was significant or an artifact generated by studying 2D image projection of 3D (three-dimensional) structures, we carried out an in-depth characterization of the foci localization by studying the acquired images in a 3D context. The nucleoplasmic and nucleolar foci seen in 2D were further characterized into perinuclear, nucleoplasmic, perinucleolar,

nucleolar in a 3D context (Figure 3.10a). This new characterization allowed us to discriminate foci that were wrongly characterized in 2D, leaving us with a much more accurate localization of the TERRA foci. This analysis confirmed that ~73% of the foci have perincuclear localization, with a small cytoplasmic fraction (18%). These results are very similar (p values >0.08) to the data obtained in our live cell studies. However, the 3D characterization of TERRA foci allowed us to determine that the nucleoplasmic (4%), perinucleolar (2%) and nucleolar (2%) fractions found in the 2D study may not have a specific biological significance (p values >0.0523), since the percentages found by 3D study were too low to discriminate them from background signal.

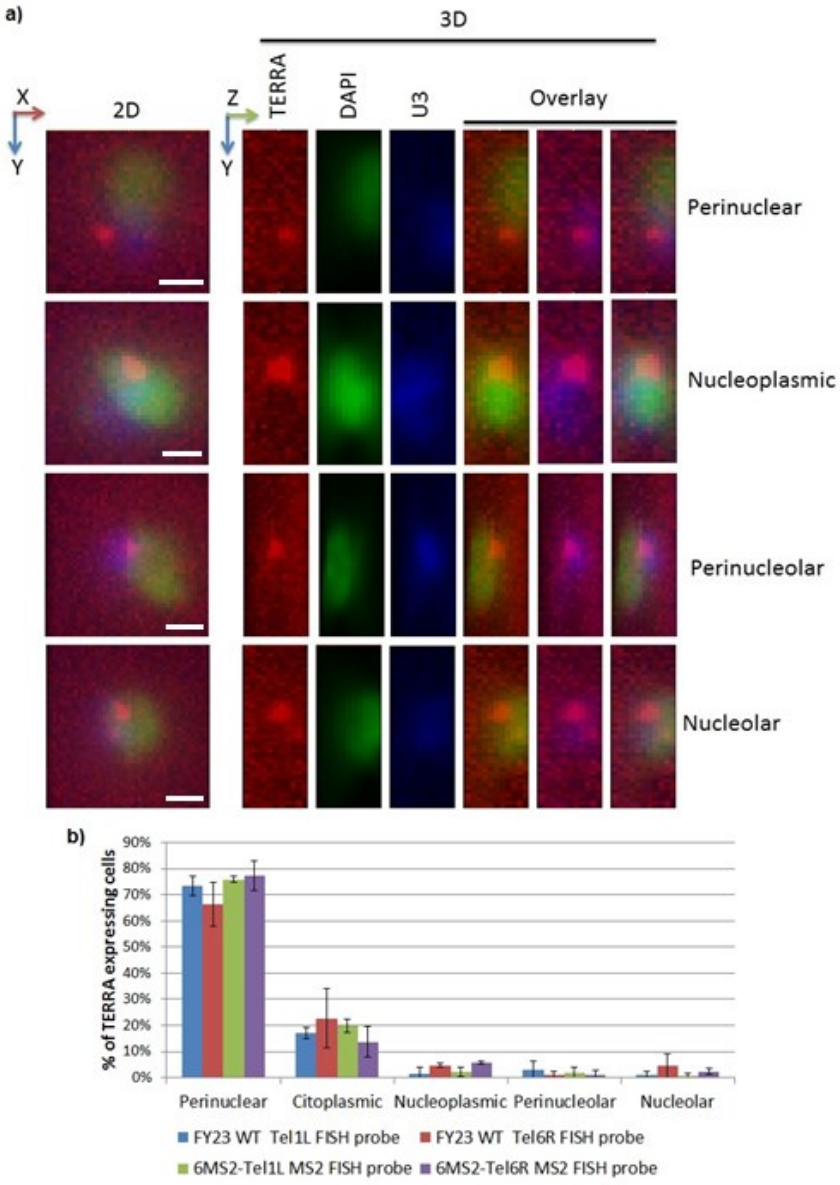

Figure 3.210 Quantitative FISH 3D image analysis characterization. a) 3D analysis revealed how a 3D perception of a body might change the localization criteria from the 2D projection of it. Examples of how TERRA foci localization can be perceived differently from 2D to 3D analysis can be seen in each panel: perinuclear, nucleoplasmic, perinucleolar, nucelolar. TERRA foci is in red. Nuclear DNA is in green, by DAPI. Nucleolus is in blue, labeled by U3 RNA FISH probe. Scale bar: 1 μm **b)** 3D analysis made easier the re-localization of some of the foci which were perceived wrongly in other categories, these also allowed us to discover that the nuclear, perinucleolar and nucleolar localization of TERRA do not have a biological significance. A minimum of 100 cells were counted in each independent experiment (N=2).

Finally, after we showed that the MS2-GFP system does not affect TERRA foci formation, quantification and localization. One last question left for us to validate the use of

the MS2-GFP system was if it does not affect TERRA RNA stability. This is an important question since the addition of stem-loops to a RNA can affect its stability, either by blocking its degradation, or by making it more accessible to degradation factors (Godlman 2005). It is known that in yeast, TERRA is degraded by 5'-3' exonuclase Rat1 (P. R. Luke 2008). The presence, in TERRA, of MS2 stem-loops tightly associated with MS2-GFP proteins, may block the progression of the Rat1 exonuclease, leading to the stabilization and accumulation of TERRA's 3' end.

To confirm that the stability or integrity of the MS2-GFP labeled TERRA is not affected, we performed an immunoprecipitation (IP) assay to enrich and detect the endogenous TERRA-MS2 RNA by quantitative RT-PCR. Advantageously, the MS2-GFP system allows us to IP the MS2-tagged RNA by using an anti-GFP antibody. Immunoprecipitation was carried in the 6xMS2-Tel1L and 6xMS2-Tel6R clones expressing MS2-GFP or not, and in WT cells, with or without MS2-GFP expression, and mock IP (without antibody) as controls. After IP, we detected the presence of the 5' and 3' ends RNA of endogenous TERRA transcripts by quantitative RT-PCR. As control, an RT-PCR reaction without reverse transcriptase (-RT) was performed to eliminate the possibility of artifact amplification from genomic DNA. RT-qPCR results were analyzed measuring the FOLD of enrichment of TERRA in the IP by comparing the signal difference between the INPUT fractions versus IP fractions.

The IP/RT-PCR experiments reveal that we can detect both 5' and 3' ends of endogenous TERRA by qPCR in the 6xMS2-tagged clones which express MS2-GFP protein but not in the controls. This experiment confirmed the interaction between MS2-tagged TERRA and MS2-GFP fusion protein, and also demonstrated that the MS2-GFP protein associated with TERRA molecules containing their 5'end and their 3' end (Figure 3.11 a, b). The difference in FOLD enrichment between the 5' and 3' ends of TERRA in our study could be due to IP enrichment difference as well as differences in primer efficiency in the RT-qPCR analysis.

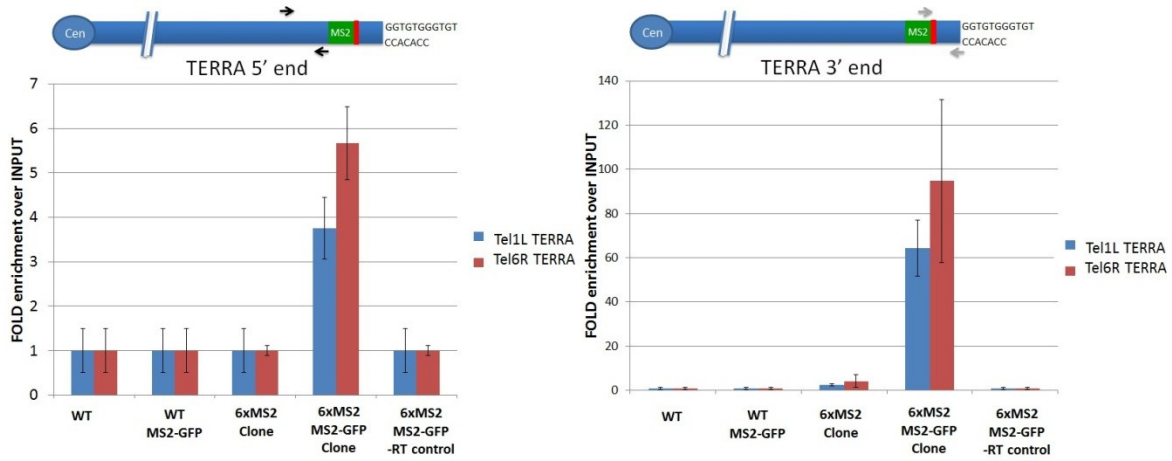

Figure 3.211 TERRA stability is unaffected by the MS2-GFP system. IP followed by RT-qPCR analysis confirmed that MS2-tagged TERRA interacts with the MS2-GFP fusion protein without affecting its stability. **a)** Different primers 80nt and 300nt from the MS2 repeats were used to assess the 5' end state, similar FOLD enrichment levels and exclusive signal in both Tel1L/Tel6R MS2 TERRA-tagged clones expressing MS2-GFP regardless of the primers used. **b)** TERRA's 3' end of TERRA show a similar excusive signal in both MS2-tagged clones expressing the MS2-GFP protein. No signal was observed in both TERRA ends in any of the controls used for the IP: WT cells with or without MS2-GFP expression, the 6xMS2-tagged TERRA clones with removed MS2-GFP expressing vector, minus RT-PCR reaction, and the mock IP incubated without antibody showed no unspecific binding noise.

Altogether, these results validate the use of the MS2-GFP system to study the expression of endogenous TERRA from a single telomere in a single cell, allowing us to perform live-cell imaging which will help to elucidate the function of TERRA in yeast cells.

3.3 TERRA interacts with the telomerase (*TLC1*) RNA *in vivo*

Previous studies in human cells have shown that both human telomerase reverse transcriptase (hTERT) and telomerase RNA (hTR) interact with TERRA *in vivo* (Redon 2010). To determine if yeast telomerase also interacts with TERRA, we decided to use our TERRA-MS2 immunoprecipitation assay, in order to enrich endogenous TERRA.

We performed a series of IP experiments in normal exponential growth conditions. First, we immunoprecipitated TERRA from the Tel1L- and Tel6R-6xMS2 clones expressing MS2-GFP, and detected the presence of the *TLC1* RNA by RT-qPCR. In these

samples, as control we measured the FOLD enrichment of MS2-tagged Tel1L- and Tel6R-TERRA after immunoprecipitation and RT-qPCR (Figure 3.12a). Once TERRA enrichment in the IP was confirmed, we measured *TLC1* RNA by RT-qPCR using specific *TLC1* primers. FOLD of enrichment was estimated calculating IP/INPUT ratio using actin (*ACT1*) primers for relative quantification. As controls, we used 6x-MS2 tagged clones which do not express MS2-GFP protein, WT cell which express MS2-GFP protein, and mock IP (without antibody). As controls for the RT-qPCR, reactions without reverse transcriptase were performed to show that the amplification is RNA dependent.

This experiment shows that the yeast telomerase (*TLC1*) RNA interacts with endogenous TERRA *in vivo*, as we detected an enrichment of *TLC1* RNA only in presence of MS2-tagged TERRA and MS2-GFP fusion protein, and not in any of the controls, which confirmed the specificity of the interaction (Figure 3.12b).

If *TLC1* and TERRA interact *in vivo,* then we should be able to validate this interaction by performing the reverse experiment, in which instead of pulling down TERRA and measuring *TLC1* RNA enrichment by RT-qPCR, we immunoprecipitate the *TLC1* RNA and measure the enrichment of TERRA by RT-qPCR. The experiment was performed by immunoprecipitation of the 10xMS2-tagged *TLC1*-RNA in the strain expressing MS2-GFP fusion protein, which was created and validated by a previous student (L. C. Gallardo 2011) (O. D. Gallardo 2008) (C. Gallardo 2011). Wild-type cells (W303 background) with no MS2 stem-loops in the *TLC1* gene, but expressing the MS2-GFP fusion protein, was used as control. A mock IP (without antibody) was used as IP controls. -RT reaction and actin (*ACT1*) housekeeping primers (relative quantification) were used as RT-qPCR controls. Endogenous *TLC1*-10xMS2 RNA was highly enriched in our IP experiment, as we detected only the 10xMS2 tagged *TLC1* RNA but not the untagged *TLC1* WT RNA (Figure 3.13a).

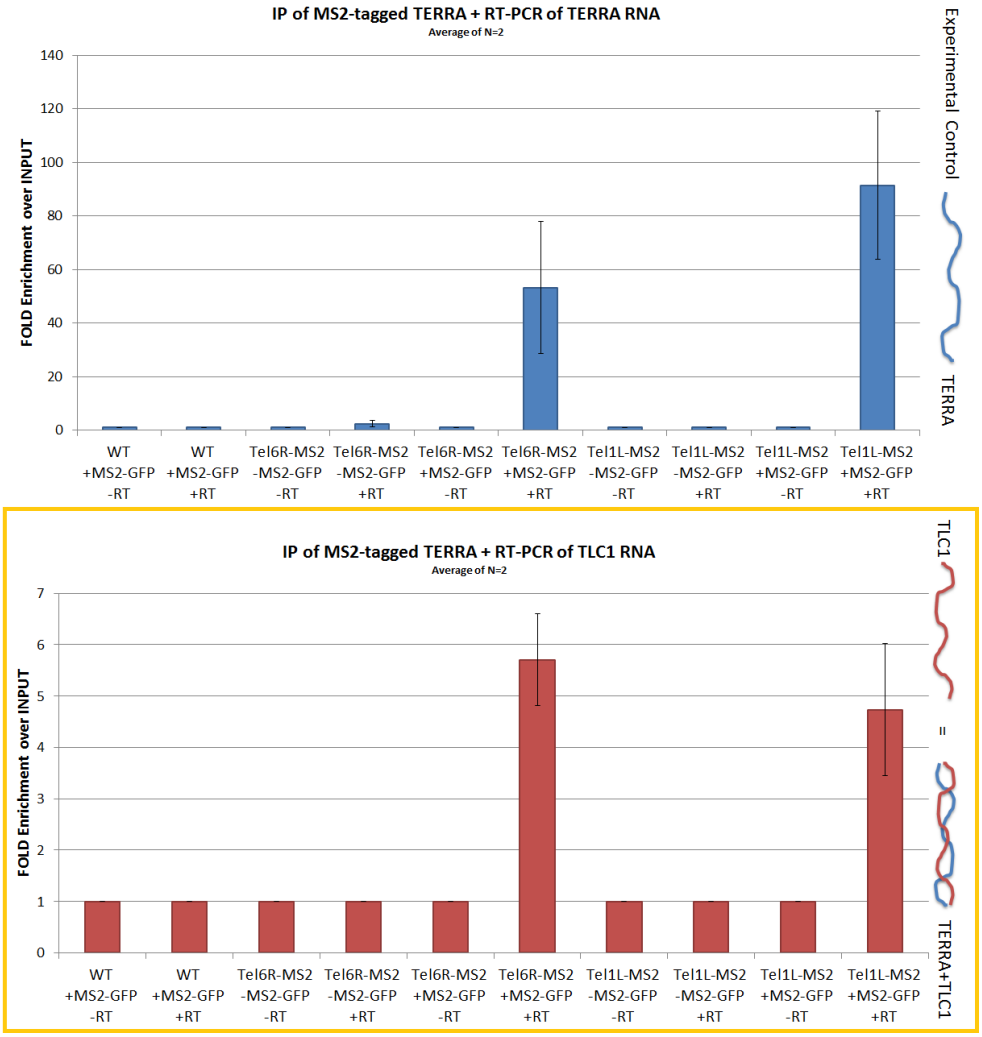

Figure 3.12 Telomerase RNA interacts with endogenous TERRA *in vivo*. IP of TERRA-Tel1L- or Tel6R-6xMS2-tagged and MS2-GFP expressing clones was performed. **a)** TERRA's IP FOLD enrichment over INPUT by RT-qPCR was used as a control to show successful TERRA pull down. **b)** A significant TLC1 FOLD enrichment was visible only on the fractions were TERRA was successfully pulled down. No unspecific interaction were observed on the IP controls (WT cells with MS2-GFP expression, 6xMS2 clones with removed MS2-GFP expressing vector, bids incubated without antibody) and RT-qPCR control (minus reverse transcriptase reaction and actin housekeeping primers used for relative quantification). N=3

Once the 10xMS2-tagged *TLC1* RNA was successfully pulled down by an anti-GFP antibody, the presence of TERRA in the pellet was assessed by specific RT-qPCR primers designed to detect TERRA expressed from Tel1L, Tel6R and from telomeres containing Y' long sub-telomeric repeat elements. This experiment shows that TERRA from different telomeres was enriched exclusively in the IP of *TLC1*-10xMS2 RNA, which confirmed the

specific of the interaction between *TCL1* RNA and TERRA *in vivo* from different telomeres regardless of clonal (MS2-tagged clones for TERRA and TLC1) and genetic background (FY23 and W303) (Figure 3.13b).

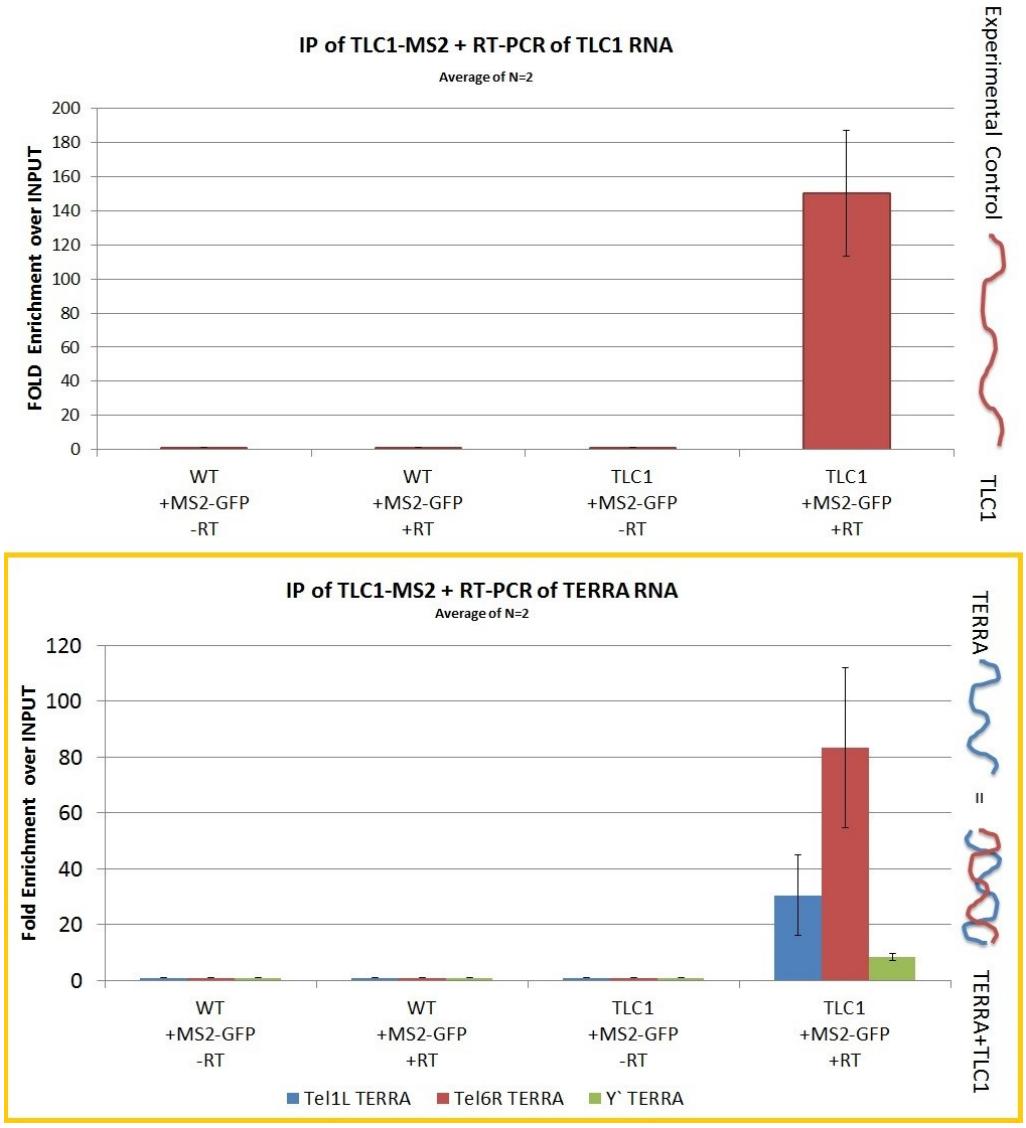

Figure 3.13 TERRA expressed from different telomeres interact with endogenous telomerase *in vivo*. a) IP of TLC1 using the MS2-GFP system as a tool allowed us to highly enrich TLC1 in the IP fractions of only the 10xMS2 TLC1 tagged TLC1 expressing the MS2-GFP protein. **b)** A significant FOLD enrichment of TERRA from different telomeres including Tel1L, Tel6R and telomeres containing Y' was observed, confirming endogenous TERRA and TLC1 interaction *in vivo*. Note: The IP controls (WT 303 cells with MS2-GFP expression, and bids incubated without antibody) and RT-qPCR control (minus reverse transcriptase reaction and actin housekeeping primers used for relative quantification) show no detectable non-specific interaction. N=2

To determine if TERRA interacts with the active telomerase, we performed immunoprecipitation experiments using the reverse transcriptase subunit of telomerase, the Est2 protein with and 18-Myc-tag. Although we were able to find a significant enrichment of telomerase *TLC1* RNA in the Est2 IP samples, we were unable to find enough levels of TERRA enrichment to discriminate from background noise (N=4, data not shown). Therefore, these results are not conclusive, since the absence of TERRA might be an experimental artifact due to an asynchronous cell population. Although we know that Est2 protein and *TLC1* RNA are associated throughout most of the cell cycle their binding peak is reached in G1, and S phase (L. C. Gallardo 2011) (Tuzon 2011) which might result in low levels of *TLC1* enrichment in unsynchronized cells experiments. So this experiment should be repeated in a synchronized cell population to determine if TERRA interacts with active telomerase, or just its RNA component.

Also, to determine if the interaction between TERRA and *TLC1* RNA's is DNA dependent, we performed a series of experiments using DNAse treatment prior to IP. Unfortunately, due to technical issues (RNA degradation during experiment), we were unable to obtain reliable results (data not shown). Other experimental approaches, such as chromatin-immunoprecipitation (ChIP) assays using the MS2-GFP system could be helpful in order to answer this question. Nevertheless, these experiments demonstrate an interaction between telomerase RNA and TERRA, which strongly suggest that TERRA might be a natural telomerase RNA ligand of telomerase in yeast, as it has already been shown by *in vitro* experiments in human cells (Redon 2010).

In order to confirm that TERRA could interact transiently with the *TLC1* RNA we performed a FISH co-localization experiment, using the foci signal seen in the 6xMS2-Tel6R TERRA tagged cells expressing the MS2-GFP fusion protein (in green), the *TLC1* FISH probes (in red), and nuclear DNA staining using DAPI (in blue) (Figure 3.14). The *TLC1* RNA FISH probes have been previously validated to detect the *TLC1* RNA by quantitative FISH analysis (C. Gallardo 2011) (O. D. Gallardo 2008). *TLC1* RNA was found to accumulate as clusters (6 to 8 more commonly) in all the yeast cells.

This approach enabled us to detect TERRA (white arrow) and *TLC1* RNA (yellow arrowhead) localization simultaneously in the same cells, which allowed us to determine if

both foci co-localize, are separated, or are side by side. By counting the number of TERRA foci in respect to *TLC1* RNA foci, we were able to find that TERRA and *TLC1* RNA foci co-localize only in 38% of the cells counted. Interestingly, we were able to find that TERRA and *TLC1* RNA co-localization occurs mostly in G1 phase, since more than 55% of the G1 phase cells present TERRA foci (Figure 3.14).

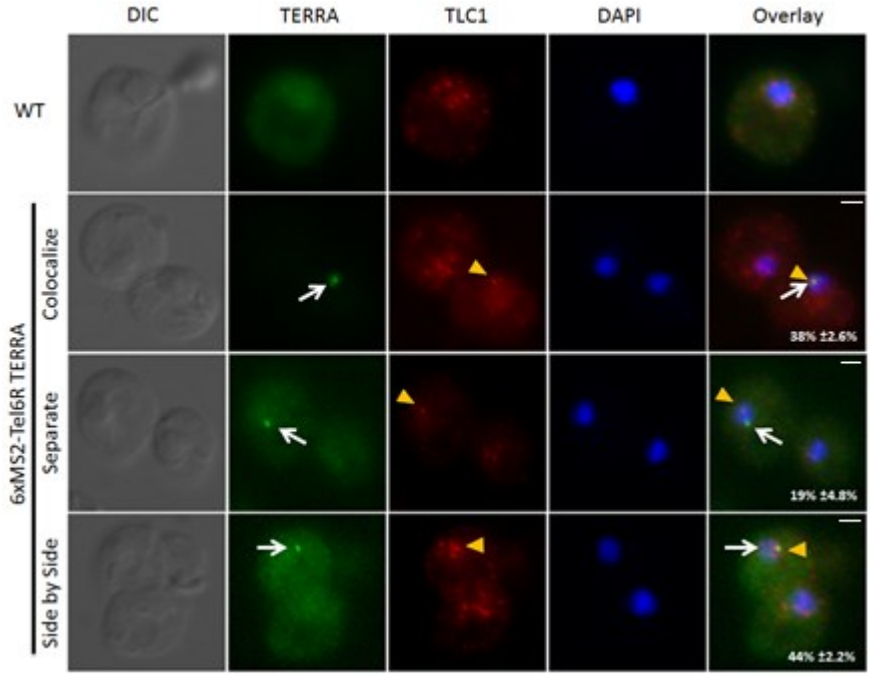

Figure 3.14 TERRA and *TLC1* RNA partially co-localize. Imaging analysis to detect TERRA MS2-GFP foci (in green and white arrow) and *TLC1* RNA foci using FISH probe (in red and yellow arrowheads). Phenotypes were scored as: colocalized, separate or side by side, and quantified (lower left corner of overlay). A minimum of 300 cells were counted in each independent experiment (N=2).

This experiment suggests a partial co-localization between TERRA and *TLC1* RNA, with co-localization happening mostly in G1 phase. A more in-depth analysis during the cell cycle by using synchronized cells and FISH studies could help to better understand the interaction between these two RNAs. We also developed the possibility to image this interaction in living cells by using the MS2 and PP7 systems to be able to label both TERRA and *TLC1* RNA with two different fluorescent proteins. We describe this system to simultaneously image TERRA and *TLC1* RNA in single living cells in the next chapter.

These experiments suggest that TERRA can be a possible ligand of the telomerase RNA component TLC1, as it might transiently interact with TLC1 in G1 phase cells, when

telomerase is known to be repressed or in an inactive state in human (Feuerhahn 2010) and yeast (O. D. Gallardo 2008) cells; these experiments also suggest a possible role of TERRA as inhibitor of telomerase in yeast cells, as it has been previously proposed in human cells (Redon 2010). It is important to note that Redon and co-workers used an *in vivo* IP TLC1 as a substrate for the *in vitro* assay where then they added TERRA-like oligos to demonstrate their inhibitory potential, our IP studies strikingly show that TERRA is already present in a little fraction of TLC1 IP *in vivo.* So it will be bold but interesting to propose that TERRA as a natural TLC1 ligand might not play an inhibitory telomerase role as has so far been proposed but might also play another yet un-described role in telomerase biology.

Indeed, we were able to show that TERRA plays an important in the spatial organization of *TLC1* RNA, in which TERRA acts as a scaffold for the nucleation of active telomerase clusters (T-Recs), which then is recruited to short telomeres. These results are presented in the next chapter.

Chapter IV

TERRA induced by telomere shortening assembles telomerase molecules at short telomeres

Emilio Cusanelli, Carmina Angelica Perez Romero, Pascal Chartrand

Paper Submitted

Authors' contribution:

Emilio Cusanelli: manuscript writing, MS2-clones tagging and genetic validation (FigS1 a,b,e,f), two-color co-localization live cell imaging of TERRA Tel6R/Tel1L or Tel6R-TERRA/telomere6R or Tel1L-TERRA/telomere6R (Fig1 b,c, Fig3 a,b, Fig4 g, FigS2, FigS7 c), telomerase KO experiments (Fig2 a,b, FigS3 a,b), telomere shortening (Fig c,d, FigS4), ChIP (Fig3 c,d), qPCR expression analysis (FigS5)

Carmina Angelica Perez Romero: FISH analysis (Fig1 a, Fig S1 c,d) TERRA/TLC1 IP experiments (Fig4 a,b, FigS6), three-color co-localization live cell imaging of Tel6R-TERRA/TLC1/telomere6R (Fig4 e,f, FigS7 a), T-recs foci formation observation, analysis and controls (Fig4 c,d, FigS7 b), video generation (movie S1, S2, S3, S4) and figures review

Pascal Chartrand: project supervisor, article and figures review, TERRA model creation (Figure 7.1)

TERRA induced by telomere shortening assembles telomerase molecules at short telomeres

Emilio Cusanelli[1], Carmina Angelica Perez Romero[1], Pascal Chartrand[1,*]

[1]Département de Biochimie, Université de Montréal, Montréal, QC, H3C 3J7, Canada
*Correspondence:

Abstract: Elongation of short telomeres depends on the action of multiple telomerase molecules, which are visible as telomerase RNA foci or clusters associated with telomeres in yeast and mammalian cells. How multiple telomerase molecules are assembled on a short telomere is still unknown. Herein, we report that TERRA, a telomeric non-coding RNA, nucleates telomerase clusters at telomeres. TERRA expression is induced when a telomere shortens, leading to the accumulation of TERRA molecules into a nuclear focus. Time-lapse imaging of TERRA expressed from a single telomere reveals that TERRA acts as a scaffold for the recruitment of telomerase molecules to generate a telomerase cluster. This cluster is subsequently recruited to the short telomere from which TERRA transcripts originate. We propose that short telomeres express non-coding RNA to assemble and spatially organize telomerase molecules, for their subsequent recruitment on these telomeres.

One sentence summary: TERRA is expressed from short telomeres to promote telomerase clustering for subsequent telomere elongation

Telomerase is a specialized ribonucleoprotein complex which promotes telomere length homeostasis by adding telomeric repeats to the ends of chromosomes (*1, 2*). In *Saccharomyces cerevisiae,* telomerase is composed of an RNA molecule (*TLC1*), a catalytic reverse transcriptase (Est2) and associated proteins (Est1, Est3, yKu). In a yeast cell, telomerase preferentially elongates the shortest telomere (*3*), and this activity is predominantly detected during late S/G2 phase (*4*). Consistently, during late S phase multiple telomerase molecules cluster, forming T-Recs (Telomerase Recruitment clusters) which co-localize with a few telomeres (*5*). How telomerase clusters assemble is still unknown. Telomeres are transcribed in a strand specific manner generating G-rich telomeric transcripts known as telomeric repeats-containing RNA or TERRA (*6, 7*). The transcription of TERRA proceeds from the subtelomeric regions towards the chromosome ends and terminates within the telomeric-repeat tract, producing long non-coding RNA (lncRNA) heterogeneous in length. The biological role of TERRA remains largely elusive. Current evidence suggest that TERRA may inhibit telomerase activity by binding both telomerase RNA and telomerase catalytic subunit (*6,8*), regulate telomere structural maintenance and heterochromatin formation (*9, 10*), and mediate the exchange of single-strand telomere binding proteins during the cell cycle (*11*). In *Saccharomyces cerevisiae*, TERRA transcripts are actively degraded by the 5'-3' exonuclease Rat1 (*12*), which makes these transcripts poorly amenable to biochemical studies in wild-type (WT) yeast cells

To elucidate the function of TERRA in yeast, we adopted a cytological approach to detect endogenous TERRA expressed from a unique telomere at single cell resolution in wild-type yeast. TERRA expression was analyzed by RNA fluorescence in situ hybridization (RNA-FISH) by using oligonucleotide probes designed to detect TERRA molecules transcribed from telomere 1L (Tel1L-TERRA), telomere 6R (Tel6R-TERRA) or from Y'-element containing telomeres (Y'-TERRA). Interestingly, TERRA signal was detected as a discrete perinuclear focus, sensitive to RNAse treatment (Fig. 1A). While Tel6R-TERRA and Tel1L-TERRA formed a single focus, Y'-TERRA were mostly detected as double or multiple foci. Cell counting analyses showed that about 15% of cells express TERRA from either telomere 1L or telomere 6R, while 28% displayed Y'-TERRA foci. These results indicate that a small population of cells expresses TERRA from a

specific telomere at a given time. In order to study TERRA in living cells, we adapted an *in vivo* assay to detect endogenous TERRA from a single telomere by using the MS2-GFP system (*13, 14*). In this assay, two or six MS2 stem-loops were integrated at telomere 1L or telomere 6R, generating different TERRA-MS2 clones (validation experiments of TERRA-MS2 clones are shown in fig. S1). Interestingly, microscopy analyses of TERRA-MS2 clones revealed the formation of a single TERRA-MS2-GFP focus at the nuclear periphery in every clone analyzed (Fig. 1B). In agreement with the data obtained by RNA-FISH in WT cells, only a small percentage of cells (~10%) expressed TERRA-MS2-GFP foci from either telomere 1L or telomere 6R.

Since a similar percentage of cells express TERRA from either telomere 1L or telomere 6R, we investigated whether Tel1L-TERRA and Tel6R-TERRA are co-expressed in the same cells by tagging both telomeric transcripts using different *in vivo* detection systems. To this aim, yeast clones containing 2xMS2 repeats at telomere 1L and 12xPP7 repeats at telomere 6R (*15*) were produced (fig. S2). Live-cell imaging analyses revealed that among the cells expressing a TERRA focus (either Tel1L-TERRA or Tel6R-TERRA), 96% contained only a single TERRA focus, while 4% showed both Tel6R-TERRA and Tel1L-TERRA foci, detected as distinct perinuclear focus, which did not co-localize (Fig. 1C). These results indicate that TERRA expression is controlled independently by each chromosome end.

We formulated the hypothesis that TERRA expression could be induced at short telomeres. Therefore, TERRA levels were analyzed in *tlc1*Δ cells, which contain short chromosome ends. RT-qPCR analysis showed upregulated levels of TERRA in *tlc1Δ* cells compared to WT cells, for all the telomeres analyzed (Fig. 2A). Moreover, exogenous expression of *TLC1* RNA restores TERRA expression in a *tlc1Δ* strain to WT levels (Fig. 2A). In agreement with these observations, live-cell imaging of *tlc1*Δ TERRA-MS2 clones showed an increased number of cells exhibiting TERRA foci, as well as increased number of foci per cell, compared to *TLC1* WT cells (Fig. 2B and fig. S3). TERRA expression from a single short telomere was also measured using a short inducible telomere assay on telomere 6R (*16*) (fig. S4). RT-qPCR analyses revealed that Tel6R-TERRA levels increased after its telomere shortening (Fig. 2C and D). Remarkably, during the course of

the experiment, Tel6R-TERRA expression correlated with the length of the telomere 6R, with the RNA levels progressively decreasing during the re-lengthening of the telomere by telomerase (Fig. 2D). Notably, the expression levels of TERRA from other telomeres (Tel7L-TERRA and Y'-TERRA) remained stable and were not influenced by the shortening of telomere 6R. Altogether, these results indicate that TERRA expression is induced at short telomeres and that TERRA levels inversely correlate with the length of their telomere of origin.

Next, whether a TERRA focus localizes at its telomere of origin was investigated by live-cell imaging of Tel6R- or Tel1L-TERRA-MS2 clones containing 112-tetO repeats integrated at telomere 6R (tetO-TERRA-MS2 clones). Microscopy analyses of tetO-TERRA-MS2 clones did not reveal a stable co-localization between Tel1L-TERRA or Tel6R-TERRA foci and telomere 6R, in the asynchronous population (data not shown). Therefore, TERRA and telomere 6R foci were monitored over time in cells from early to late S phase. These analyses showed that the Tel6R-TERRA focus transiently co-localizes with telomere 6R during mid-late S phase of the cell cycle (Fig. 3A and movie S1). Notably, Tel6R-TERRA foci colocalized with telomere 6R in 70% of the time-lapse analyses, while Tel1L-TERRA foci colocalized with telomere 6R in only 9% of the time courses (Fig. 3B and movie S2). In order to confirm the cell-cycle dependent association of TERRA with its telomere, chromatin immunoprecipitation experiments (ChIP) were performed using a 6xMS2-Tel6R-TERRA strain. Immunoprecipitation of chromatin-TERRA-MS2-GFP complexes with anti-GFP antibody resulted in specific enrichment of telomere 6R, but not telomere 1L, during S phase (Fig. 3C and D; see also fig. S5). Altogether, both live-cell imaging and ChIP indicate that TERRA transcripts associate preferentially with their telomere of origin during S phase.

Since TERRA is expressed from short telomeres (Fig. 2) and interacts *in trans* with its telomere of origin in S phase (Fig. 3), we investigated whether TERRA may associates with telomerase, which also acts preferentially on short telomeres in S phase (*17, 18*). Tel1L-TERRA-MS2-GFP and Tel6R-TERRA-MS2-GFP pull-down experiments resulted in the specific enrichment of endogenous *TLC1* RNA in both samples (Fig. 4A and fig. S6A). Similarly, using a strain expressing the endogenous *TLC1* RNA containing 10xMS2

repeats (*TLC1*-MS2 cells), *TLC1*-MS2 RNA pull-down resulted in a consistent enrichment of TERRA from various telomeres (Fig. 4B and fig. S6B), indicating that *TLC1* RNA interacts with TERRA transcripts generated from different telomeres *in vivo*. In support of these results, two-color acquisition analyses using a strain expressing endogenous *TLC1*-MS2-CFP and a GFP-PP7 labeled Tel6R-TERRA revealed that 93% of Tel6R-TERRA-GFP foci co-localized with a *TLC1*-CFP cluster, or T-Recs, in S phase (data not shown). Remarkably, imaging cells expressing Tel6R-TERRA foci by time-lapse experiments revealed spontaneous events of *TLC1* RNA nucleation onto the TERRA foci, starting as early as late G1/early S phase (Fig. 4C and movie S3). Post-acquisition analyses confirmed that the area of the *TLC1* RNA cluster increases over time, as *TLC1* RNA molecules nucleate on the TERRA focus, with a median half-time of formation of 5.2 minutes (Fig. 4D and fig. S7). Altogether, these results suggest that TERRA foci act as a scaffold to promote the nucleation of *TLC1* RNA molecules and generate telomerase clusters, or T-Recs, in S phase.

These results prompted us to investigate whether TERRA localize at their telomeres of origin, during S phase, as a TERRA-*TLC1* RNA cluster. To this aim, multicolor live-cell imaging analyses were performed to monitor the localization of PP7-Tel6R-TERRA, *TLC1-MS2* RNA and 112-TetO repeats-containing telomere 6R, by imaging PP7-GFP, MS2-CFP and TetR-RFP fusion proteins, respectively (fig. S7). In 70% of the cells analyzed, *TLC1* RNA clusters and Tel6R-TERRA foci simultaneously co-localize with telomere 6R during S phase (Fig. 4E-F and movie S4). In all these cells, the colocalization of *TLC1* RNA with TERRA occurred prior to their recruitment on telomere 6R. Notably, in cells that do not express a Tel6R-TERRA focus, the *TLC1* RNA cluster co-localizes with telomere 6R in only 15% of the cells analyzed (Fig. 4F). Interestingly, live cell imaging analyses of TERRA foci in mutant strains in which the recruitment of telomerase at telomeres is compromised, such as *mre11Δ*, *tel1Δ* and *yku70Δ* (*19, 20*), showed significantly impaired co-localization between Tel6R-TERRA and telomere 6R (Fig. 4G), as well as a consistently decreased residence time of Tel6R-TERRA foci at telomere 6R, as compared to colocalization events in WT cells (fig. S7). Thus these results indicate that TERRA-*TLC1* RNA clusters are recruited preferentially to the telomere of origin of

TERRA, and that factors controlling telomerase recruitment at telomeres are involved in the localization of TERRA at its telomere.

Our data suggest a model in which a threshold of telomere erosion induces TERRA expression. Upon transcription, TERRA molecules are rapidly displaced from their telomere of origin and accumulate into a focus. In early S phase, a TERRA focus acts as a seed to nucleate telomerase RNA, directly or via binding to different telomerase components, leading to the formation of a telomerase cluster or T-Rec. Later in S phase, the T-Rec is recruited to the telomere from which TERRA originates, which would then be elongated by telomerase. Thus TERRA expression might represent a signal induced by short telomeres to trigger telomerase clustering and subsequent telomere elongation. Interestingly, in cancer cells, formation of telomerase RNA (hTR) foci at telomeres has been linked to a distributive action of telomerase at telomeres, in which several telomerase molecules elongate a short telomere (*21*). Whether TERRA also acts as a scaffold for the formation of hTR foci remains to be established. Our data reveal that lncRNAs do not only act as regulators of gene expression, but also actively organize catalytic activities involved in genome maintenance.

Figure Legends

Fig. 1. Endogenous TERRA accumulates as a focus in WT yeast cells. (**A**) RNA-FISH on endogenous Tel6R, Tel1L and Y' TERRA transcripts. Nuclei are stained with DAPI. Percentage: mean±SD, N=4. (**B**) Live-cell microscopy analysis of Tel6R and Tel1L TERRA-MS2 clones. Nuclei were visualized using Rap1-mCherry. Percentage: mean±SD, N=3. (**C**) Representative images of cells expressing a Tel1L-TERRA-MS2-GFP focus (white arrow) or a Tel6R-TERRA-PP7-Tomato focus (yellow arrowhead), or co-expressing both foci. Numbers on the right represent the percentage of cells with the indicated phenotype (N=2). Scale bars: 1 μm

Fig. 2. TERRA expression is induced at short telomeres. (**A**) RT-qPCR analyses of Tel7L, Tel6R and Y' TERRA expression in *tlc1*Δ cells. g = generations. Data shown represent mean±SD (N=2). (**B**) Examples of TERRA-MS2-GFP foci expressed in cells with normal (*TLC1*) or shorter (*tlc1Δ*) telomeres. (**C**) Southern blot analysis of telomere 6R length in short inducible telomere strain (short) and CTR strain (CTR). GAL: galactose. g:

generations after telomere shortening. (**D**) RT-qPCR analyses of TERRA expression. Values shown represent FOLD of induction of $2^{\wedge-Dct}$ TERRA values detected in the short inducible strain over the control (CTR) strain. Data shown represent mean±SD from triplicate samples of the experiment in (C) out of three independent experiments.

Fig. 3. TERRA associates with its telomere of origin during S phase. (**A**) Time-lapse confocal microscopy of Tel6R-TERRA-MS2-GFP and telomere 6R-TetR-RFP localization. Two colors z-stack acquisitions were performed every two minutes. White arrows indicate co-localization events. Scale bar: 1µm. (**B**) Quantification of colocalization occurrence between TERRA-MS2-GFP foci and telomere 6R-RFP in time-lapse experiments. (**C**) Cell cycle synchronization analyzes by FACS after G1 arrest by α-factor and subsequent release of the cell cycle. (**D**) Chromatin immunoprecipitation (ChIP) experiment. Tel6R-TERRA-MS2-GFP was immunoprecipitated using anti-GFP antibody. Telomere 1L or 6R DNA enrichment was determined by qPCR. IgG antibody was used as control (CTR). Data shown represent mean±SD (N=3). *** $p < 0.001$ using unpaired t-test.

Fig. 4. TERRA foci act as a scaffold to trigger the formation of telomerase clusters. (**A**) Enrichment of *TLC1* RNA in TERRA-MS2-GFP immunoprecipitates. *TLC1* RNA enrichment is shown as FOLD of enrichment in IP samples versus INPUT. (N=3). (**B**) Enrichment of TERRA transcripts in *TLC1*-MS2-GFP immunoprecipitates. TERRA enrichment is shown as FOLD of enrichment in IP samples versus INPUT. (N=2). (**C**) Confocal microcopy images of *TLC1*-MS2-CFP and Tel6R-TERRA-PP7-GFP from Movie S3 at indicated time points. (**D**) Quantification analysis of *TLC1*-CFP and TERRA-GFP foci areas. The graph shows the analysis of time course shown in (C). (**E**) Colocalization between Tel6R-TERRA-PP7-GFP focus, *TLC1*-MS2-CFP cluster and telomere 6R-Tet-RFP focus in S phase cell. (**F**) Occurrence of T-Recs localization at telomere 6R during S-phase, in cells not expressing Tel6R-TERRA foci (- Tel6R TERRA) or in cells which express a Tel6R-TERRA focus (+ Tel6R-TERRA). (**G**) Localization of Tel6R-TERRA foci at telomere 6R in WT and mutant strains. (N=10). Scale bars: 1µm.

References and Notes

1. C. W. Greider, E. H. Blackburn, Identification of a specific telomere terminal transferase activity in Tetrahymena extracts. *Cell* **43**, 405 (1985).

2. N. Hug, J. Lingner, Telomere length homeostasis. *Chromosoma* **115**, 413 (2006).

3. M. T. Teixeira, M. Arneric, P. Sperisen, J. Lingner, Telomere Length Homeostasis Is Achieved via a Switch between Telomerase- Extendible and -Nonextendible States. *Cell* **117**, 323 (2004).

4. S. Marcand, V. Brevet, C. Mann, E. Gilson, Cell cycle restriction of telomere elongation. *Current Biology* **10**, 487 (2000).

5. F. Gallardo *et al.*, Live Cell Imaging of Telomerase RNA Dynamics Reveals Cell Cycle-Dependent Clustering of Telomerase at Elongating Telomeres. *Molecular Cell* **44**, 819 (2011).

6. S. Schoeftner, M. A. Blasco, Developmentally regulated transcription of mammalian telomeres by DNA-dependent RNA polymerase II. *Nat Cell Biol* **10**, 228 (2008).

7. C. M. Azzalin, P. Reichenbach, L. Khoriauli, E. Giulotto, J. Lingner, Telomeric Repeat Containing RNA and RNA Surveillance Factors at Mammalian Chromosome Ends. *Science* **318**, 798 (November 2, 2007, 2007).

8. S. Redon, P. Reichenbach, J. Lingner, The non-coding RNA TERRA is a natural ligand and direct inhibitor of human telomerase. *Nucleic Acids Research* **38**, 5797 (September 1, 2010, 2010).

9. Z. Deng, J. Norseen, A. Wiedmer, H. Riethman, P. M. Lieberman, TERRA RNA Binding to TRF2 Facilitates Heterochromatin Formation and ORC Recruitment at Telomeres. *Molecular Cell* **35**, 403 (2009).

10. N. Arnoult, A. Van Beneden, A. Decottignies, Telomere length regulates TERRA levels through increased trimethylation of telomeric H3K9 and HP1alpha. *Nat Struct Mol Biol* **19**, 948 (2012).

11. R. L. Flynn *et al.*, TERRA and hnRNPA1 orchestrate an RPA-to-POT1 switch on telomeric single-stranded DNA. *Nature* **471**, 532 (2011).

12. B. Luke *et al.*, The Rat1p 5' to 3' Exonuclease Degrades Telomeric Repeat-Containing RNA and Promotes Telomere Elongation in Saccharomyces cerevisiae. *Molecular Cell* **32**, 465 (2008).

13. E. Bertrand *et al.*, Localization of ASH1 mRNA particles in living yeast. *Mol. Cell* **2**, 437 (1998).

14. F. Gallardo, P. Chartrand, Visualizing mRNAs in fixed and living yeast cells. *Methods in Molecular Biology* **714**, 203 (2011).

15. D. R. Larson, D. Zenklusen, B. Wu, J. A. Chao, R. H. Singer, Real-Time Observation of Transcription Initiation and Elongation on an Endogenous Yeast Gene. *Science* **332**, 475 (April 22, 2011, 2011).

16. S. Marcand, V. Brevet, E. Gilson, Progressive cis-inhibition of telomerase upon telomere elongation. *EMBO J* **18**, 3509 (1999).

17. A. Bianchi, D. Shore, Increased association of telomerase with short telomeres in yeast. *Genes & Development* **21**, 1726 (July 15, 2007, 2007).

18. M. Sabourin, C. T. Tuzon, V. A. Zakian, Telomerase and Tel1p Preferentially Associate with Short Telomeres in S. cerevisiae. *Molecular Cell* **27**, 550 (2007).

19. L. K. Goudsouzian, C. T. Tuzon, V. A. Zakian, S. cerevisiae Tel1p and Mre11p Are Required for Normal Levels of Est1p and Est2p Telomere Association. *Molecular Cell* **24**, 603 (2006).

20. T. S. Fisher, A. K. P. Taggart, V. A. Zakian, Cell cycle-dependent regulation of yeast telomerase by Ku. *Nat Struct Mol Biol* **11**, 1198 (2004).

21. Y. Zhao *et al.*, Processive and distributive extension of human telomeres by telomerase under homeostatic and nonequilibrium conditions. *Molecular Cell* **42**, 297 (2011).

Acknowledgments: The authors thank C. Cole, K. Nasmyth, S. Marcand, D. Zenklusen, E. Querido, M. Marcotte, D. Guérit and M. Vasseur for plasmids, strains and helpful comments; Danièle Gagné and Gaël Dulude for technical support with FACS analysis. We also thank the Cell Imaging Analytical Network (CIAN, McGill University) for access to their imaging stations. This project was funded by a grant from the Canadian Institutes of Health Research (CHIR) MOP-89768 to PC. C.A.P.R is supported by a CDMC/CREATE fellowship from the Natural Sciences and Engineering Research Council of Canada (NSERC). P.C is a Senior Fellow of the Fonds de Recherche du Québec-Santé (FRQS).

Figures

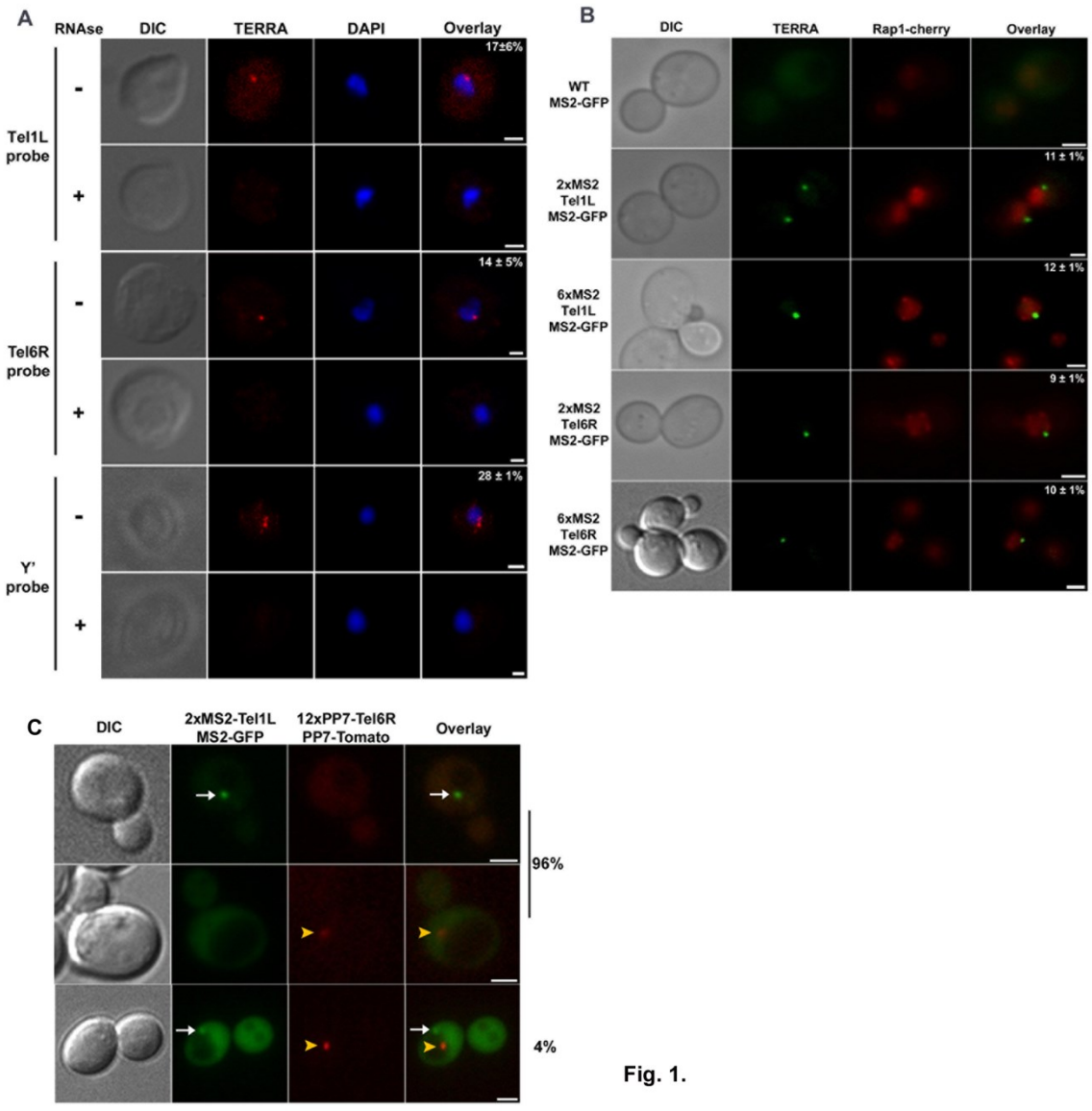

Fig. 1.

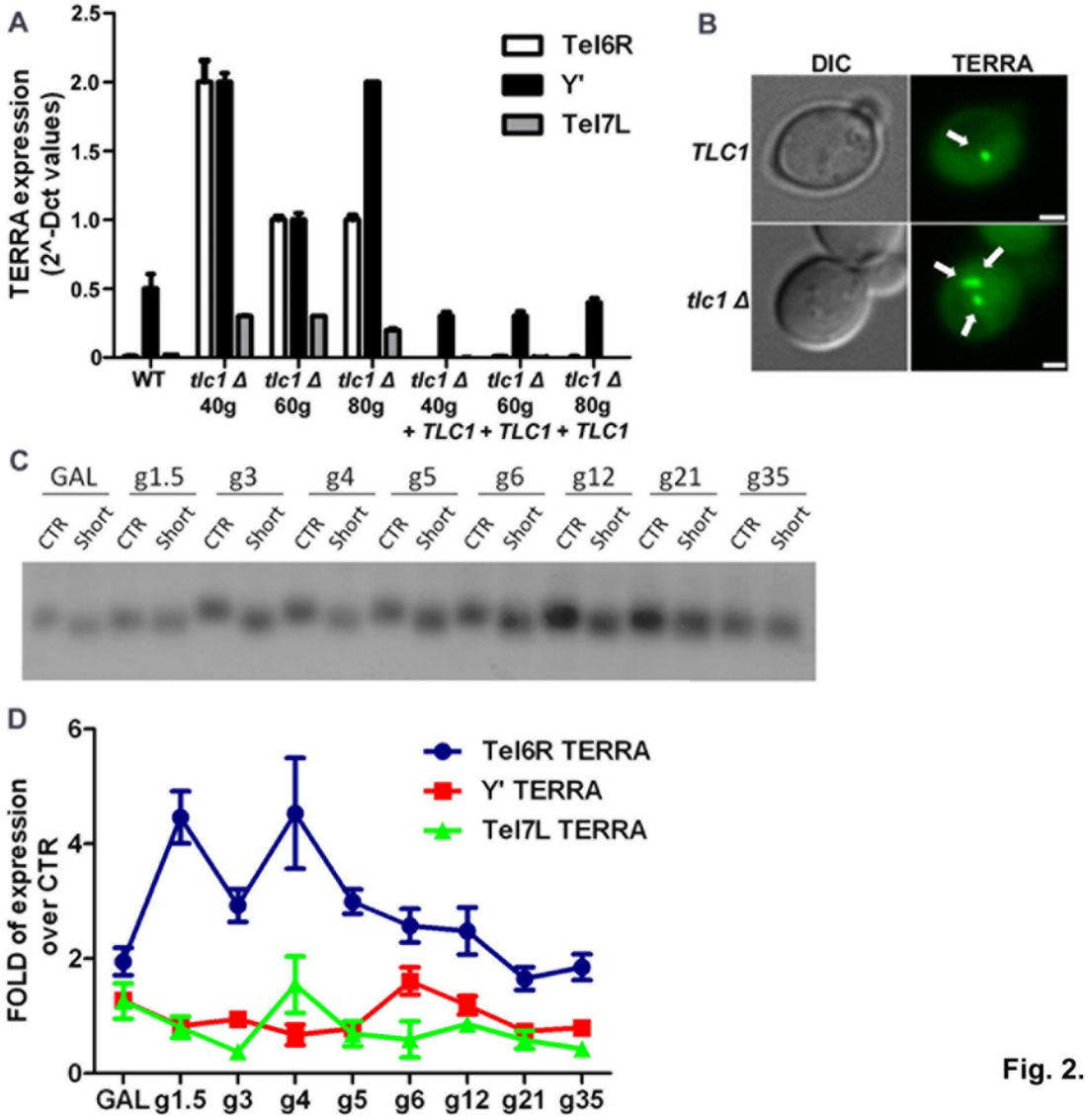
A
TERRA expression (2^-Dct values)
2.5
2.0
1.5
1.0
0.5
0
Tel6R
Y'
Tel7L
WT
tlc1 Δ 40g
tlc1 Δ 60g
tlc1 Δ 80g
tlc1 Δ 40g + TLC1
tlc1 Δ 60g + TLC1
tlc1 Δ 80g + TLC1
B
DIC
TERRA
TLC1
tlc1 Δ
C
GAL
g1.5
g3
g4
g5
g6
g12
g21
g35
CTR
Short
D
FOLD of expression over CTR
6
4
2
0
Tel6R TERRA
Y' TERRA
Tel7L TERRA
GAL g1.5 g3 g4 g5 g6 g12 g21 g35

Fig. 2.

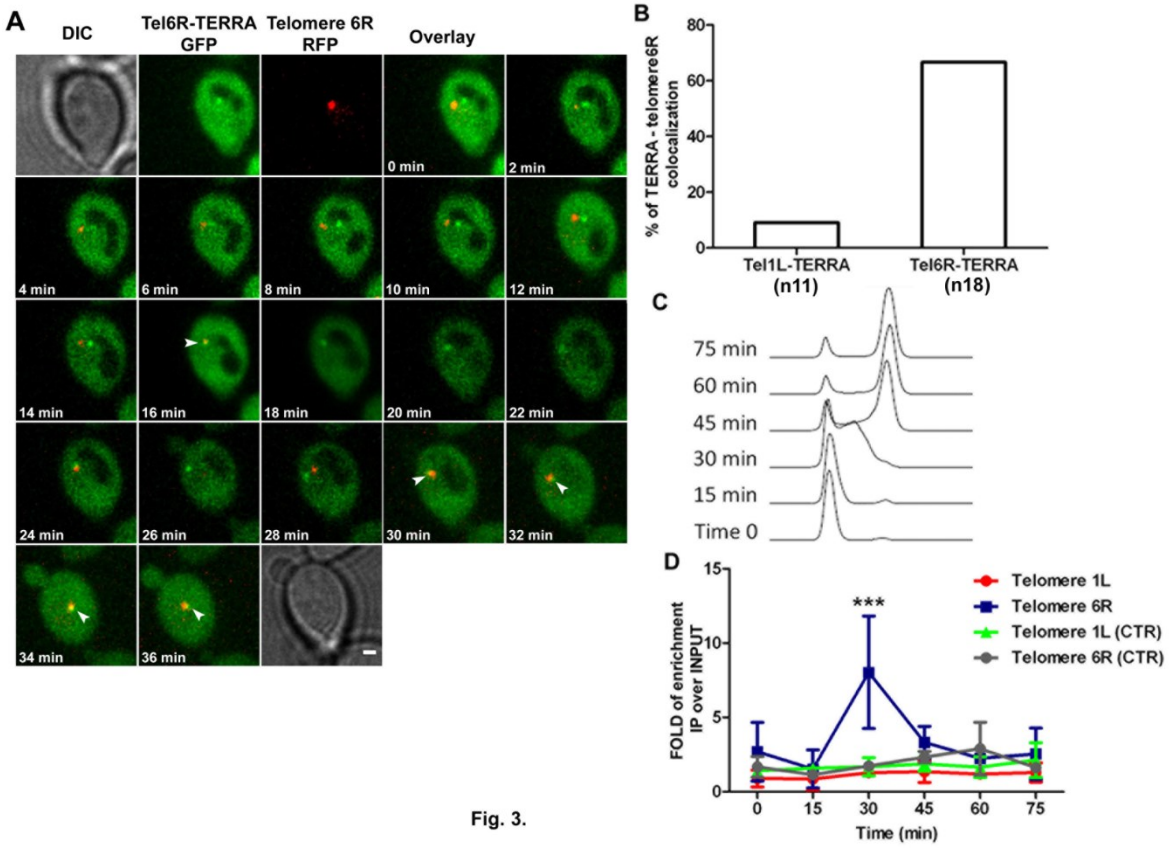
A
DIC
Tel6R-TERRA GFP
Telomere 6R RFP
Overlay
0 min
2 min
4 min
6 min
8 min
10 min
12 min
14 min
16 min
18 min
20 min
22 min
24 min
26 min
28 min
30 min
32 min
34 min
36 min
B
% of TERRA - telomere6R colocalization
Tel1L-TERRA (n11)
Tel6R-TERRA (n18)
C
75 min
60 min
45 min
30 min
15 min
Time 0
D
FOLD of enrichment IP over INPUT
***
Telomere 1L
Telomere 6R
Telomere 1L (CTR)
Telomere 6R (CTR)
Time (min)

Fig. 3.

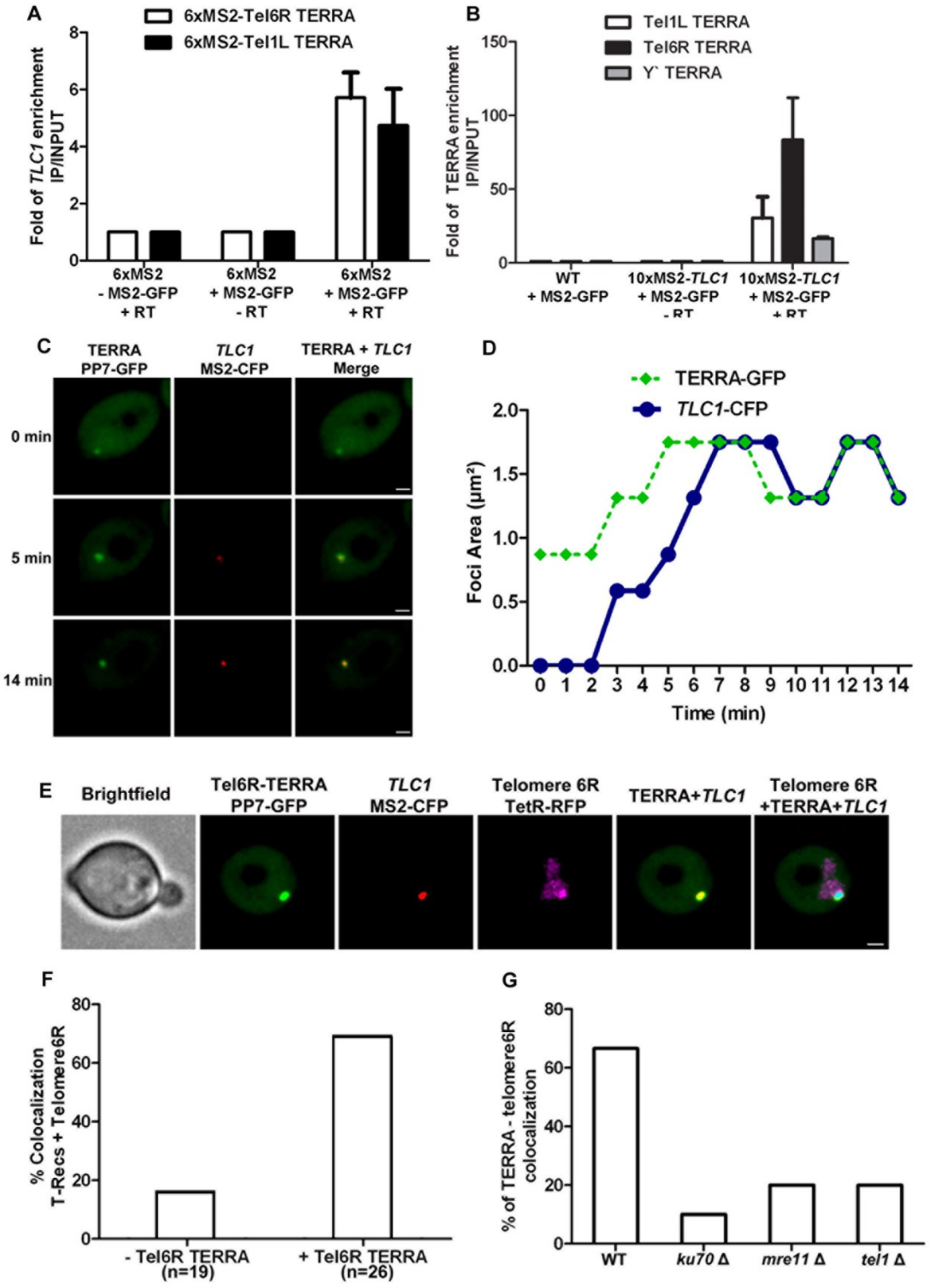
A
6xMS2-Tel6R TERRA
6xMS2-Tel1L TERRA
Fold of TLC1 enrichment IP/INPUT
6xMS2 - MS2-GFP + RT
6xMS2 + MS2-GFP - RT
6xMS2 + MS2-GFP + RT
B
Tel1L TERRA
Tel6R TERRA
Y` TERRA
Fold of TERRA enrichment IP/INPUT
WT + MS2-GFP
10xMS2-TLC1 + MS2-GFP - RT
10xMS2-TLC1 + MS2-GFP + RT
C
TERRA PP7-GFP
TLC1 MS2-CFP
TERRA + TLC1 Merge
0 min
5 min
14 min
D
TERRA-GFP
TLC1-CFP
Foci Area (µm²)
Time (min)
E
Brightfield
Tel6R-TERRA PP7-GFP
TLC1 MS2-CFP
Telomere 6R TetR-RFP
TERRA+TLC1
Telomere 6R +TERRA+TLC1
F
% Colocalization T-Recs + Telomere6R
- Tel6R TERRA (n=19)
+ Tel6R TERRA (n=26)
G
% of TERRA - telomere6R colocalization
WT
ku70 Δ
mre11 Δ
tel1 Δ

Fig. 4.

Supplementary Materials:

Material and Methods

Yeast strains

All the strains used in this study were generated in a FY23 background, with the exception of the strains used in the ChIP experiments, where the W303 *bar1Δ* background was used (see Table S1). Insertion of 2xMS2 and 6xMS2 at telomere 1L or telomere 6R was performed by the integration of a PCR cassette containing the MS2 sequences and a G418 resistance (*KAN*) gene, flanked by lox-p sites. *KAN* marker gene was eliminated by expression of the Cre recombinase. The MS2-*KAN* cassette was PCR amplified from the 6xMS2-pUG6-loxp-*KAN* plasmid by using the following primer pairs: HRchr6prS-MS2-6s and HRchr6prAS for the integration of 2xMS2 at telomere 6R; HRchr6prS-MS2-6sB and HRchr6prAS for the integration of 6xMS2 at telomere 6R; HRchr1LprS-MS2s and HRchr1LprAS for 2xMS2 at telomere 1L; HRchr1LprS-MS2-6s and HRchr1LprAS for the integration of 6xMS2 at telomere 1L (see Table S4 for primers sequences). After integration of the MS2-*KAN* cassette, the selection marker was removed using the Cre recombinase expressed from the plasmid pSH47-Gal1-Cre (*URA3*), which was subsequently eliminated by growing the cells on 5-FOA. The MS2 integration site was PCR amplified and PCR products verified by sequencing (fig. S1A). The single integration of the MS2 repeats sequence was confirmed by Southern blot using an MS2 specific probe, while the length of telomere 1L and telomere 6R after MS2 integration was analyzed by Southern blot using telomere specific probes (fig. S1B). For Southern blot analyses, genomic DNA was digested PvuII or EcoRV for the analyses of telomere 6R or telomere 1L, respectively. The MS2 repeats were integrated at about 80 nucleotides upstream from the telomeric repeats tracts of both telomere 1L and telomere 6R.

The integration of the 12xPP7 sequence at telomere 6R was performed by integrating a cassette containing 12xPP7 repeats and a *KAN* gene flanked by lox-p sites. The cassette was PCR amplified from the 12xPP7 pUG6-lox-p-*KAN* plasmid, using the primers pUG6-prHR-TEL6R-S and HRchr6prAS. After *KAN* elimination, the 12xPP7 integration site was sequence-verified and clones analyzed by Southern blot using the telomere 6R specific probe and a PP7 specific probe (PvuII digestion).

Integration of 112-tetO repeats at chromosome 6R, at a distance of ~3 kb from the telomeric repeats tract, was performed by transforming the NheI linearized pRS306-112tetO-Tel6R vector. Integration was confirmed by Southern blotting using a TetO-repeats specific probe and a chromosome 6R specific probe mapping within the genomic region of the integration site (genomic DNA were digested SpeI). After integration, the length of the telomeric repeats tract at telomere 6R

was verified by a single telomere 6R specific probe, which revealed no difference in length compared with the WT telomere 6R. TetR-RFP expression was achieved by integration of a TetR-RFP expressing cassette containing the nourseothricine resistance gene (NAT) in chromosome VIIL.

Generation of the strains containing a short inducible telomere 6R was carried out as follows: first, a cassette containing the galactose inducible Flp1 recombinase was integrated at the LEU2 gene locus. This integration was achieved by linearizing the pFV17-Gal1-Flp vector using BsteII enzyme. LEU+ clones were grown on galactose plates to test potential toxicity due to Flp1 recombinase expression, and then transformed with a cassette containing a short inducible telomere 6R sequence WT or containing 2xMS2 sequences. This cassette was obtained by digestion of the plasmids Sp225-Tel6R, Sp229-Tel6R and Sp242-Tel6R using EcoRI, either WT or containing 2xMS2 repeats (see plasmids generation paragraph). For each clone, the integration site of the short inducible telomere 6R cassette was PCR amplified and sequence-verified. The specificity of the integration and the shortening of telomere 6R following Flp1 recombinase expression, were verified by Southern blot using MS2 specific probe or, in the absence of MS2 repeats, the primer HRchr6RprAS was used as a probe. It should be noted that the shortened telomere 6R retains the complete sub-telomeric sequence, thus maintaining native sequences of TERRA and its promoter regions.

Clones expressing endogenous *TLC1* RNA tagged with 10xMS2 were generated by integrating a cassette containing 10xMS2 repeats and a *KAN* resistance gene flanked by lox-p sites, at the 3' of *TLC1* gene. The MS2 repeats integration was performed at the nucleotide 1140 of the *TLC1* gene. This integration was previously shown to maintain a functional telomerase activity (*22*). The 10xMS2-*KAN* cassette was obtained by PCR amplification using 3'TLC1-10xMS2-pUG6-lox-p-*KAN* plasmid as template and the following primer pair: 3'TLC1-prS and TLC1-3'HR-prAS. *KAN* resistance gene was eliminated by expression of the Cre recombinase, as described above. After *KAN* elimination, the 3' of the endogenous *TLC1*-10xMS2 gene was verified by sequencing.

Plasmids constructions

Plasmids used in this study are listed in Table S2. **MS2-pUG6-lox-p-Kan plasmid:** the 330nt sequence containing 6xMS2 repeats was obtained by digesting the vector pSL-MS2-6 with the restriction enzymes BamHI/EcorV. The 6xMS2 sequence was then cloned in SalI restriction site (filled-in) in pUG6-lox-p-*KAN* vector. **12xPP7-pUG6-lox-p-Kan vector**: the 737nt sequence containing 12xPP7 repeats was obtained by digesting BamHI/xhoI the vector 214ycpLac33-

12xPP7SSA4 (gift from Daniel Zenklusen). The 12xPP7 fragment was then cloned PvuII/SalI in pUG6-lox-p-*KAN* vector. **pRS306-112tetO-Tel6R vector:** the 853nt sequence mapping ~3kb from the telomeric repeats tract of telomere 6R was PCR amplified from FY23 background cells. The sequence was then cloned BglII/SalI in the vector pRS306-112tetO (gift from K. Nasmyth). The 853nt cloned sequence carries a NheI restriction enzyme site which was used to linearize the vector and allow the integration of the vector at ~3kb from telomere 6R. **sp225-Tel6R, sp229-Tel6R and sp242-Tel6R plasmids**: the 480nt fragment corresponding to the subtelomeric sequence of telomere 6R adjacent to the telomeric repeat tract was PCR amplified from WT cells (FY23 strain) or the 2XMS2-Tel6R clone; the sequence was then HindIII cloned in the vectors Sp225, Sp229 and Sp242 (gift from Stéphane Marcand). EcoRI digestion of the resulting plasmids allows the extraction of the cassette containing the subtelomeric region of telomere 6R, a URA3 marker gene and 0, 270nt or 540nt telomeric tract used for the selection of the strains CTR, short and short-dc, respectively; **3'TLC1-10xMS2-pUG6-lox-p-Kan plasmid**: 500nt sequence containing the 3' of *TLC1* RNA (from nt1063 to nt1227 of the gene) and 10xMS2 repeats inserted at the nt 1140 of the *TLC1* gene, was PCR amplified from the vector pRS314-3'TLC1-10xMS2 (*22*). The PCR product was PvuII cloned in pUG6-lox-p-Kan vector. **Ycp111-MS2CFP**: first the sequence of the ADH1 terminator was PCR amplified from pFA6-13Myc plasmid and cloned in pECFP-MS2 vector, using the NotI restriction site present at the 3' end of the sequence codifying for the MS2-CFP fusion protein. Then the MS2-CFP-ADH1-terminator cassette was removed by EcoRI digestion and cloned in ycp111-MS2GFP plasmid, replacing GFP gene with CFP (one EcoRI site is present in the MS2 coding sequence). Each plasmid cloned in this study was verified by sequencing.

Validation of MS2-tagged TERRA expression and foci formation

To confirm that MS2-GFP foci observed in strains with MS2 repeats integrated at telomere 6R or telomere 1L contain TERRA-MS2 RNA, fluorescent in situ hybridization on TERRA-MS2 was performed using an MS2 sequence-specific probe. Co-localization between Tel6R- or Tel1L-TERRA-MS2 transcripts and MS2-GFP focus was observed (fig. S1C). These results confirm that the MS2-GFP foci correspond to the TERRA foci detected by RNA-FISH. Fluorescent in situ hybridization was also performed on Tel1L- or Tel6R- TERRA-MS2 clones not expressing MS2-GFP. These results indicate that the expression of the MS2-GFP fusion protein does not influence TERRA transcripts localization (fig. S1D).

Quantification of TERRA levels by qRT-PCR confirmed that the integration of 2xMS2 repeats at telomere 1L or telomere 6R does not influence TERRA expression levels, while the integration of 6xMS2 resulted in an increased expression of Tel6R- and Tel1L-TERRA (fig. S1E).

We therefore used the strains expressing 2xMS2 tagged TERRA for all the imaging analyses. To further confirm that the TERRA-MS2-GFP foci reflects TERRA expression, expression of MS2-tagged Tel6R-TERRA and Tel1L-TERRA was measured in a temperature-sensitive mutant of the 5'-3' exonuclease Rat1. An increased number of cells expressing TERRA-MS2-GFP foci were detected in the *rat1-1* strain when grown at semi-permissive temperature (30°C), compared to TERRA-MS2 WT strain (fig. S1F). These results indicate that expression of TERRA-MS2-GFP foci is sensitive to Rat1, as expected if the formation of these foci depends on TERRA expression. Altogether, these results show that the expression and localization of TERRA-MS2-GFP is identical to endogenous TERRA detected by FISH. Therefore, the MS2-tagged TERRA can be used as a marker of TERRA expression and trafficking in single living cells.

Fluorescent In Situ Hybridization (FISH)

Probe design: FISH assay was performed as described previously (*23*) with minor modifications. The FISH probes used in this study to target TERRA are as follows: MS2-TERRA (5-AGT'CGACCTGCAGACAT'GGGTGATCCTCAT'GTTTTCTAGGCAATT'A-3), Tel1L-TERRA (5-CCAT'CCCTCTACTT'ACTACCACT' CACCCACCGT'TACCCTCCAAT'TACCCATATC-3), Tel6R-TERRA (5-ACGCACACGT'ATGCTAA AGT'ATATATTACT'TCACTCCATT'GCGC CCCAT'GACCC-3) and a control probe targeting the small nucleolar RNA U3 (5-TT'CTATAGA AATGATCCT'ATGA AGTACGTCGACTT'A-3) was used as described in (*24*). All probes were synthesized with amino-allyl modified T residues where stated (T').

FISH Probe labeling: The TERRA specific probes were labeled with Cy3 dye, while the control RNA U3probe used for quantification analyses in Figure 1 was labeled with Cy5. For the labeling reaction, 10µg of probe were resuspended in 35µl of sodium carbonate buffer pH 8.8, followed by the addition of 15µL of monoreactive Cy3 or Cy5 dye (GE Healthcare). The mixture was incubated for 24 hours at room temperature in the dark, with occasional vortexing. The probes were then purified using an RNAse free Sephadex G-25 column (Roche Applied Bioscience). Subsequently, probe concentration and labeling efficiency were measured by reading absorbance at OD_{260} and OD_{552}, respectively. Fluorophore incorporation efficiency was calculated and rectified to be higher than 70% as quality control for our labeling. The labeled probes were then diluted to a final concentration of 1ng/µL in DEPC water for further use.

Cell fixation and spheroplast formation: 50 ml of yeast cultures in early log phase, at OD_{600} between 0.2-0.4 were collected and washed in 1xPBS buffer (10mM KH_2PO_4, 1.4M NaCl, 40mM KCl, 100mM Na_2HPO_4, pH 7.5). The cells were fixed in PBS for 45 min at room temperature by adding 6.25 mL of 32% paraformaldehyde (Electron Microscope Sciences), and subsequently

washed 3 times in 1x ice-cold Buffer B (1.2M Sorbitol, 0.1M potassium phosphate, pH 7.5). Samples were resuspended in 1mL of buffer B containing 20mM vanadyl ribonucleoside complex (VRC), 28mM β-mercaptoethanol, 0.06 mg/mL phenylmethylsulfonyl fluoride, 5µg/mL pepstatin, 5µg/mL leupeptin, 5µg/mL aprotinin, and 120U/mL of RNAse inhibitor (Qiagen), and incubated for 15 min at 30°C in presence of oxalyticase for spheroplast formation. Spheroplast were resuspended in 750µL of 1x ice-cold buffer B and 100 µL were placed on a poly-L-lysine coated coverslip and let adhere for 30 min at 4°C. The coverslips were washed with ice-cold buffer B, and spheroplasts were dehydrated in 70% DEPC ethanol for at least 30 min at -20°C.

In situ hybridization: 10µL of TERRA specific probe or 2µL RNA U3 probe, previously labeled, were mixed with 4 µL of *E.coli* tRNA (5 µg/µL) and lyophilize. Probes were resuspended in 12µL of 80% formamide and 10mM sodium phosphate, pH 7. Meanwhile the coverslips containing spheroplasts were rehydrated by washing them in 8 ml of 2xSSC buffer for 5 min at room temperature in a Columbia coplin jar. Cells were incubated in 8ml 2xSSC containing 35% formamide for the hybridization of MS2-TERRA probe, 40% formamide for the Y'element TERRA probe, and 50% formamide for the Tel1L and Tel6R TERRA probes. During this incubation the probe solutions were heated for 3 min at 95°C, and 12µL of 4xSSC solution containing 20 mM VRC, 4µg/mL RNAse free BSA and 50U of RNAse inhibitor were added to each tube. Hybridization was performed at 37°C overnight in the dark. Coverslips were subsequently washed twice with 8 ml of pre-heated 2xSSC with the required percentage of formamide, at 37°C for 15 min, and once with 8mL of 2xSSC solution containing 0,1% Triton X-100, for 15 min at room temperature (for the endogenous Tel1L TERRA probe, this step was repeated 2 times). Two more washes were carried out using 8 ml of 1xSSC solution, at room temperature for 15 min (for the endogenous Tel1L TERRA probe this step was repeated 4 times). Cells were then incubated with 8 ml of 1xPBS containing 1ng/ml of 4',6 diamidino-2-phenylindole (DAPI) (Invitrogen) for 2 min at room temperature, for DNA staining. The coverslips were mounted on a glass slide with the surface containing the spheroplasts on a 10µl drop of mounting medium. The slides were sealed by applying nail polish.

Image Acquisition and Analysis: The prepared slides were imaged using an epifluorescence microscope Nikon Eclipse TE2000U equipped with Cy3.0, Cy5.0, FITC, and DAPI filters, a 100x/1.46 NA objective, and a CoolSNAP HQ2 camera from Photometrics. Images were acquired using NIS Elements software ND acquisition (from Nikon), with at least 15 z-stack images with a 0.20 µm step size. Endogenous TERRA foci were detected using a Cy3.0 filter, while MS2-GFP tagged TERRA foci were detected using a FITC filter. An RNA U3 control probe, used to confirm

the quality of spheroplasting and FISH, was detected using a Cy5.0 filter. All the images were processed equally using a self-made macros on ImageJ software to perform: maximum intensity projection, adjust brightness/contrast of each channel using the same levels for all the FISH experiments and modifying channel LUTs to desired colors (endogenous TERRA foci in red, MS2-tagged TERRA foci in green, DAPI in blue and DIC in gray scale) to visualize the final merged images. The number of TERRA foci in the cell population was quantified by taking into account the number of cells with foci and its localization. As control, only cells labeled with the U3 RNA control probe were quantified. For quantification, between 300 and 400 cells were analyzed in each experiment.

Live cell imaging

For TERRA-MS2-GFP foci imaging and TERRA-telomere 6R co-localization experiments, TERRA foci were detected using an exposition time of 100 ms, binning 1 x 1, and 488-laser power at 12%. Telomere 6R foci were detected using the following camera setting: 100 ms exposure time, binning 1 x 1, 532-laser power 20%, 375 EM gain. For time course experiments, seven z-stack images were taken every 2 minutes for at least 30 minutes, using a 0.24 µm step size in the Z axis. Analyses were performed using the ZEN software (Zeiss). For imaging of TERRA-MS2-GFP/Rap1-mCherry clones, an epi-fluorescence microscope Nikon Eclipse E800 was used, equipped with a 100x/1.46 NA objective and a Evolve512 EM-CCD camera (Photometrics). TERRA signal was detected by using a FITC fluorescence filter and the following camera setting: 80 ms exposure time, binning 1 x 1, 50 EM gain. Rap1-mCherry signal was detected using Texas-Red fluorescence filter and the following camera setting: 200 ms exposure time, binning 1 x 1, 100 EM gain. Acquisitions were analyzed using Metamorph software.

For simultaneous TERRA-MS-GFP, *TLC1-PP7*-CFP RNA and telomere 6R-TetR-RFP imaging, Tet-RFP-tagged telomere 6R foci were detected using a diode laser for RFP (568nm/50mW) and an ET 620/60 emission filter with the following set up: 25% laser power, 250 ms exposure time, 1x1 binning. PP7-GFP labeled TERRA foci were detected using a diode laser for GFP (491nm/50mW) and a ET 525/50 emission filter with the following set up: 15% laser power, 100ms exposure time, 1x1 binning. MS2-CFP labeled *TLC1* RNA foci were detected using a diode laser for CFP (446nm/40Mw) and a HQ 470/40 emission filter with the following set up: 25% laser power, 200ms exposure time, 1x1 binning. Brightfield images were captured to identify cell cycle stage with 250ms exposure time, 1x1 binning. For the time-lapse experiments, seven z-stack images were taken every minute for at least 20 minutes, using a 0.25 µm step size, capturing multiple

channels at each Z plane going from the longest wavelength (568 nm) to the shortest wavelength (446 nm) using Velocity software (PerkinElmer). Analyses were performed using Image J software.

Colocalization analysis

Colocalization between TERRA, *TLC1* RNA and telomere 6R (strain FY23 12xPP7-Tel6R/10xMS2-TLC1/TetO-Kan-Tel6R TetR-RFP, see Table S1) was assessed plane by plane between each channel during the whole time course using the acquisition software. Colocalization was positive if two foci overlapped in the same focal plane. Of note, post-acquisition analyzes revealed no variation in TERRA foci intensity between time points acquired before or after TERRA localization with telomere 6R (data not shown). These observations indicate that TERRA foci analyzed correspond to the same foci tracked over time, and do not represent newly synthesized TERRA particles. Representative movie of the cells was generated by performing a maximum projection of the planes in which foci colocalized (for Supplemental movies 1, 3 and 4). In case of no colocalization maximum projection of all the stacks was performed using ImageJ software (for Supplemental movies 2).

Analysis of *TLC1* RNA cluster (T-Recs) formation

Time course images of TERRA, *TCL1* RNA and telomere 6R (strain FY23 12xPP7-Tel6R/10xMS2-TLC1/TetO-Kan-Tel6R TetR-RFP, see Table S1) were analyzed plane by plane between each channel during each time point using Volocity software. The time courses which were found to have a formation of T-Recs were imported into ImageJ, where maximum projection of the planes in which the focus appeared was produced. The area of T-Recs and TERRA foci was measured over the complete period of the time-lapse using ImageJ. Thirteen cells showing spontaneous T-Recs formation were analyzed and the areas information were plotted on graphs using GraphPad software to fit the graphs into a non-linear regression, one phase association model with the equation: $Y= Y_0 + (Plateau-Y_0)*(1-exp(-K*x))$, using a constrain of plateau value to be equal to zero. These regressions allowed us to calculate the initial foci area values as well as the maximum foci area for both T-Recs clusters and TERRA foci. The half time of foci formation was calculated using the rate constant (ln(2)/K) of T-Recs clusters formation for each data set. To compile the data obtained from each time course into a generalized data median and standard deviation, values were calculated for the initial and maximum foci area, and the half time of foci formation was represented on a dot plot. We found that T-Recs clusters started with an area of 0

μm^2 and reached a maximal area of 1.3±0.2 μm^2, TERRA foci started with an area of 0.8±0.3 μm^2 and reached a maximal area of 1.4±0.2 μm^2. The average cell area was 156±11 μm^2.

Telomere shortening experiment

Cells were grown overnight at 30° in YPD medium containing raffinose as carbon source. The following day the expression of Flp1 recombinase was induced by diluting the cells to the OD_{600} of 0.2, in 30° pre-warmed YPD medium, containing 3% galactose as carbon source. Cells were grown in galactose for 3 hours, then collected, washed twice in YPD + glucose, and diluted in glucose containing YPD medium, at the OD_{600} of 0.2. After telomere shortening, the cells were grown in glucose rich medium and maintained in exponential growth ($OD_{600} < 2$) by regular dilutions. At the indicated generations of growth two cellular pellets were collected for RNA and DNA extraction.

Chromatin immunoprecipitation (ChIP)

Cells were grown in selection medium at 30°C until an OD_{600} of 0.7-0.8. Then α-factor was added to 2.5µM final concentration for 2 hours. The cells were subsequently collected and washed twice in YPD medium, re-suspended in YPD and grown at room temperature (23°C) for the indicated time. Each 15 minutes time point, 50 ml aliquots of cells were fixed in 1% formaldehyde. Cells were collected and washed twice in ice-cold PBS. Pellets were resuspended in 400µl Lysis buffer (50mM HEPES pH8, 140mM NaCl, 1mM EDTA, 1% sodium deoxycholate, 1% Triton-x100) containing protease inhibitors (EDTA free protease inhibitor mix and 1mM PMSF, Roche), and RNase inhibitor (2mM VRC). Cells were lysed using glass beads by vortexing 6 times x 45 second. Lysates were eluted in new tubes by needle puncturing, centrifuged 5 minutes, 3000 rpm at 4°C, and supernatant transferred in a new tube. Pellets were resuspended in 200µl lysis buffer, centrifuged again, and supernatant added to the corresponding tube. Samples were sonicated on ice, 4 times, 20 second each, and subsequently pre-cleared 1 hour at 4°C with 45µl of equilibrated magnetic beads (Millipore). After a pre-clearing step, immunoprecipitation was performed overnight using monoclonal anti-GFP antibody (Roche) or mouse IgG. The following day, 45 µl magnetic beads were added to each sample, and binding to the antibodies was allowed for 1 hour at 4°C. Protein-beads complexes were collected, washed 4 times for 5 minutes each, at room temperature, using the following wash buffers: wash 1: 700µl of lysis buffer; wash 2: 1ml lysis buffer containing 500mM NaCl; wash 3: 700µl LiCl buffer (10mM Tris pH8, 1mM EDTA pH 8, 0.25M LiCl, 0.5% NP-40, 0.5% sodium deoxycholate); wash 4: 700µl of wash buffer 4 (10mM Tris pH8, 1mM EDTA pH8, 100mM NaCl). Protein-beads complexes were eluted and de-crosslinked in 200µl elution buffer (10mM Tris pH8, 1mM EDTA pH8, 0.5% SDS) at 65°C overnight. The

following day, 225µl of solution containing 10mM Tris pH8, 1mM EDTA pH8 and 25µg proteinase K was added to each tube and samples were incubated 6 hours at 37^{0}C. Phenol/chloroform and chloroform extractions were performed, followed by DNA precipitation overnight at -20^{0}C. DNA was resuspended in 40µl of H_2O, and qPCR experiments were performed in triplicates using 3µl of sample per reaction. Telomere 1L and 6R DNA enrichment was assessed by calculating 2^-Dct values using actin normalization, in both IP and INPUT samples, and expressed as FOLD of enrichment IP over INPUT.

RNA extraction and RT-qPCR analyses

Cells were harvested during logarithmic phase, washed in ice cold PBS and re-suspended in 400µl of ice cold TES solution (10 mM Tris pH7.5, 10 mM EDTA, 0.5% SDS). 400ul of acid phenol were added to each sample and tubes were incubated for 1 hour at 65^{o}C, vortexing 5sec every 10 minutes. Samples were then chilled in ice for 5 minutes and centrifuged at 13000 Rpm, 5 minutes at room temperature. After chloroform extraction, RNA was precipitated by addition of 1/10 volume of 3M NaAc pH5.2 and 2 volumes 100% ETOH. RNA were subsequently collected by centrifugation and washed with 500µl of ethanol 70%. Pellets were re-suspended in DEPC water, run on 1xMOPS agarose gel for quantification and quality control. 3µg of RNA were treated with DNase I (Fermentas) for 1 hour at 37 ^{o}C, and 200ng of DNase I treated RNA were reverse transcribed by using H-MULV–H enzyme (Fermentas) at 42^{o}C for 1 hour. For TERRA, a C-rich primer was used for reverse transcription (RT), while a specific primer was used for *TLC1* RNA (Table S3). 3µl of the RT reaction were used for the qPCR experiments. qPCR were performed in triplicates, using primers shown in Table S3, and the qPCR master mix "SsoFAST EVAGreen Super MIX" from Biorad. qPCR was carried out on a Roche LightCycler 480 sequence-detection system. Analyses were performed by calculating the averages and standard deviations of the actin normalized 2^-Dct values of each triplicate.

DNA extraction and Southern blot analyses

Cells were harvested during logarithmic phase and washed in ice cold PBS. Pellets were re-suspended in 200µl of lysis buffer (0.01M Tris pH8, 0.1M NaCl, 1mM EDTA pH8, 1% SDS, 2% Triton-X100) and transferred in new tubes containing 200µl of phenol/chloroform and the equivalent of 200µl of glass beads. Lysis was performed by vortexing samples 10 minutes at room temperature. After vortexing, 200µl of TE was added to each tube and samples centrifuged for 5 minutes at 13000 Rpm. After one step of chloroform extraction, DNA was precipitated at -20^{o}C for 1 hour adding 2 volumes of EtOH 100%. DNA was resuspended in 200µl RNAse A-water solution and incubated at least 1 hour at 37^{o}C. Genomic DNA was subsequently quantified on agarose gel.

For southern blot analyses, 10µg of genomic DNA were digested with the appropriate restriction enzyme, run overnight (30 V) in 1% agarose gel, and processed for DNA hybridization.

Cell cycle analysis by FACS

The appropriate cell culture volume (1-2x10^7 cells) was pelleted and cells fixed in ethanol 70% over night at 4^o C. Fixed cells were washed in 1ml Tris 50mM pH7.5 and an RNAse A treatment was performed for 3h at 42^{o}C. Cells were subsequently resuspended in a Tris 50mM pH7.5 solution containing 200µg proteinase K, incubated for 30 min at 50^{o}C. Proteinase K was removed by centrifugation and cells resuspended in 300µl of Tris 50mM pH7.5 solution. 100µl of cells were stained using a Sytox green staining solution (1 uM final concentration in Tris buffer) and analyzed by flow cytometry. Cell cycle analyses were carried out using a BD-FACS Canto II instrument (BD BIOSCIENCE).

Co-immunoprecipitation assay

50 ml culture of logarithmic phase growing cells were pelleted and washed in ice cold PBS. Cells were lysed using glass beads by vortexing in 400ul lysis buffer (20mM Hepes pH7.9, 20% glycerol, 0.2mM EDTA, 150 mM NaCl, 0.05% NP40) containing 10mM β-mercaptoethanol, 1mM PMSF, EDTA free protease inhibitor mix, VRC 2mM, 3µl/ml of RNAse inhibitor "RNAse OUT" (INVITROGEN). Lysates were pre-cleared and ~ 200ug of protein lysate were used for the immunoprecipitation experiment overnight, using 2µg of mouse monoclonal anti-GFP antibody (Roche) per sample, while ~40µg of protein lysate was used for the INPUT. Complexes associated with anti-GFP antibody were collected using protein-G Sepharose (Millipore, GE heathcare), and binding allowed by incubation for 1 hour at 4^{o}C. Samples were washed four times in lysis buffer and RNA was extracted by adding 500µl of TRIZOL reagent to the IP and INPUT samples. RNA extraction was performed according to manufacturer instruction and isopropanol precipitation allowed for 2 hours at room temperature in the presence of glycogen (20µg per sample). INPUT and IP samples were resuspended in 30µl and 20µl of H_2O, respectively. Of these, 2µl were used for RT reaction. RT and qPCR reactions were performed as described above.

Supplementary Figures

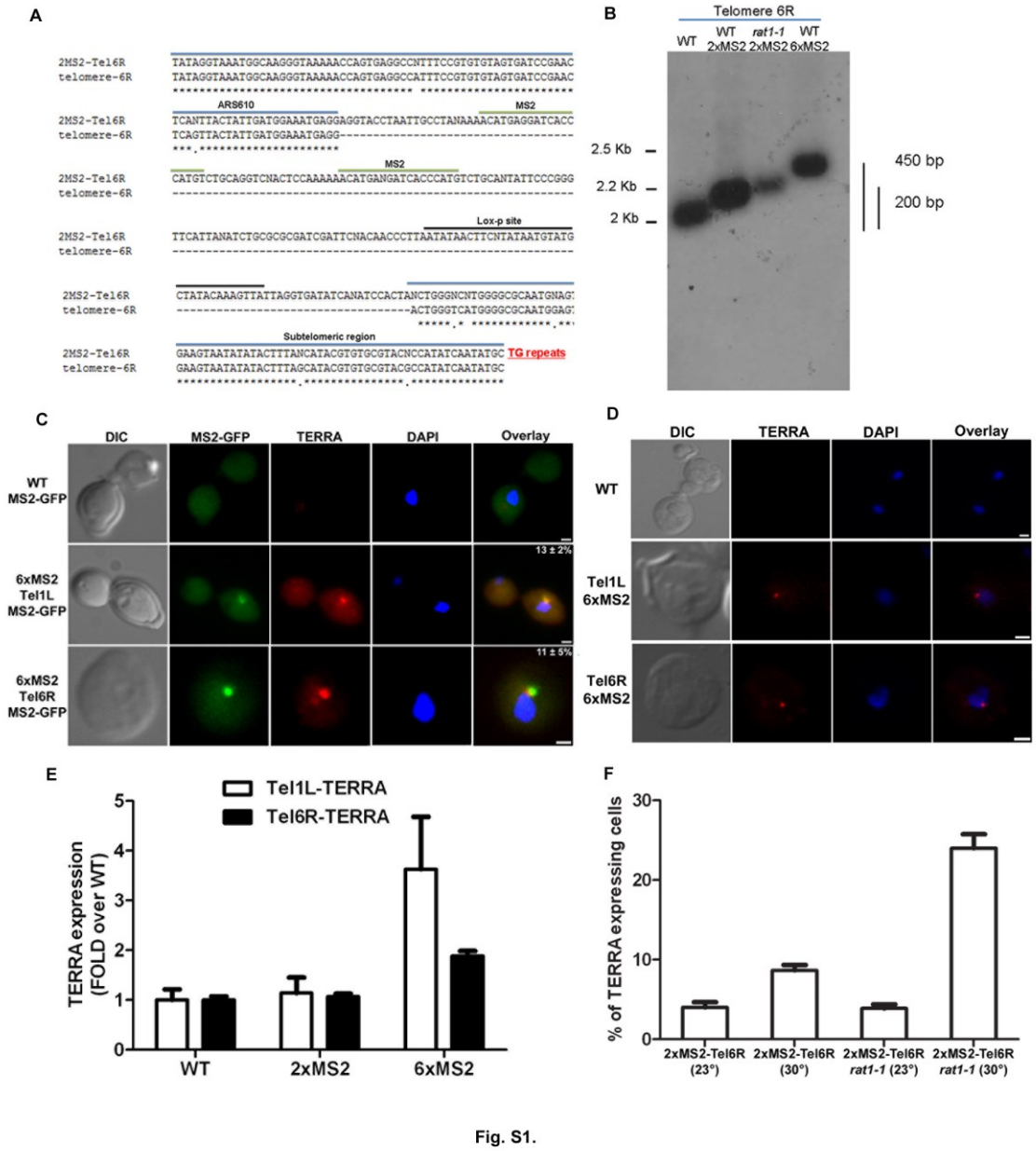

Fig. S1.

Fig. S1. Validation of TERRA-MS2 clones. (**A**) Sequencing analysis confirms that the MS2-tagged telomeres retain full-length native subtelomeric sequence. Sequence alignment of the subtelomeric regions of telomere 6R in 2MS2-Tel6R clone and WT clone. The sequence precedes 5'-3' from top to down, terminating at the nucleotides adjacent to the telomeric repeat tract. The two MS2 sequences and the lox-p site integrated are shown. (**B**) Southern blot analyses confirmed that the integration of the MS2 repeats does not significantly affect the length of the telomeric-repeat tracts of the specific chromosome end. Telomere 6R length analysis by Southern blot in WT, 2xMS2- and 6xMS2-Tel6R-TERRA clones. A telomere 6R specific probe was used for the hybridization (probe sequence: TGTGTAGTGATCCGAACTCAGT). Marker is shown on the left. The expected length of the integrated sequences correspond to 190 nt and 450 nt, for the integration of 2 or 6 MS2 sequences, respectively. (**C**) Fluorescent in situ hybridization on TERRA-MS2 shows co-

localization between Tel6R- or Tel1L-TERRA-MS2 focus (red) and MS2-GFP focus (green). MS2 sequence-specific probe was used to detect TERRA-MS2 transcripts. The percentage of cells where a focus is detected is indicated (mean±SD, N=3). Scale bar: 1 μm. (**D**) Fluorescent in situ hybridization shows perinuclear Tel1L- or Tel6R-TERRA foci in TERRA-MS2 clones not expressing MS2-GFP. RNA-FISH was performed using an MS2 specific probe. TERRA signal is shown in red and nucleus stained by DAPI is in blue. WT: negative control. Scale bar: 1 μm. (**E**) RT-qPCR analysis shows Tel1L-TERRA and Tel6R-TERRA expression levels in WT and TERRA-MS2 clones. Data shown represent mean±SD (N=2). (**F**) Percentage of cells with TERRA-MS2-GFP foci in WT or *rat1-1* background at the indicated temperature. Data shown represents mean ± SD (N=3). At least 300 cells were analyzed in each experiment.

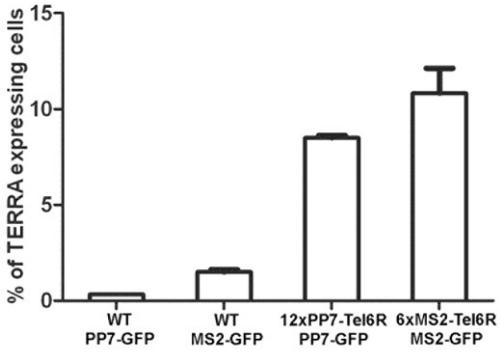

Fig. S2. Validation of MS2/PP7 clones sensitivity. Comparison of 2xMS2-Tel6R-TERRA- and 12xPP7-Tel6R-TERRA foci occurrence. WT cells expressing PP7-GFP or MS2-GFP were counted as controls for the occurrence of non-specific GFP foci. Data shown represent mean SD (N=2). At least 300 cells per clone were counted in each experiment. These results indicate that the specific numbers of MS2 and PP7 repeats used allows a similar sensitivity of the two *in vivo* detection systems.

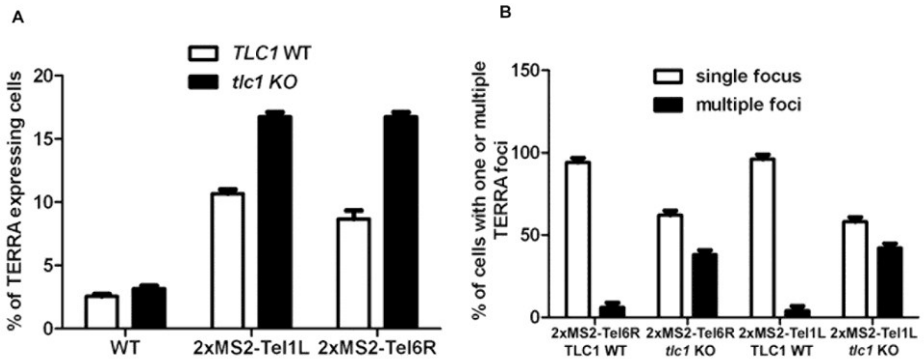

Fig. S3. Quantification of TERRA foci in *tlc1*Δ cells. (**A**) Occurrence of TERRA-MS2-GFP foci in cells containing normal (*TLC1* WT) or shorter (*tlc1*Δ) telomeres. Data shown represent mean ± SD (N=2), in which at least 100 cells expressing TERRA were analyzed for each clone. WT cells expressing MS2-GFP were counted as controls for the occurrence of non-specific GFP foci. (**B**) Quantification of TERRA-MS2-GFP foci in cells with normal (*TLC1* WT) or shorter (*tlc1*Δ) telomeres. Data shown represent mean ± SD (N=2), in which at least 100 cells were counted for each clone.

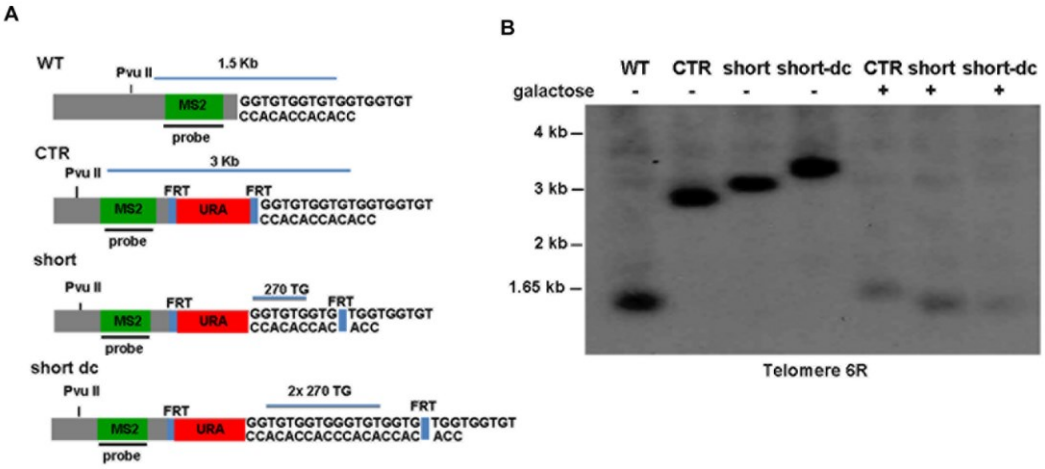

Fig. S4. Southern blot analysis of short inducible telomere 6R. (**A**) Schematic representation of short inducible telomere 6R. Representative images of telomere 6R in wild-type strain with 2xMS2 repeats at telomere 6R (WT), control clone (CTR) and short inducible clones containing a single 270 TG tract (Short) or a double 270 TG tract (Short dc). (**B**) Galactose induction of Flp1 recombinase results in telomere 6R shortening in both short and short dc clones. Telomere 6R length was analyzed using an MS2-sequence specific probe (probe sequence: ACATGAGGATCACCCATGTCTG). The presence of a cassette containing a double 270 TG tract does not induce further shortening of telomere 6R, as compared to the short clone.

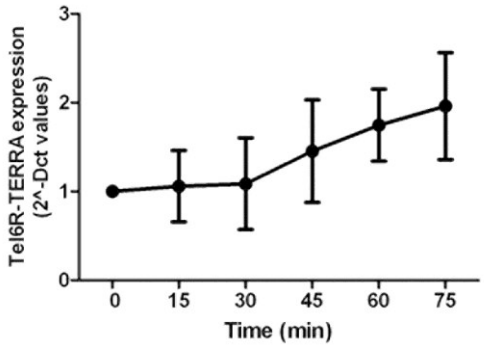

Fig. S5. RT-qPCR analysis of Tel6R-TERRA-MS2 expression in yeast after G1 arrest by α-factor and subsequent release of the cell cycle. Data shown represent mean±SD (N=3). These results confirm that Tel6R-TERRA levels do not significantly vary during the different time points analyzed (see Fig. 3D), suggesting that the enrichment of Tel6R-TERRA at telomere 6R during S phase (30 min timepoint) is not due to the detection of nascent Tel6R-TERRA transcripts.

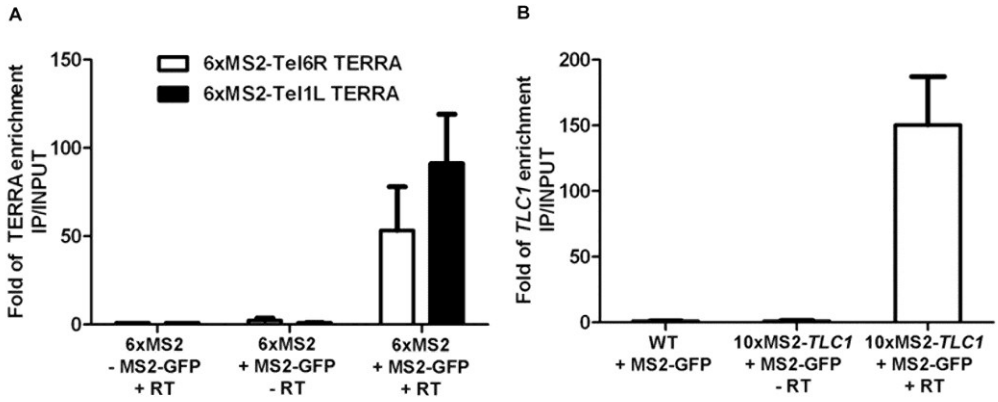

Fig. S6. Control experiments of TERRA-MS2 and *TLC1*-MS2 immunoprecipitation (**A**) RT-qPCR analyses confirm enrichment of TERRA-MS2 in MS2-GFP immunnoprecipitates. TERRA-MS2 transcript enrichment is shown as fold of enrichment of IP samples over INPUT. Data shown represent mean ± SD (N=2). (**B**) RT-qPCR analyzes confirm enrichment of *TLC1*-MS2 in MS2-GFP immunoprecipitates. *TLC1*-MS2 transcript enrichment is shown as fold of enrichment of IP samples over INPUT. Data shown represent mean ± SD (N=2).

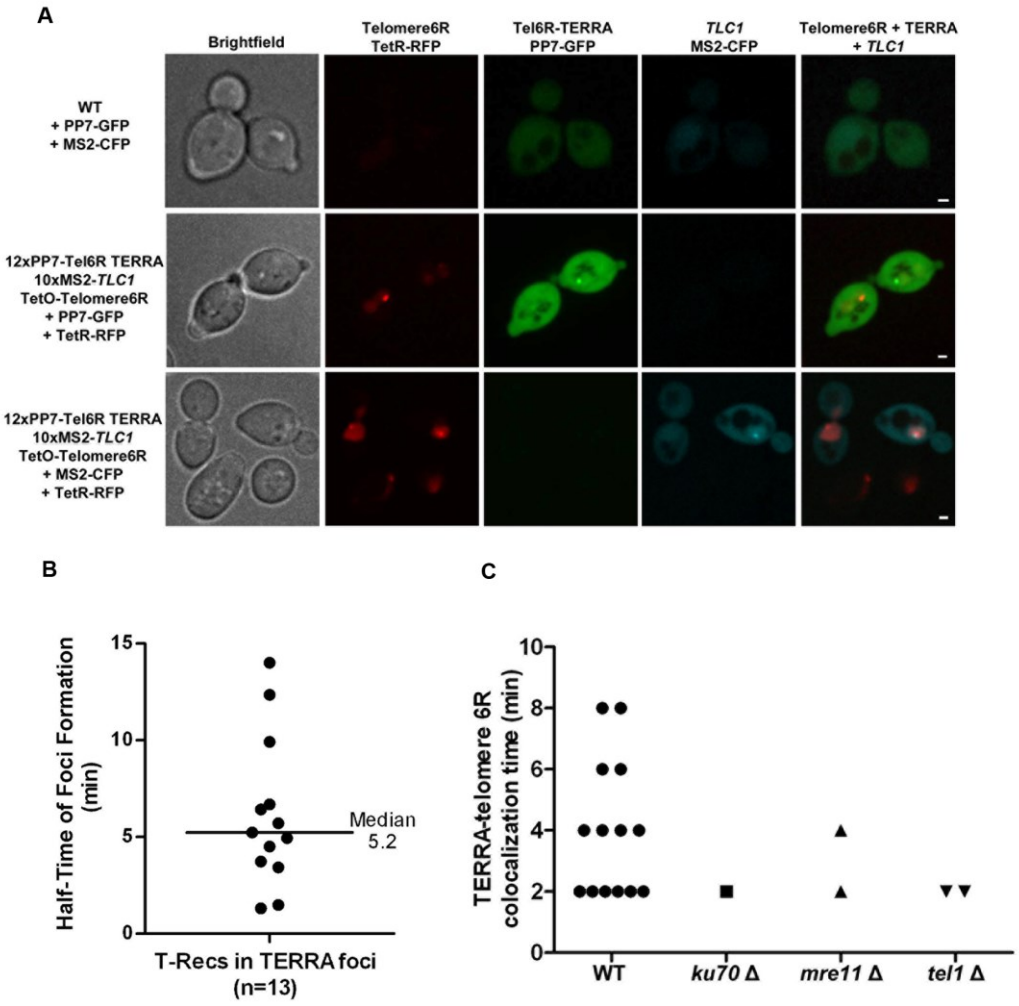

Fig. S7. Control experiments for the simultaneous imaging of Tel6R-TERRA-PP7-GFP, *TLC1*-MS2-CFP and telomere 6R-TetR-RFP in living cells. **(A)** Bleed-through verification experiment. Three color imaging analyses confirm the absence of bleed-through occurrences during acquisitions of TetR-RFP, MS2-CFP and PP7-GFP fusion proteins. Representative confocal microscopy images of clones expressing different combinations of the three fluorescent proteins. Scale bar: 1 μm. **(B)** Half-time of formation of *TLC1* RNA clusters (T-Recs). Thirteen cells showing spontaneous T-Recs formation were analyzed. The areas information calculated using imageJ were plotted on graphs using GraphPad software. Median value is shown. **(C)** Residence time of Tel6R-TERRA focus at the telomere 6R in WT and mutant strains. Each symbol represents a single time course experiment.

Legends of Supplementary Movies

Movie S1. Tel6R-TERRA focus co-localizes with telomere 6R during S phase, related to Figure 4A. Localization of Tel6R-TERRA focus (green) and tetR-RFP labeled telomere 6R (red) was monitored over time by imaging MS2-GFP and tetR-RFP fusion proteins, respectively, using a

spinning disk confocal microscope. Seven Z-stack images were acquired in each channel, at a 2 minutes time interval. Arrowheads point to colocalization events between the two foci. Maximal intensity projection is shown. Scale bar: 1µm

Movie S2. Tel1L-TERRA focus does not colocalizes with telomere 6R in time-lapse experiments. Localization of Tel1L-TERRA focus (green) and tetR-RFP labeled telomere 6R (red) was monitored over time by imaging MS2-GFP and tetR-RFP fusion proteins, respectively, using a spinning disk confocal microscope. Seven Z-stack images were acquired in each channel, at a 2 minutes time interval. Maximal intensity projection is shown. Scale bar: 1µm

Movie S3. Time-lapse imaging of *TLC1* RNA-CFP clustering on a Tel6R-TERRA focus, related to figure 5C. *TLC1-10xMS2* RNA and Tel6R-TERRA-12xPP7 were detected using MS2-CFP and PP7-GFP fusion proteins, respectively, using a spinning disk confocal microscope. Formation of *TLC1* RNA-CFP cluster (red) can be detected as it nucleates on the TERRA-PP7-GFP focus (green). Seven Z-stack images were acquired in each channel, at a 1 minute time interval. Maximal intensity projection is shown. Scale bar: 1µm

Movie S4. Tel6R-TERRA foci and TLC1 RNA clusters co-localize with telomere 6R during S phase, related to figure 6A. Localization of *TLC1-10xMS2* RNA (red), Tel6R-TERRA-12xPP7 (green) and tetO-telomere 6R (pink) was monitored over time by imaging MS2-CFP, PP7-GFP and tetR-RFP fusion proteins, respectively, using a spinning disk confocal microscope. Seven Z-stack images were acquired in each channel, at a 1 minute time interval. Arrowheads point to colocalization events between the three foci. Maximal intensity projection is shown. Scale bar: 1µm

Supplementary Tables

Table S1. Strains used in this study

Strain	**Genotype**	**Source**
FY23	Mat A *ura 3-52 trp1-Δ63 leu2-Δ1*	C. Cole
FY23-2MS2 Tel1L	Mat A *ura 3-52 trp1-Δ63 leu2-Δ1* 2MS2::telomere1L	this study
FY23-6MS2-Tel1L	Mat A *ura 3-52 trp1-Δ63 leu2-Δ1* 6MS2::telomere1L	this study
FY23-2MS2-Tel6R	Mat A *ura 3-52 trp1-Δ63 leu2-Δ1* 2MS2::telomere6R	this study
FY23-6MS2-Tel6R	Mat A *ura 3-52 trp1-Δ63 leu2-Δ1* 6MS2::telomere6R	this study
FY23-2MS2 Tel1L Rap1-cherry	Mat A *ura 3-52 trp1-Δ63 leu2-Δ1* 2MS2::telomere1L	this study
FY23-6MS2-Tel1L Rap1-cherry	Mat A *ura 3-52 trp1-Δ63 leu2-Δ1* 6MS2::telomere1L cherry-KAN::Rap1	this study

FY23-2MS2-Tel6R Rap1-cherry	Mat A *ura 3-52 trp1-Δ63 leu2-Δ1* 2MS2::telomere6R cherry-KAN::Rap1	this study
FY23-6MS2-Tel6R Rap1-cherry	Mat A *ura 3-52 trp1-Δ63 leu2-Δ1* 6MS2::telomere6R cherry-KAN::Rap1	this study
FY23-2MS2-Tel1L/12PP7-Tel6R	Mat A *ura 3-52 trp1-Δ63 leu2-Δ1* 2MS2::telomere1L 12PP7::telomere6R	this study
Rat1-1	Mat α *ura 3-52 trp1-Δ63 leu2-Δ1*	C. Cole
Rat1-1 2MS2-Tel6R	Mat α *ura 3-52 trp1-Δ63 leu2-Δ1* 2MS2::telomere6R	this study
FY23 *tlc1 Δ*	Mat A *ura 3-52 trp1-Δ63 leu2-Δ1 tlc1 Δ::*KAN	this study
FY23-2MS2-Tel1L *tlc1 Δ*	Mat A *ura 3-52 trp1-Δ63 leu2-Δ1 tlc1 Δ::*KAN 2MS2::telomere1L	this study
FY23-2MS2-Tel6R *tlc1 Δ*	Mat A *ura 3-52 trp1-Δ63 leu2-Δ1 tlc1 Δ::*KAN 2MS2::telomere6R	this study
FY23 225-CTR (short inducible telomere 6R-CTR)	Mat A *ura 3-52 trp1-Δ63 leu2-Δ1,* 225-URA::telomere6R Flp1cassette::LEU2 2MS2::telomere6R	this study
FY23 229-short (short inducible telomere 6R)	Mat A *ura 3-52 trp1-Δ63 leu2-Δ1,* 229-URA::telomere6R Flp1cassette::LEU 2MS2::telomere6R	this study
FY23 2MS2-Tel6R 225-CTR	Mat A *ura 3-52 trp1-Δ63 leu2-Δ1,* 225-2MS2-URA::telomere6R Flp1cassette::LEU	this study
FY23 2MS2-Tel6R 229-short	Mat A *ura 3-52 trp1-Δ63 leu2-Δ1,* 229-2MS2-URA::telomere6R Flp1cassette::LEU	this study
FY23 2MS2-Tel6R 242-short-dc	Mat A *ura 3-52 trp1-Δ63 leu2-Δ1,* 242-2MS2-URA::telomere6R Flp1cassette::LEU	this study
FY23 2MS2-Tel1L/112TeTO-Tel6R/TetR-RFP	Mat A *ura 3-52 trp1-Δ63 leu2-Δ1* 2MS2::telomere1L 112TetO-URA::telomere6R TetR-RFP-NAT::chrVII	this study
FY23 2MS2-Tel6R/112TeTO-Tel6R/TetR-RFP	Mat A *ura 3-52 trp1-Δ63 leu2-Δ1* 2MS2::telomere6R 112TetO-URA::telomere6R TetR-RFP-NAT::chrVII	this study
FY23 2MS2-Tel6R/112TeTO-Tel6R/TetR-RFP *ku70* Δ	Mat A *ura 3-52 trp1-Δ63 leu2-Δ1* 2MS2::telomere6R 112TetO-URA::telomere6R TetR-RFP-NAT::chrVII *yku70* Δ::KAN	this study
FY23 2MS2-Tel6R/112TeTO-Tel6R/TetR-RFP *mre11* Δ	Mat A *ura 3-52 trp1-Δ63 leu2-Δ1* 2MS2::telomere6R 112TetO-URA::telomere6R TetR-RFP-NAT::chrVII *mre11* Δ::Hygro	this study
FY23 2MS2-Tel6R/112TeTO-Tel6R/TetR-RFP *tel1* Δ	Mat A *ura 3-52 trp1-Δ63 leu2-Δ1* 2MS2::telomere6R 112TetO-URA::telomere6R TetR-RFP-NAT::chrVII *tel1* Δ::Hygro	this study
FY23 12xPP7-Tel6R	Mat A *ura 3-52 trp1-Δ63 leu2-Δ1* 12PP7::telomere6R	this study
FY23 12xPP7-Tel6R/2xMS2 Tel1L	Mat A *ura 3-52 trp1-Δ63 leu2-Δ1* 12PP7::telomere6R 2MS2::telomere1L	this study
Fy23 10xMS2-TLC1	Mat A *ura 3-52 trp1-Δ63 leu2-Δ1,* 10MS2::TLC1	this study
FY23 12xPP7-Tel6R/10xMS2-TLC1	Mat A *ura 3-52 trp1-Δ63 leu2-Δ1,* 12PP7::telomere6R 10MS2::TLC1	this study

FY23 12xPP7-Tel6R/10xMS2-TLC1/TetO-Kan-Tel6R TetR-RFP	Mat A *ura 3-52 trp1-Δ63 leu2-Δ1,* 12PP7::telomere6R 10MS2::TLC1 112tetO-KAN::telomere6R TetR-RFP-NAT::chrVIIL	this study
W303 *bar*1 Δ	Mat A *ura 3-52 trp1-Δ63 leu2-Δ1 bar1 Δ::LEU2*	R. Wellinger
W303 *bar*1 Δ 6MS2 Tel6R	Mat A *ura 3-52 trp1-Δ63 leu2-Δ1 bar1 Δ::LEU2* 6MS2::telomere 6R	this study

Table S2. Plasmids used in this study

Plasmids	**Source**
pUG6 -lox-p-Kan	P.Chartrand
MS2-pUG6	this study
pFA6-cherry	P. Chartrand
pSH47-Gal1-Cre	P. Chartrand
12xPP7-pUG6	this study
pRS306-112tetO	K. Nasmyth
pRS306-112tetO Tel6R	this study
pFA6-Hygro	P. Chartrand
sp225	S. Marcand
sp225-Tel6R	this study
sp225-2MS2-Tel6R	this study
sp229	S. Marcand
sp229-Tel6R	this study
sp229-2MS2-Tel6R	this study
sp242	S. Marcand
sp242-2MS2-Tel6R	this study
pFV17-Gal1-Flp	S. Marcand
3'TLC1-10xMS2-pUG6-Kan	this study
YCP33-MS2-GFPΔNLS	P. Chartrand
YCP111-MS2-CFP	this study
pTRP-PP7-tomato	D. Zenklusen
pURA-PP7-2xGFP (ADE promoter)	D. Zenklusen

Table S3. Primers used for qPCR in this study

Primers	Sequence
Tel 1L primer S	GGTAATGGAGGGTAAGTTGAGAG
Tel 1L primer AS	CATCCTAACACTACCCTAACACAG
Tel 6R primer S	GTCATGGGGCGCAATGGAGTG
Tel 6R primer AS	TAGCATATTGATATGGCGTACGC
Tel VIIL primer S	ACGGTTATGATGGGCGGTGGA

Tel VIIL primer AS	CTACCCTAACCCTATTCTAACCCAGATC
Tel8R (Y') primer S	CTCGCTGTCACTCCTTACCCG
Tel 8R (Y') primer AS	GGCTTGGAGGAGACGTACATG
TLC1 primer S	CTTAAGCATCGGTTAGGTTTGCG
TLC1 primer AS	AATGAACACACGGTTCCTTCCG
ACTIN primer S	TTCCAGCCTTCTACGTTTCC
ACTIN primer AS	ACGACGTGAGTAACACCATC
RT telomere AS oligo	CACCACACCCACACACCACACCCACA
RT TLC1 primer	CGAAGGCATTAGGAGAAGTAGC

Table S4. Primers used for strains constructions

Primers	**Sequence**
HRchr6prS-MS2-6s	AACCAGTGAGGCCATTTCCGTGTGTAGTGATCCGAACTCAGTTACTATTGATGGAAATGAGGAGGTACCTAATTGCCTAG
HRchr6prS-MS2-6sB	AACCAGTGAGGCCATTTCCGTGTGTAGTGATCCGAACTCAGTTACTATTGATGGAAATGAGGCCAGCTGAAGCTTCGTACG
HRchr6prAS	GGCGTACGCACACGTATGCTAAAGTATATATTACTTCACTCCATTGCGCCCCATGACCCAGTTAGTGGATCTGATATCACC
HRchr1LprS-MS2s	GTAGAGGGATGGATGGTGGTTCGGAGTGGTATGGTTGAATGGGACAGGGTAACGAGTGGAGGCAAGGTACCTAATTGCCTAG
HRchr1LprS-MS2-6s	GTAGAGGGATGGATGGTGGTTCGGAGTGGTATGGTTGAATGGGACAGGGTAACGAGTGGAGGCACCAGCTGAAGCTTCGTACG
HRchr1LprAS	CTACCCTAACACAGCCCTAATCTAACCCTGGCCAACCTGTCTCTCAACTTACCCTCCATTACCCTAGTGGATCTGATATCACC
pUG6-prHR-TEL6R-s	AACCAGTGAGGCCATTTCCGTGTGTAGTGATCCGAACTCAGTTACTATTGATGGAAATGAGGTTAGGTGACACTATAGAACGC
Rap1-5'HRcherry	AAACTGGTTAAAAAGCATGGAACTGGTAGAATGGAAATGAGGAAAAGATTTTTGAGAAGGACTGTTACGGATCCCCGGGTTAATTAA
Rap1-3'HRcherry	TAGAAAACGTGAATCAGTGAAATAAAGGAGTAAAATAAGTTAAACAATGATGTTACTTAATTCAATTACGAATTCGAGCTCGTTTAAAC
3'TLC1-prS	TTCCAAGCGGAAGGAACCGTG
TLC1-3'HR-prAS	GCATACCTCCGCCTATCCGCCTATCCTCGTCATGAACAATCAATTAAAAGCGCTTATAAAGCATAGGCCACTAGTGGATCTG
ku70 Δ S	ATTTGTTAAGTGACTCTAAGCCTGATTTTAAAACGGGAATATTGCTGAAGCTTCGTACGC
ku70 Δ AS	AAATATTGTATGTAACGTTATAGATATGAAGGATTTCAATCGTCTGCATAGGCCACTAGTGGATCTG
tel1 Δ prS	GCAGGAAATTCGAAAAAAAAGCCTTCAAAGAAAAGGGAAATCAGTGTAACATAGACGAAGCTTCGTACGCTGCAGG

tel1 Δ prAS	GTACATTACTTTTCGTATTTCTATAAACAAAAAAAAGAAGTATAAAGCATCT GCATAGCAACTAGTGGATCTGATATCACC
mre11 Δ prS	TTAAGAGAATGCAGACAATTGACGCAAGTTGTACCTGCTCAGATCCGATAAA ACTCGACTGCTGAAGCTTCGTACGCTGC
mre11 Δ prAS	TCGCGAAGGCAAGCCCTTGGTTATAAATAGGATATAATATAATATAGGGATC AAGTACAAGCATAGGCCACTAGTGGATCTG
tlc1 Δ prS	TCAAGGTTCTCAATTAAAAGACCTTCTTTGTAGCTTTTAGTGTGATTTTTCTGG TTTGAGGCTGAAGCTTCGTACGCTGC
tlc1 Δ prAS	TATTTGTATATTGTATATTCTAAAAAGAAGAAGCCATTTGGTGGGCTTTATTA GCATAGGCCACTAGTGGATCTG
ChrVIIL-TetR-RFP-S	AGCAACGCTAATCCTTCTGCC
ChrVIIL-TetR-RFP-AS	AATTCTTGTAAGTCCACTGACGG

Supplementary References

22. F. Gallardo *et al.*, Live Cell Imaging of Telomerase RNA Dynamics Reveals Cell Cycle-Dependent Clustering of Telomerase at Elongating Telomeres. *Molecular Cell* **44**, 819 (2011).

23. F. Gallardo, P. Chartrand, Visualizing mRNAs in fixed and living yeast cells. *Methods in Molecular Biology* **714**, 203 (2011).

24. C. Verheggen *et al.*, Box C/D small nucleolar RNA trafficking involves small nucleolar RNP proteins, nucleolar factors and a novel nuclear domain. *EMBO J* **20**, 5480 (2001).

Chapter V

Expression and localization of TERRA and *TLC1* RNA during yeast growth in diauxic shift and stationary phase

Authors' contribution:

Unless otherwise stated all other figures and analysis were made by Carmina Angélica Pérez Romero

Emilio Cusanelli: first observation of TERRA induction during diauxic shift (Figure 5.1a,b)

Before starting this section let me tell you an interesting anecdote that happened in our journey to uncover the secrets of TERRA.

…Once upon a time after a long day of experiments in normal growing conditions, our yeast cells were left to their own fates in the incubator overnight and over half of the next day. Until finally a curious scientist noticed they had been left there all alone and instead of throwing them away and calling it a day, he went to the microscope and discovered that TERRA was no longer only one single perinuclear foci, but many more and had instead a cytoplasmic localization (Figure 5.1a). After several repetitions and the same phenomenon appearing a stubborn student decided this could not be coincidence and performed a series of experiments and time courses to try understanding the big mystery of this multiple cytoplasmic TERRA foci, and so this story started…

5.1 TERRA expression and localization changes during diauxic shift

In the previous chapter, we described how we used live cell imaging to study the expression of TERRA and its role in the cell cycle regulation of telomerase. In this chapter, we aim to understand how TERRA and *TLC1* RNA might be regulated during the different phases of yeast cell growth.

Yeasts preferred source of carbon is glucose, which is metabolized into ethanol as a by-product of fermentation. When glucose becomes limiting (typically after 1 day of growth), the cells enter diauxic shift, characterized by decreased growth rate and by a metabolic switch to aerobic respiration which utilizes the generated ethanol as a carbon source. When ethanol is depleted from the medium (after 5 days of continues culture), cells enter quiescent or stationary phase G0 (Brauer 2005). Cells in diauxic shift and stationary phase are stressed by the lack of nutrients and by accumulation of toxic metabolites, primarily from the oxidative metabolism, and are differentiated in ways that allow them to maintain viability for extended periods of time (Galdieri 2010). To ensure that the cells we were working with were in the right growth condition (diauxic shift, and stationary stage), the OD_{600} of the culture was continuously monitored, to develop growth curves (Lui 2010).

This growth curves were then used to ensure that we have reached the diauxic shift and stationary phase conditions for each clone in each individual experiment, an example of this growth curve in WT cells can be found on (Figure 5.1).

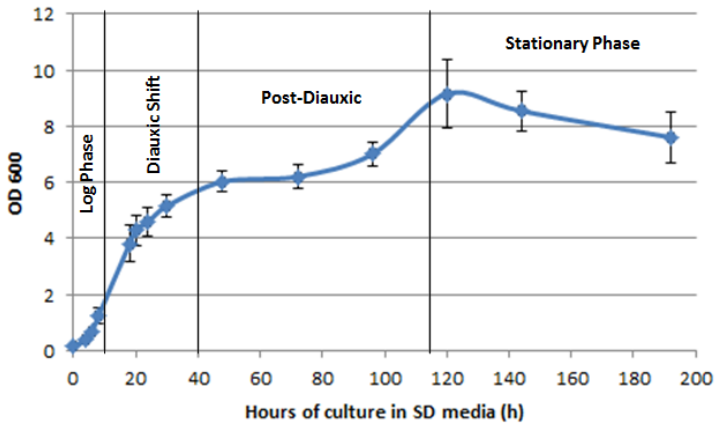

Figure 5.1 WT cells growth curve in SD media. Typical yeast cell growth stages characterized by their culture optical density (y-axis, OD_{600}) and time in culture (x-axis, hours): logarithmic phase, diauxic shift, post-diauxic shift and stationary phase. N=4

Our first observation was that TERRA-MS2-GFP foci were over-expressed and display a cytoplasmic localization when yeast cells are in high density cultures (Figure 5.2a). The experiment was repeated to confirm this intriguing characteristic. Indeed, in yeast cultures at high optical density TERRA foci were more abundant and brighter in all the MS2-TERRA tagged clones tested (Figure 5.2b) and they display a predominantly cytoplasmic localization (Figure 5.2d). Most of the cells expressing TERRA were in G1 or early S (Figure 5.2c). However, cell cycle analysis might not be significant for this growth stages since during diauxic shift cells decrease their growth rate favoring cell population in G1 (Brauer 2005). WT cells expressing MS2-GFP protein were used as control, for GFP aggregation in cells undergoing diauxic shit and stationary phase conditions (Figure 5.2b, and Annex III).

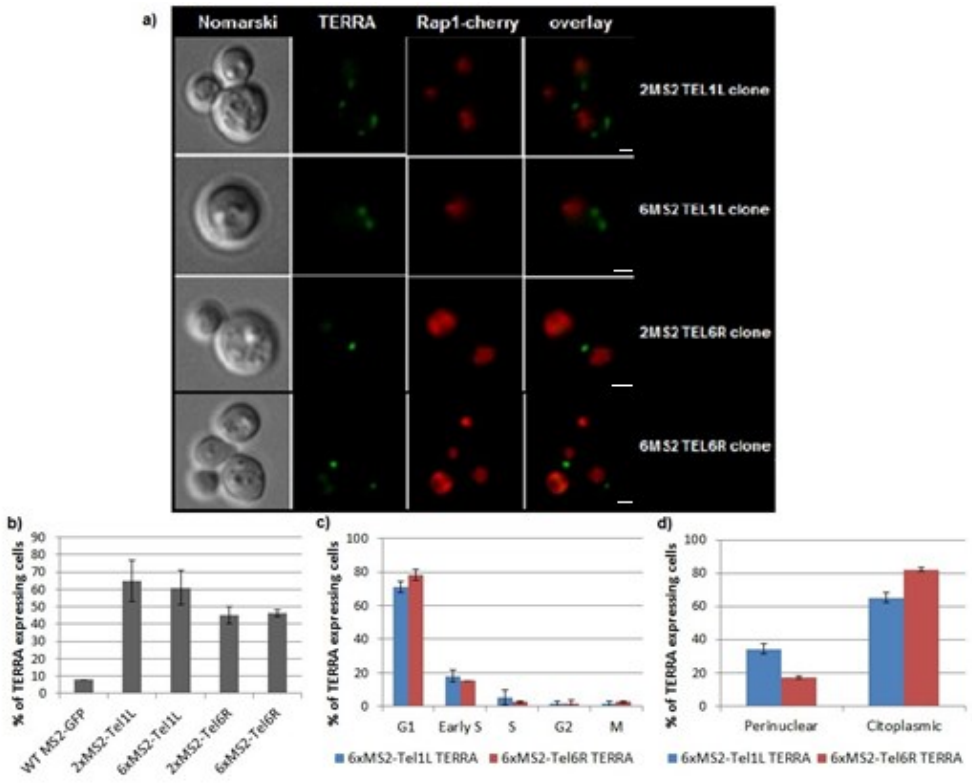

Figure 5.2 TERRA foci induction during diauxic shift. a) Microscopy analysis of the TERRA MS2-tagged clones reveals TERRA localization to be cytoplasmic, with the formation of multiple and brighter foci per cells. TERRA-MS2-GFP foci are in green, mCherry-labeled telomeres are in red by Dr. Emilio Cusanelli. Scale bar: 1 μm. **b)** Percentage of cells expressing TERRA foci in the various clones tested. WT show little background, showing that MS2-GFP protein aggregation is negligible. **c)** TERRA foci are mostly found in G1 yeast cells, due to diauxic shift conditions. **d)** Most of cells presenting TERRA foci have a cytoplasmic localization. A minimum of 300 cells were scored for quantification analysis in each independent experiment N=3.

Therefore, we decided to confirm TERRA overexpression during diauxic shift conditions by RT-qPCR. For this purpose, we grew cells in YPD medium and performed a time course experiment, taking samples every 2 hrs for 18hrs, and then every 8 hrs for a total of 34hrs. Afterwards, total RNA was extracted, TERRA expressed from telomere 6R, 1L and the Y'telomeres was quantified by RT-qPCR. We used the *ALG9* mRNA for normalization, since other commonly used housekeeping genes like actin, are down-regulated during these stages, but not *ALG9* (Teste 2009). This way, we were able to confirm the induction of TERRA during diauxic shift (Figure 5.3). It is important to notice that telomere 6R and 1L TERRA are more highly induced than TERRA expressed from Y' element containing telomeres. Although this result could be due to qPCR primer efficiency

differences, it might also suggest a different regulation of TERRA expression in this condition depending on the kind of telomere they originated from, either X core telomere (like 6R and 1L) or Y' element telomeres.

Since we know that TERRA interacts with *TLC1* RNA *in vivo,* we decided to measure *TLC1* RNA expression by RT-qPCR using samples from the time course. We were able to find a significant (p value=0.0167) up-regulation of *TLC1* expression in diauxic shift compared to its expression during log phase (Figure 5.4). The up-regulation of *TLC1* expression is interesting since most housekeeping genes like actin are known to be down-regulated during diauxic shift (Teste 2009). So we compiled together the *TLC1* and TERRA RT-qPCR data and we were able to observe that *TLC1* up-regulation (OD_{600} 21.5) comes after TERRA over expression (OD_{600} 12.5).

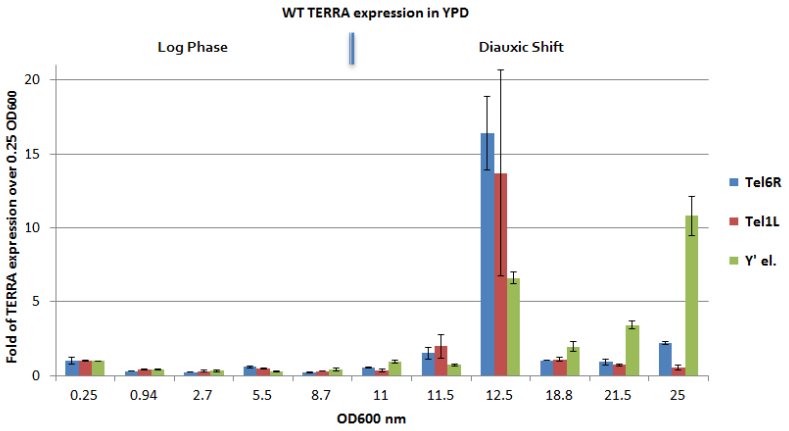

Figure 5.3 TERRA expression is up-regulated during diauxic shift growth. RT-qPCR analysis shows that TERRA expression form all telomeres is at least 7 times higher in diauxic shift compared to its expression level during logarithmic growth than during normal conditions.

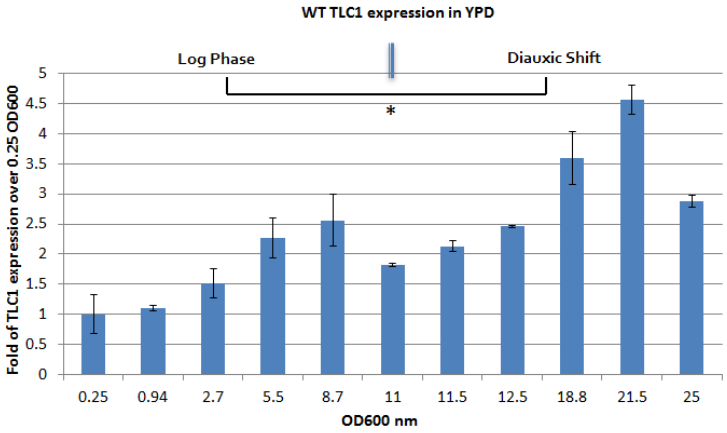

Figure 5.4 *TLC1* RNA expression is up-regulated during diauxic shift. RT-qPCR analysis on *TLC1* RNA at different optical densities of yeast cultures, it shows that its expression is 2 times higher during diauxic shift.

5.2 TERRA and *TLC1* RNA interact *in vivo* during diauxic shift

To further investigate a possible relationship between TERRA and *TLC1* RNA during diauxic shift, we decided to carry out immunoprecipitation experiments in these growth conditions. Surprisingly, after IP of *TLC1* RNA containing 10xMS2 stem-loops using an anti-GFP antibody (we confirmed the enrichment of *TLC1*-10xMS2 RNA by RT-qPCR in Figure 5.5b), we measured an enrichment of telomere 6R/1L TERRA in diauxic shift conditions (Figure 5.5a). Interestingly, we did not found any enrichment of TERRA from the Y' elements, which suggests that TERRA from X core and Y' element telomeres might be differently regulated in this conditions. To confirm the interaction between TERRA and *TLC1* RNA in this stage of cell growth, we performed an immunoprecipitation of Tel6R/1L TERRA from the 6xMS2 tagged clones (we confirmed enrichment of TERRA by RT-qPCR in Figure 5.5d) and measured the enrichment for *TLC1* RNA. We found an enrichment of *TLC1* RNA in the TERRA IP, which confirms a specific interaction between these two RNAs in diauxic shift conditions (Figure 5.5c) since no enrichment was found in any of the WT cells used as control.

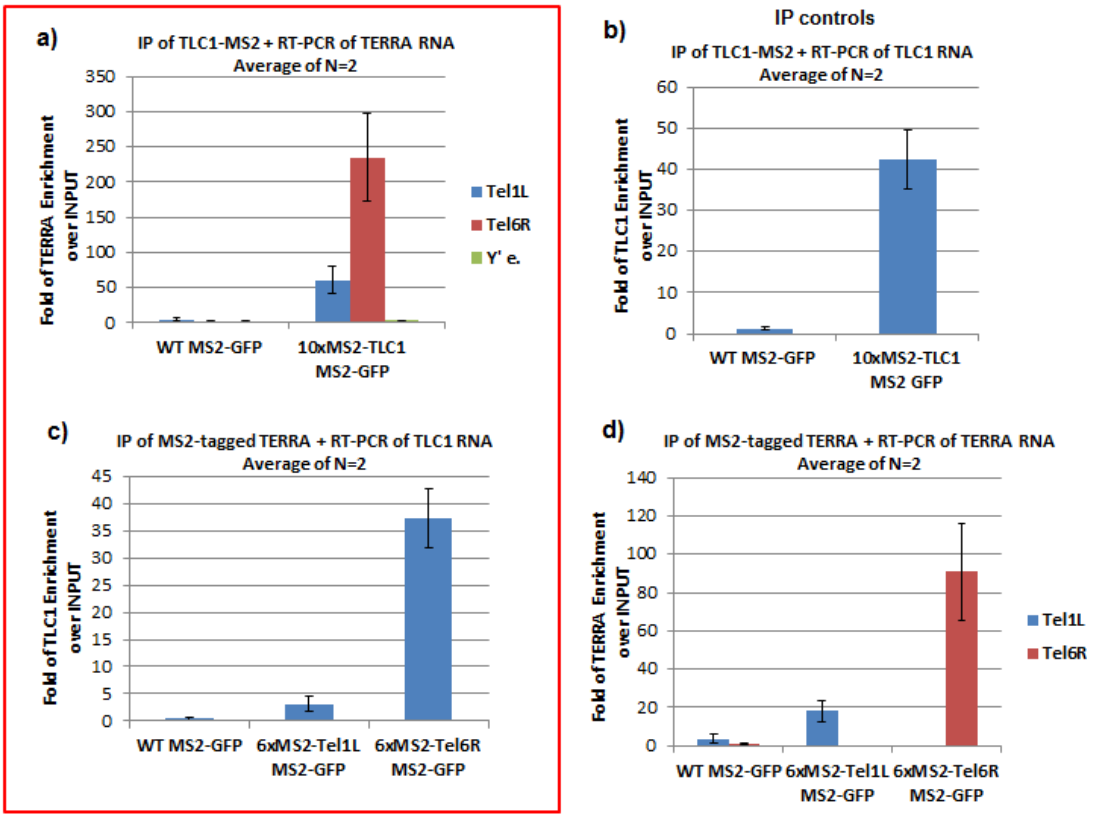

Figure 5.25 TERRA and *TLC1* RNA interact during diauxic shift. a) TERRA from telomere 6R/1L but not from the Y`elements was enriched only in the 10xMS2-*TLC1* RNA IP. **b)** *TLC1* RNA was successfully enriched in the clone containing the 10xMS2 tag, this RT-qPCR was used as a control for the IP of *TLC1* RNA. **c)** TLC1 RNA was enriched only in the 6xMS2 tagged TERRA IP. **d)** TERRA was successfully IP in the clones containing the 6xMS2 tag, this RT-qPCR was used as a control for the IP of TERRA. ALG9 was used for normalization and no signal was seen in any of the minus reverse transcriptase reaction. The culture OD_{600} and TERRA overexpression confirmed by live cell microscopy were used as markers to ensure diauxic shift conditions, for the IP experiment to be performed.

5.3 *TLC1* RNA foci can be observed in the cytoplasm during diauxic shift conditions

Once we found an interaction between *TLC1* RNA and telomere 6R/1L TERRA during diauxic shift conditions, we decided to perform FISH experiments in these growth conditions to confirm TERRA induction and change in their cellular localization, as well as to determine the localization of *TLC1* RNA localization. However, FISH experiments with the normal protocol failed in diauxic shift condition, since the yeast cell wall in this stage is

more resistant, making it harder to digestion by conventional spheroplasting (Klis 2006). Therefore, we optimized the spheroplasting protocol for FISH in order to digest the harder cell walls by using a tube containing 2x the normal amount of oxalyticase and 60 µl of zymolase 5 µg/mL. The cells were left to digest at 30 °C for 20 minutes. FISH was performed on WT cells and 6xMS2 Tel1L/Tel6R TERRA clones, using probes to detect endogenous Tel6R- and Tel1L-TERRA or MS2-tagged TERRA. The U3 RNA was used to control the efficiency of the spheroplasting conditions, and quantify TERRA foci expression and localization. *TLC1* probes were also used to characterize *TLC1* RNA localization during these conditions.

We were able to detect cytoplasmic TERRA and *TLC1* RNA foci (yellow arrows) by FISH in diauxic shift conditions (Figure 5.6a); TERRA foci quantification confirms a significant increase ($p = 0.001$) of foci during diauxic shift compared to logarithmic growth (Figure 5.6b), as well as very significant increase ($p = 0.0003$) in TERRA cytoplasmic localization (Figure 5.6c). *TLC1* RNA foci expression did not show any significant variation during diauxic shift. However, a very significant ($p = 0.0001$) cytoplasmic percentage of *TLC1* RNA was found at the cytoplasm (Figure 5.6d). Since we found that both TERRA and *TLC1* RNA interact during diauxic shift by IP, and we now have evidence that a fraction of TLC1 RNA is found in the cytoplasm during diauxic shift, we may propose that TERRA might play a role in TLC1 RNA export and localization during this growth stage. Although, we would have to label TLC1 and TERRA probes with different flourophores (Cy3.0 and Cy3.5 could be used) and optimize the protocol to confirm this idea by FISH.

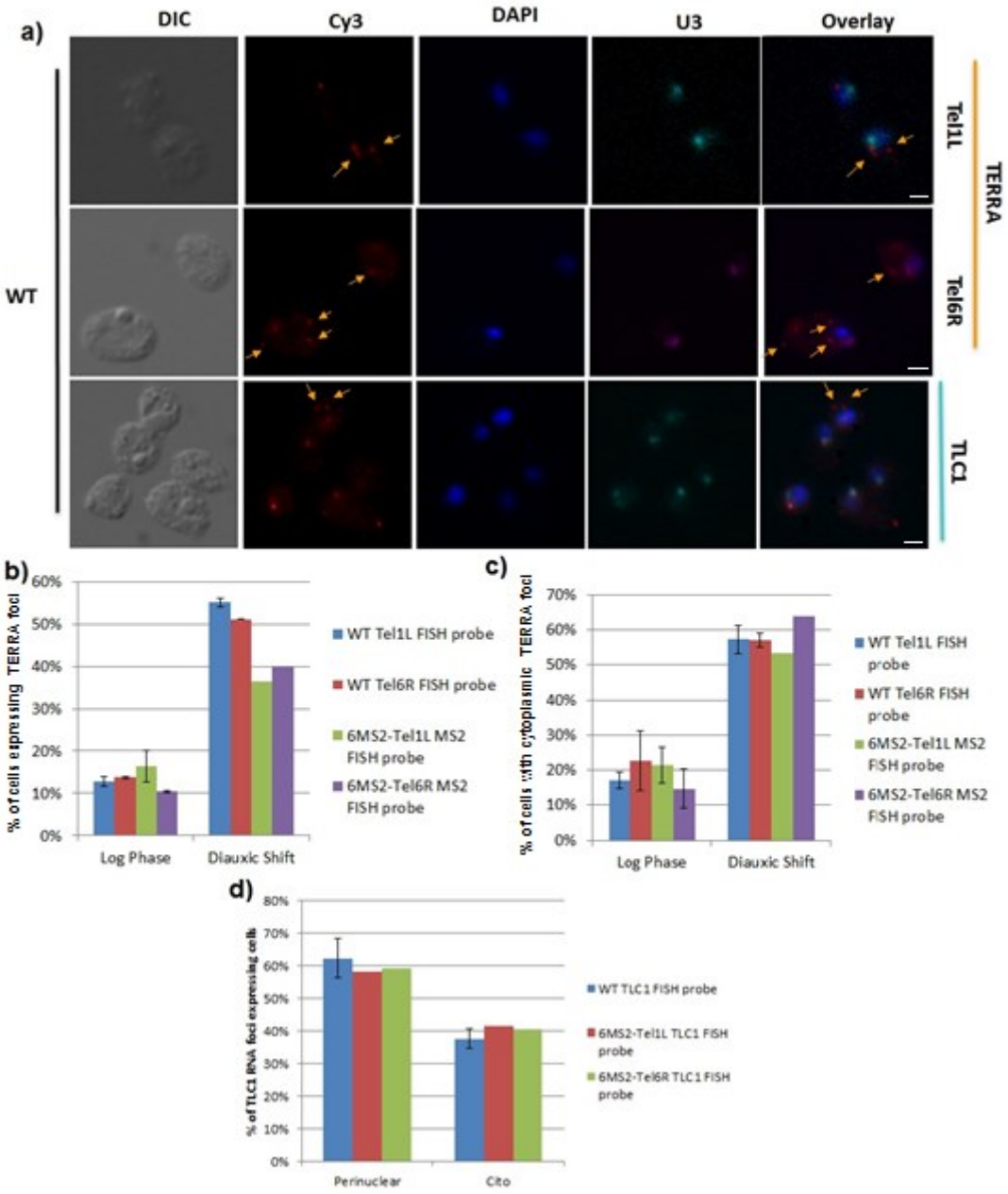

Figure 5.6 Characterization of TERRA and *TLC1* RNA foci during diauxic shift by FISH. a) Quantitative FISH analysis shows cytoplasmic foci of TERRA and *TLC1* RNA (yellow arrows). TERRA foci are in red by endogenous Tel1L- or Tel6R-TERRA FISH probe, and *TLC1* RNA foci are in red by *TLC1* FISH probes in FY23 WT yeast cells. Nuclear DNA is in blue, by DAPI. Nucleolus is in light green or purple, labeled by U3 RNA FISH probe. Scale bar: 1 μm. **b)** qFISH signal in 6xMS2 tagged expressing cells (using MS2 FISH probe) and in WT cells (using endougenous Tel1L/Tel6R TERRA FISH probes) confirm TERRA foci induction in cell population during diauxic shift. **c)** A greater percentage of TERRA foci have a cytoplasmic localization during diauxic shift compared to log phase. **d)** Interestingly, *TLC1* RNA which has a nuclear localization

during logarithmic growth has a significant cytoplasmic fraction in diauxic shift. A minimum of 300 cells were scored for quantification in each independent experiment (N=3).

5.4 TERRA and *TLC1* expression is reduced after diauxic shift and stationary phase, but their foci stay in the cytoplasm

To further investigate the link between TERRA and *TLC1* RNA localization, we decided to perform live cell imaging experiments to assess the localization of these RNAs during cell growth. We followed and counted at least 300 cells of 6xMS2-Tel6R TERRA, 6xMS2-Tel1L TERRA, 10xMS2-*TLC1* and WT cells expressing MS2-GFP and mCherry-labeled Rap1 during logarithmic phase, diauxic shift, post-diauxic shift and stationary phase in three independent experiments.

As shown previously, we observed an induction of telomere 1L/6R TERRA foci in diauxic shift, with a main localization in the cytoplasm. We were able to follow the foci until post-diauxic shift or early stationary phase, where TERRA foci expression was reduced, but their localization was still mainly cytoplasmic (Figure 5.7). However, due to a high level of auto-florescence, we were unable to properly monitor TERRA foci expression during later stationary phase (see Annex I for Tel1L and Annex II for Tel6R TERRA time course).

By live-cell imaging, *TLC1* RNA in normal growth conditions is in the nucleus, in the form of small foci, unless the cell is in late S phase, where an aggregation of active telomerase can be observed, resulting in the formation of *TLC1* clusters or T-Recs that elongate short telomeres (L. C. Gallardo 2011). Surprisingly, we observed *TLC1* RNA clusters in G1, and 28±8% of these clusters showed a cytoplasmic localization during diauxic shift, which is a very significant ($p = 0.012$) difference compared to exclusively nuclear T-Recs found in log phase (Figure 5.8). It is important to notice that the *TLC1* RNA clusters in diauxic shift were found in G1 cells and not in late S phase cells as in log phase. Moreover, *TLC1* RNA clusters expression was unchanged during diauxic shift compared to logarithmic growth, where T-Recs can be identified. However, *TLC1* RNA foci expression

as well as TERRA foci expression was reduced during post-diauxic shift, but increased during late stationary phase (Figure 5.7). The clusters were not caused by the aggregation of the MS2-GFP protein, since WT cells expressing only MS2-GFP show much fewer clusters during diauxic shift and stationary phase (Figure 5.7). Moreover, there is a significant difference (p value ~0.02) between the brightness of these MS2-GFP aggregates compared to *TLC1* RNA clusters or TERRA foci (see Annex III for WT time course).

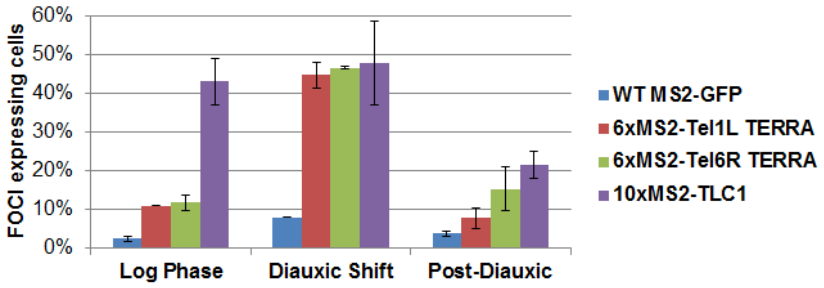

Figure 5.7 Foci expressing cells during different growth stages. Clones expressing Tel1L or Tel6R 6xMS2-taged TERRA, 10xMS2-taged *TLC1* RNA, and WT cells expressing the MS2-GFP protein, were scored during different phases of yeast cell growth: logarithmic growth, diauxic shift and post diauxic stage. At least 300 cells of each clone were scored for each clone and each cell growth stage N=4.

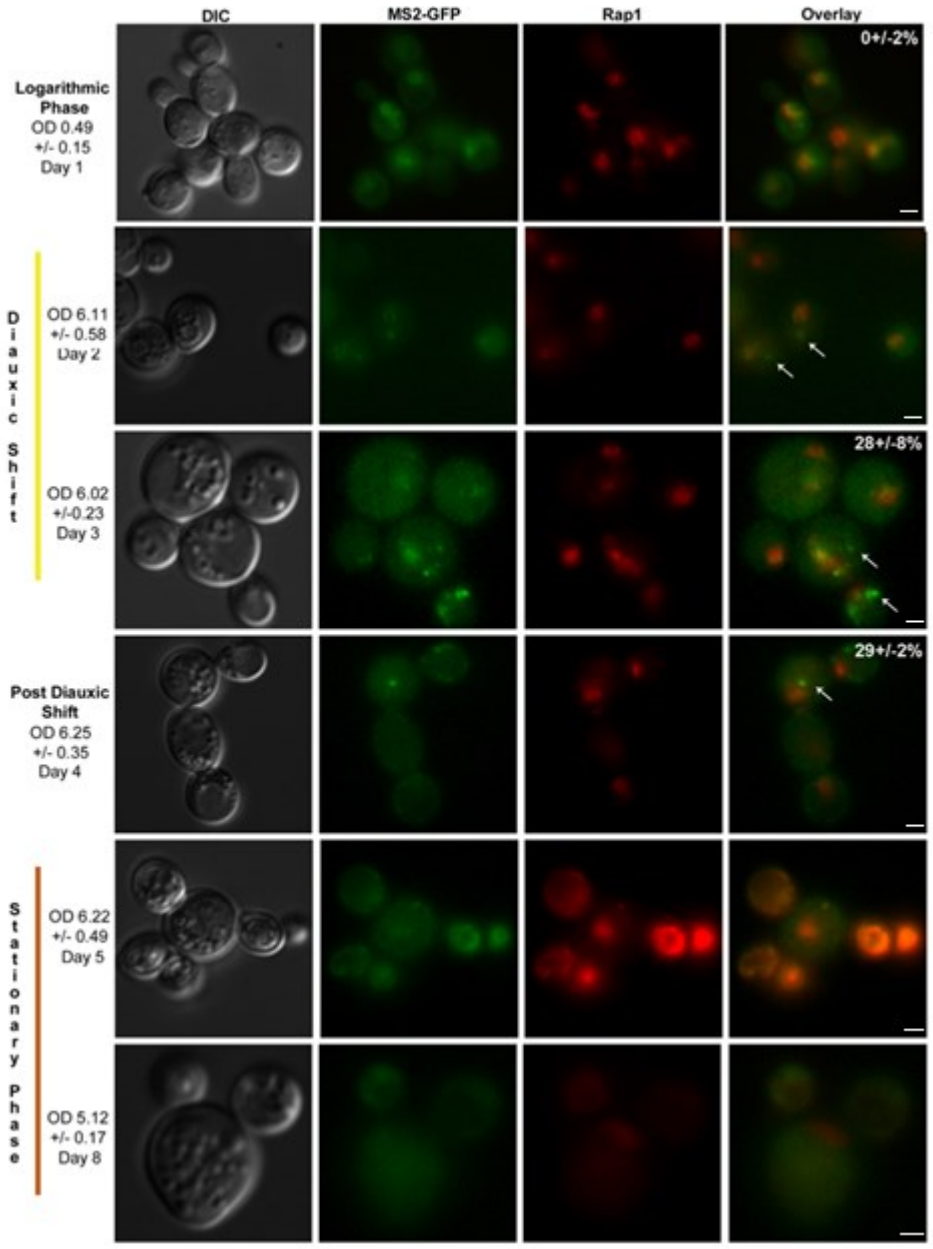

Figure 5.85.4 10xMS2-TLC1 time course during different yeast cell growth stages. Live cell imaging of the 10xMS2-tagged *TLC1* RNA, revealed cytoplasmic *TLC1* RNA (white arrows) cluster formation during diauxic shift and post-diauxic shift conditions. TLC1-MS2-GFP foci are in green, mCherry-labeled telomeres are in red. Quantification of the number of cytoplasmic *TLC1* RNA clusters(superior-right corner of the overlay), indicates a significant cytoplasmic localization of *TLC1* RNA during late cell growth stages compared to logarithmic growth; where *TLC1* RNA has a fuzzy nuclear signal and only form clusters (T-recs) in late S phase were telomerase is recruited to telomeres. A minimum of 300 cells were counted in each independent experiment N=4. Scale bar: 1 μm.

5.5 TERRA and *TLC1* RNA nuclear localization is partially restored in fresh media

After noticing that TERRA and some *TLC1* RNA foci keep a cytoplasmic localization after diauxic shift, we wondered if their nuclear localization could be re-establish if fresh media was added and normal growth conditions were acquired again. For this purpose, cells that had been growing for a week in same media were diluted in fresh media (OD_{600} 0.15), and samples of the culture were taken every 2 hours for a period of 8 hours, then every 24 hours until stationary phase was reached again.

For the 6xMS2-Tel6R TERRA tagged cells, we were able to see that the percentage of Tel6R-TERRA cytoplasmic foci was reduced from 62±9% before glucose to 38±6% after 2h in glucose (Figure 5.9). We did not observe a significant increase in the expression of TERRA foci compared to the number of foci already present before glucose addition by live cell imaging (Figure 5.10a). However, TERRA expression levels 2h after glucose was added is very low, similar to the levels seen in logarithmic phase by RT-qPCR in WT cells (Figure 5.10b), although this cells are in lag phase. This may suggests that a significant ($p = 0.002$) amount of TERRA foci get imported back into the nucleus. The old cells take more than a couple of hours to restart cell division, which can be seen by the slow increase in OD_{600} after addition of glucose. However, after 6 and 8 hrs of growth in fresh media, cells reach the logarithmic growth phase (Figure 5.9). In this phase, we observe an increase in TERRA expression, by both microscopy (Figure 5.10a) and qPCR (Figure 5.10b) and TERRA foci are mainly nucleopasmic (73%). However, the percentage of cells with cytoplasmic foci is still slightly higher ($p. = 0.013$) than in normal logarithmic conditions (Figure 5.9), which suggest that a percentage of TERRA stays cytoplasmic. After 24 hrs of growth in fresh media, TERRA expression levels go back to normal logarithmic growth levels in the RT-qPCR analysis (Figure 6.10b), although TERRA foci count in live cell analysis and the optical density of the culture demonstrate cells are in diauxic shift conditions (Figure 6.9, 6.10a). After 48h and 72h, the cells go thru diauxic shift, and then into stationary phase following a similar trend as the live microscopy experiment. The

difference between the RT-qPCR results and the live cell experiments could be due to RNA degradation during the RT-qPCR, so this experiment should be repeated once more and with different set of primers to make the RT-qPCR these results more reliable.

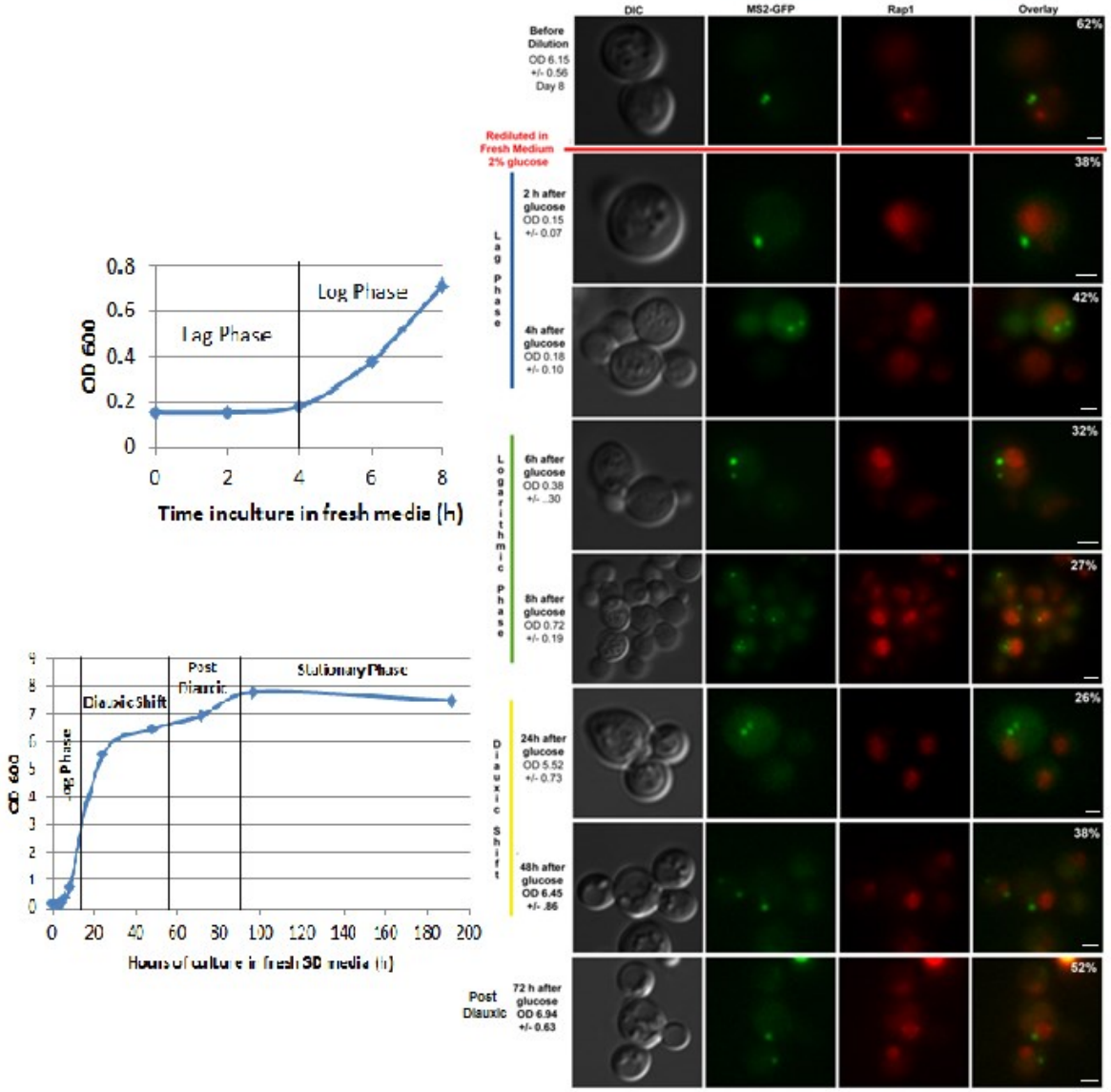

Figure 5.9 6xMS2-Tel6R TERRA time course after old cell were diluted in fresh media. *On left panel,* optical density of the culture in fresh glucose SD media was monitored to develop, growth curves that let us know in which phase of yeast cell growth we were on (OD_{600}, y-axis. hours of culture in fresh media, x-axis). The cell growth stages are noted: lag, log, diauxic shift, post diauxic and stationary phase. Logarithmic growth conditions are reached after 6h and 8h, diauxic shift conditions are reached at 24h and 48h. *On the right panel*, live cell imaging of the 6xMS2-Tel6R TERRA, revealed that the cytoplasmic TERRA foci fraction (superior-right corner of the overlay) dropped shortly after cells were diluted in fresh media. TERRA-MS2-GFP foci are in

green, mCherry-labeled telomeres are in red. A minimum of 300 cells were counted in each independent experiment N=2. Scale bar: 1 μm.

Cells from the 6xMS2-Te1L TERRA clone were unable to recover any visible phenotype shortly after glucose addition. However, they developed survivors after 72h of culture and TERRA foci were able to be visualized by microscopy (Figure 5.10a). Interestingly, RT-qPCR experiment using WT cells which have been through the same growth process reveals that Tel1L and Y'element TERRA follow a similar trend as Tel6R TERRA described above (Figure 5.10b).

WT cells expressing MS2-GFP were used as control for microscopy experiments, and no significant GFP foci aggregation was observed in these cells during the time course (Figure 5.10a). RNA was extracted from WT cells at each time point to perform RT-qPCR analysis (Figure 5.10b,c).

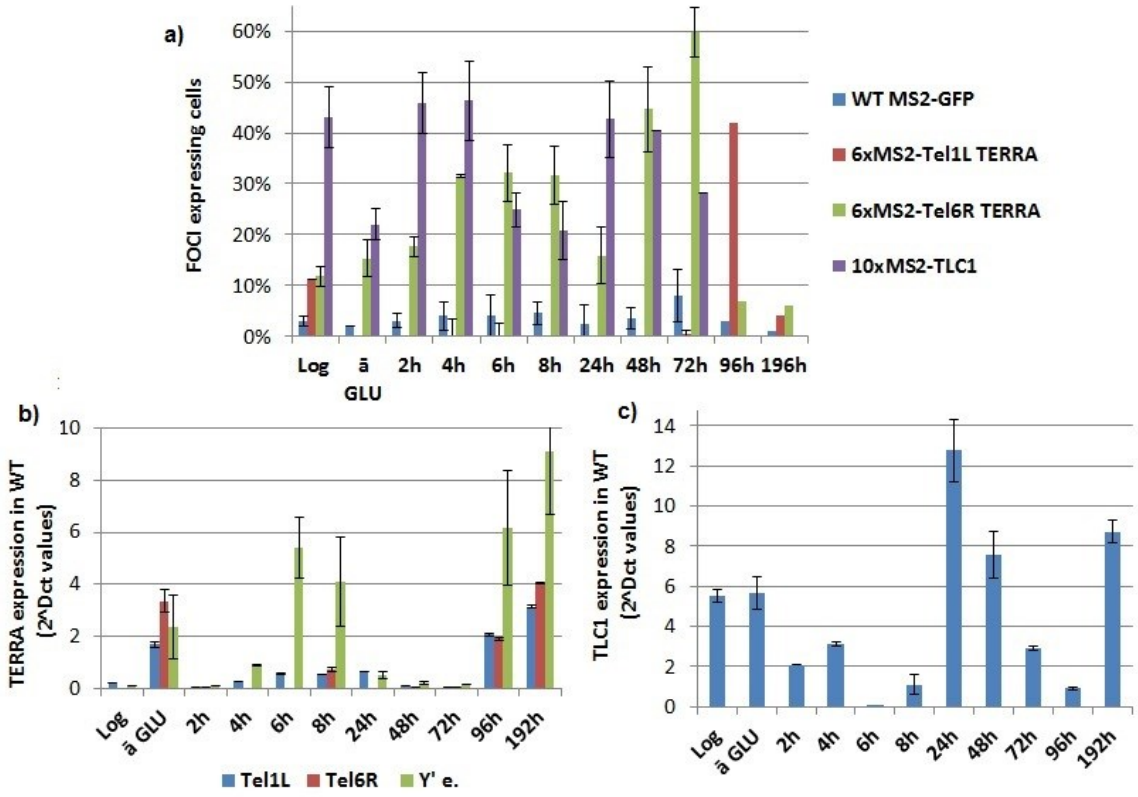

Figure 5.105.5 Characterization of TERRA and *TLC1* RNA expression after old cell were diluted in fresh media. Please note that the time line shown in these graphs are absolute however, due to clonal differences the cells might reach diauxic shift conditions at different time points **a)** At least 300 cells were counted to determine TERRA and *TLC1* foci expression N=2. **b)** TERRA

expression levels in WT cells during the time course as calculated by qPCR 2^Dct values. **c)** TLC1 RNA expression levels in WT cells during the time course. Note: normal logarthimic growth conditions were included in graphs for easy expression comparison (Log), the time point before glucose fresh media was added is also included for the analysis (ā GLU). *ALG9* mRNA was used as for normalization of the qPCR analysis.

A similar time course was performed using yeast cells expressing *TLC1-10xMS2* RNA to determine the localization of *TLC1* clusters during the time course. In cells expressing 10xMS2-TLC1 RNA, we were able to observe a small but significant ($p = 0.0003$) decrease of *TLC1* clusters in the cytoplasm 2 hrs after glucose addition, from 29±2% to 22±-2% (Figure 5.11). While an increase of *TLC1* clusters was observed by live cell imaging after 2 hrs (Figure 5.10a), this increase is not due to new transcription of *TLC1* RNA, since *TLC1* expression levels are lower than in normal logarithmic conditions (Figure 5.10c). These results let us argue that a small nuclear TLC1 RNA may be taking place between the 2 hours after glucose was added, however cells will have to be continuously monitored in finer time points to be able to confirm a cyto-nucleoplasmic trafficking of TLC1 RNA. After 6 or 8 hrs of culture, cells finally reach logarithmic growth conditions, and during this period, *TLC1* clusters accumulation and *TLC1* RNA expression is the lowest (Figure 5.10a, c). It would have been expected by this point that all or most of *TLC1* clusters had a nuclear localization. However, still 22+/-2% of T-recs foci had a significant ($p = 0.0001$) cytoplasmic localization (Figure 5.11), this suggests that *TLC1* RNA might play another role in the cytoplasm after stress, or a fraction of it might be getting targeted for degradation, however further experimentation is needed to arrive at any conclusion. After 24h of growth in fresh medium, cells reach diauxic shift condition, we see an increase in T-recs foci formation as well as an over expression of *TLC1* RNA by qPCR (Figure 5.10a, c). We were surprised to find that at this time point *TLC1* RNA expression was much higher than in any other time points. This made us believe that the up-regulation of telomerase might be due to the need of re-lengthening a short telomere. After 48h the cells go into diauxic shift condition without any big change in T-recs or TLC1 expression, and after 72h the cell are in post-diauxic shift conditions were expression levels following a similar trend as the live microscopy experiment described before.

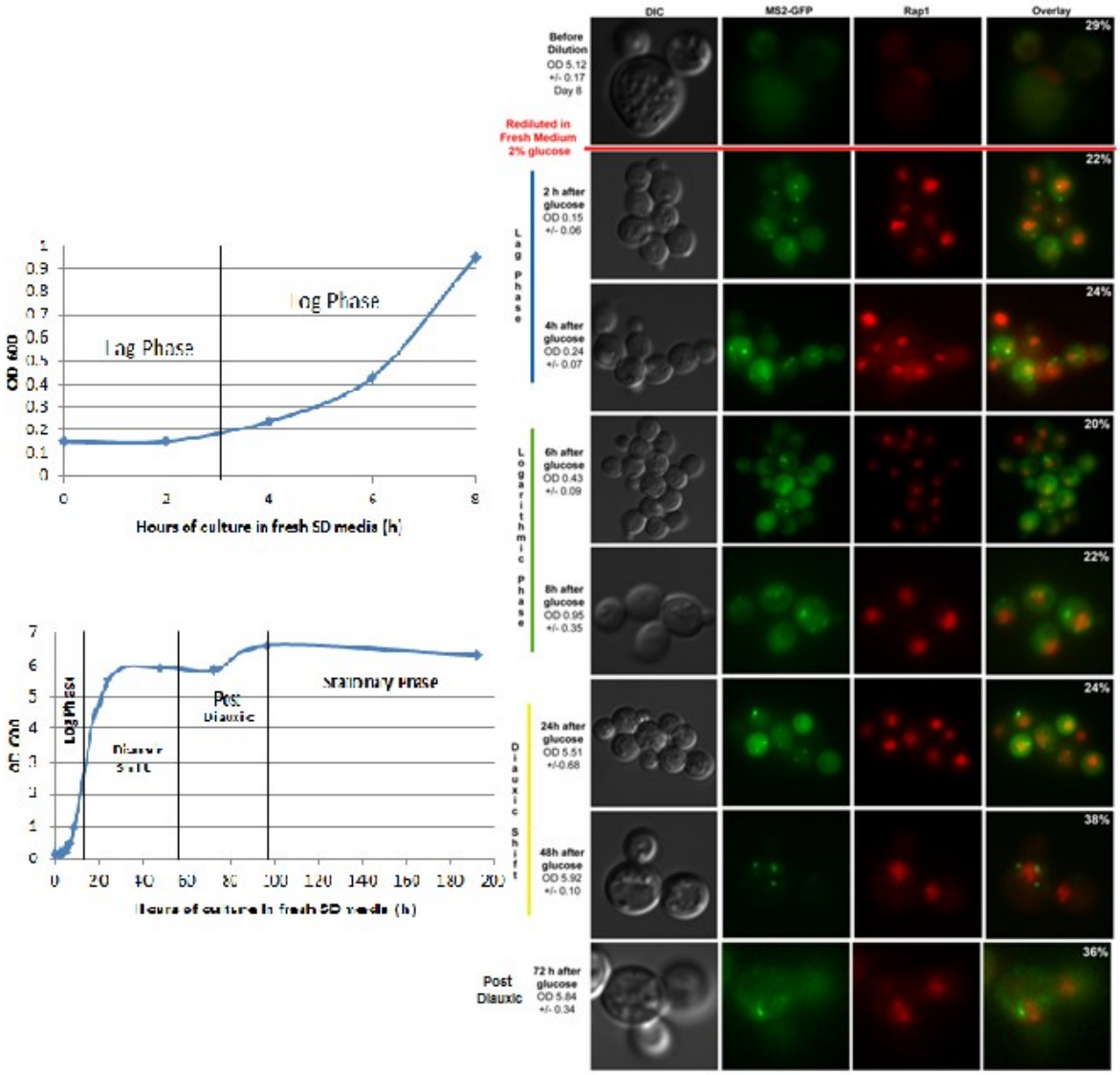

Figure 5.11 Time course of *TLC1*-10xMS2 RNA cluster localization. *On left panel,* optical density of the culture in fresh glucose SD media was monitored to develop, growth curves that let us know in which phase of yeast cell growth we were on (OD_{600}, y-axis. hours of culture in fresh media, x-axis). The cell growth stages are noted: lag, log, diauxic shift, post diauxic and stationary phase. Logarithmic growth conditions are reached after 6h and 8h, diauxic shift conditions are reached at 24h and 48h. *On the right panel*, live cell imaging of the *TLC1*-10xMS2 RNA, revealed that some of the cytoplasmic *TLC1* RNA clusters (superior-right corner of the overlay) dropped shortly after cells were diluted in fresh media. TLC1-MS2-GFP foci are in green, mCherry-labeled telomeres are in red. A minimum of 300 cells were counted in each independent experiment N=2. Scale bar: 1 μm.

Since we saw the sudden over expression of *TLC1* RNA as the cells were entering the second diauxic shift after 24hr of growth in fresh media, we sought to assess the telomere length conditions during this time course experiments.

5.6 Telomere shortening occurs before, *TLC1* RNA expression increases, which restores telomere length

To determine the length of telomeres by Southern blot analysis, we extracted DNA from 6xMS2 Tel6R/Tel1L TERRA tagged clones and WT cells at each time point of the time course described above. We determined the length of telomere 6R in the 6xMS2 Tel6R-TERRA clone by digesting the genomic DNA with PvuII, and this telomere was detected using an MS2 probe (Figure 5.12). We did not find any significant difference in telomere size at the beginning of the time course. However, we were surprised to find no signal at 24h, and a slightly shorter telomere 48 and 72hrs after fresh media was added. We confirmed that there was DNA in the sample taken at 24h, since DNA gel was run and checked before blotting (data not shown), but we were unable to see any signal on the southern blot. This result might had been due to telomere shortening, since the DNA band might have been so small that it might pass through the membrane during the blotting which unable use to see any result.

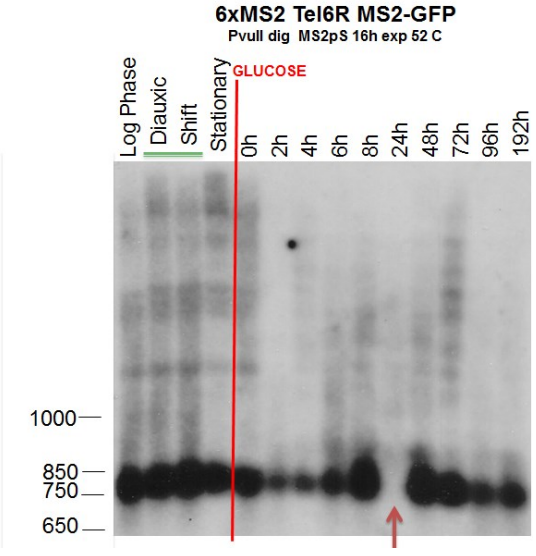

Figure 5.12 Southern blot analysis of 6xMS2-Tel6R-TERRA time course. The expected 6xMS2-tagged telomere 6R size is ~800 bp with the conditions mentioned in the upper part of the blot. No signal can be seen at 24h and a slightly shorter telomere can be observed after this time point, suggesting telomere shortening just before second diauxic shift happens.

To confirm this model, we measured the length of telomere 6R in WT cells that have been through the same time course experiment. Genomic DNA was digested with PvuII, transferred on a nylon membrane and hybridized at 53°C using the GprobeTel6R probe (Figure 5.13). Interestingly, we were able to confirm the shortening of telomere 6R in WT cells after 24h of culture in fresh media when the second diauxic shift started. A full recovery of telomere size was also observed after 72/96h of culture, corresponding to post-diauxic shift and stationary phase conditions.

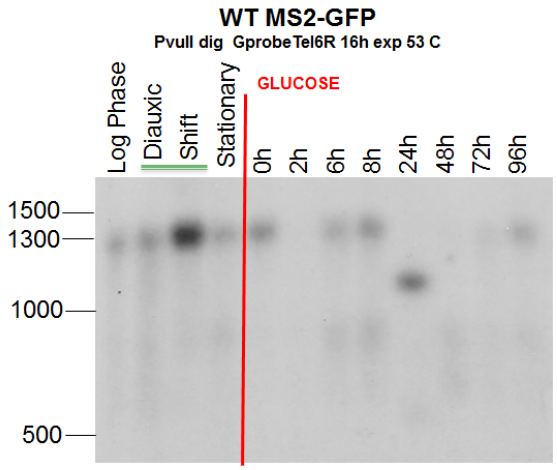

Figure 5.13 Southern blot analysis of WT + MS2-GFP cells time course. The expected WT telomere 6R size is ~1350 bp with the conditions mentioned in the upper part of the blot. Telomere 6R shortening can be confirmed 24h after fresh media was added, while normal telomere size is attained after 72h of culture.

In order to demonstrate that the telomere 6R shortening observed at 24h in both 6xMS2-Tel6R TERRA and WT clones is real and is not an artefact of DNA degradation, we performed a control experiment by blotting a specific gene that could be visualized with a PvuII digested genomic DNA. We stripped both membranes and hybridized using a probe against the *SIR4* gene (Figure 5.14). Since we were able to detect a specific band for the *SIR4* gene in all the time points, we were able to confirm that the shortened telomere 6R band detected at 24hrs by Southern blot (Figure 5.12 and 5.13) is due to telomere shortening, and is not an artefact due to blotting or DNA degradation.

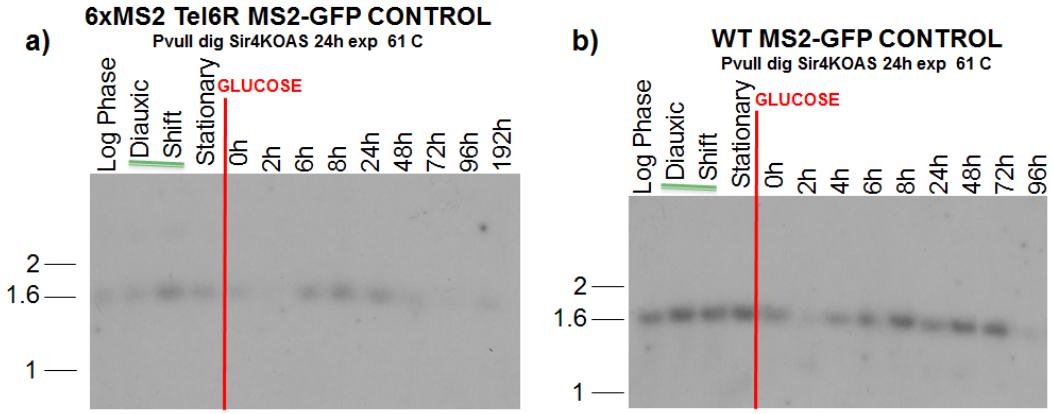

Figure 5.14 Southern blot control analysis. The expected size for Sir4 gene in is ~1350 bp with the conditions mentioned in the upper part of the blots. **a)** Sir4 gene in the 6xMS2-tagged telomere 6R blot. Note that a band can be seen at the 24h time point, were no band was seen before due telomere 6R shortening. **b)** Sir4 gene in the WT + MS2-GFP time course. No blotting artifact or DNA quality problems were found in any of the control southern blot.

The absence of telomere shortening in the first diauxic shift might be explained by the low amount of time points taken at this stage, where telomere shortening and its repair might occur between the 24 hour time points missing the event, therefore higher resolution time points must be done on this stage to show telomere shortening is also happening at this stage, as we find evidence of telomere shortening before/during the second diauxic shift. Interestingly, we can observe that the shortened telomere is lengthen is restored when the cell reaches post-diauxic shift and stationary phase conditions.

These results show for the first time that telomere shortening might be happening during diauxic shift in yeast cells. It will be adventurous, but interesting to propose that re-lengthening of short telomeres must be achieved before cells can achieve a quiescent stage in stationary phase. Since quiescent yeast cells in stationary phase are known to have normal telomere lengths (Ashrafi 1999).

5.7 Three-color live cell imaging confirm cytoplasmic TERRA and *TLC1* RNA cluster during diauxic shift

In the previous chapter, we described how we used the MS2 and PP7 systems to label TERRA and *TLC1* RNA in live cells. Recently, we used this clone containing 112-

tetO repeats integrated at telomere 6R, with Tel6R-TERRA labeled with 12PP7 stem-loops, and *TLC1* RNA labeled with 10MS2 stem-loops, to confirm TERRA and *TLC1* RNA cytoplasmic localization during diauxic shift. The cells were grown until diauxic shift was reached, and imaged in a confocal microscope to detect TERRA-PP7-GFP foci, *TLC1*-MS2-CFP clusters and Telomere6R-TetR-RFP. TERRA and *TLC1* RNA foci as well as co-localization events between TERRA/*TLC1,* TERRA/telomere6R, and *TLCI*/telomere6R were quantified. Seven hundred cells were quantified, a minimum of 100 cells expressing TERRA and *TLC1* were qualified for their co-localization status (69 of these cells were co-expressing TERRA/*TLC1* foci).

Preliminary results show that TERRA foci and *TLC1* clusters co-localize in the cytoplasm in 64% of the cells co-expressing both foci (Figure 5.15), these TERRA/*TCL1* clusters are dynamic as can be seen in Movie 5. These results in conjunction with the immunopresipitation experiments carried out during diauxic shift confirm the cytoplasmic localization of TERRA and *TLC1* RNA and the *in vivo* interaction between this two RNAs during diauxic shift.

Interestingly, during early diauxic shift (18 to 24h after cell culture) 14% of the cells expressing TERRA foci co-localize with telomere 6R (Figure 5.15), but only 1% of the cells expressing *TLC1* RNA clusters and TERRA foci co-localize with telomere 6R. Which suggests that perinuclear TERRA fraction may plays a role in telomere maintenance, while cytoplasmic TERRA/*TLC1* cluster may have a yet un-described function.

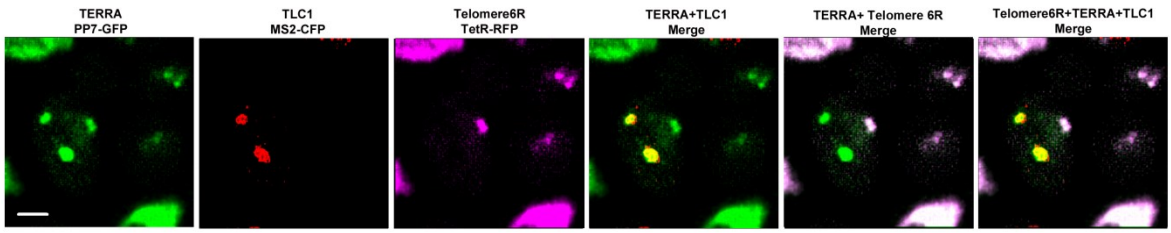

Figure 5.15 Three color live cell imaging during diauxic shift. Microscopy analysis of the 12xPP7-Tel6R TERRA, *TLC1*-10xMS2 and TetO-Telomere6R, reveals TERRA and *TLC1* RNA foci co-colocalizing in the cytoplasm (TERRA+TLC1 merge), while a part of TERRA foci co-localizes with telomere6R (TERRA+Telomere6R merge). TERRA-PP7-GFP foci are in green, *TLC1*-MS2-CFP clusters are in red, telomere6R-TetR-RFP is in pink. Scale bar: 1 μm.

Movie 5 TERRA and *TLC1* RNA co-localize in the cytoplasm during diauxic shift. Tel6R-TERRA foci and *TLC1* RNA clusters co-localize in the cytoplasm (related to figure 5.15), while a TERRA foci co-localize with telomere6R. TLC1-10xMS2 RNA (red), Tel6R-TERRA-12xPP7 (green) and tetO-telomere 6R (pink) was monitored over time by imaging MS2-CFP, PP7-GFP and tetR-RFP fusion proteins, respectively, using a spinning disk confocal microscope. Seven Z-stack images were acquired in each channel, at a 1 minute time interval for 20 minutes. Maximal intensity projection is shown.

Interestingly, during a time course experiment of this clone during diauxic shit, we were able to find evidence of TERRA export to the cytoplasm in one of the cells. At the beginning Tel6R-TERRA foci was co-localizing with its telomere, however after 15 minutes the foci was exported to the cytoplasm, were the foci disappeared (Figure 5.16 and Movie 6). Unfortunately, this cell was not expressing *TLC1*-MS2-CFP, therefore more time courses and co-localization analysis must be done to understand how *TLC1* and TERRA cytoplasmic export occur, as well as to find the significance of this result.

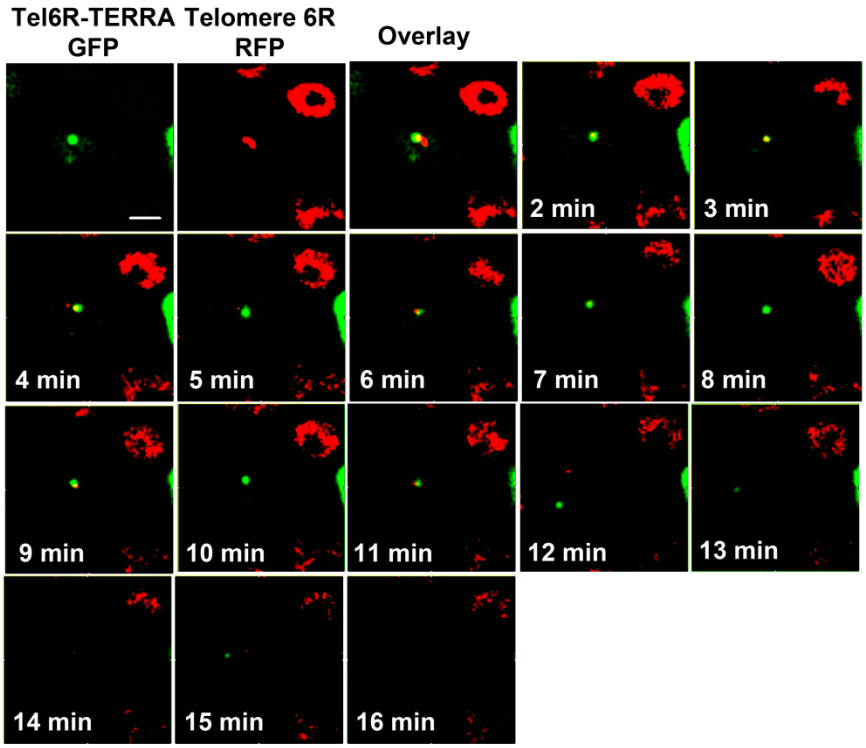

Figure 5.16 TERRA co-localize with telomere 6R and later get exported to the cytoplasm. Time course microscopy analysis of the 12xPP7-Tel6R TERRA, and TetO-Telomere6R, reveals TERRA co-localizes with telomere 6R for 10 minutes during early diauxic shift before, getting exported into the cytoplasm, were the TERRA foci disappears. Persumably by RNA degradation, although photo-bleaching should also be considered. TERRA-PP7-GFP foci are in green, Telomere6R-TetR-RFP clusters are in red. Time points every 1 minute. Scale bar: 1 μm.

Movie 6 TERRA foci co-localize with its telomere and later get exported into the cytoplasm. Tel6R-TERRA foci and telomere 6R co-localize for 10 minutes during early diauxic shift before,

getting exported into the cytoplasm, were the TERRA foci disappears. Persumably by RNA degradation, although photo-bleaching should also be considered. The cell was not expressing TLC1-10xMS2 RNA. Tel6R-TERRA-12xPP7 (green) and tetO-telomere 6R (red) was monitored over time by imaging PP7-GFP and tetR-RFP fusion proteins, respectively, using a spinning disk confocal microscope. Seven Z-stack images were acquired in each channel, at a 1 minute time interval for 16 minutes. Maximal intensity projection is shown.

Further experiments and the repetition of the dilution of stationary phase cells in fresh media utilizing these clones could shed light on the function of the cytoplasmic function of TERRA/*TLC1* clusters during late cell growth stages.

All these experiments led to more questions than answers, to the mystery of the cytoplasmic TERRA foci, the observations carried out here are just the tip of the treasure waiting to be uncovered under the sand… with what we now have, we can only suppose on what can be find underneath it… and that is where most of my discussion next will focus on…

So now bear with me and my crazy ideas a little longer as you get welcome to this student mind…

Chapter VI

Discussion

The first step in our journey to uncover the mysteries behind TERRA was to find a way to detect TERRA transcripts expressed from a unique telomere in single WT cells, since its study in budding yeast has been limited due to its rapid degradation by the Rat1p exo-nucalease (P. R. Luke 2008). So we used cytological approaches which involve the use of the MS2-GFP system to detect transcribed TERRA from the telomeres to enable to study its localization and expression in live cells. However, first we needed to prove that the system did not affect our subject of study, so the MS2 system had to be validated for use with this non-coding RNA.

6.1 WT TERRA from a single telomere can be visualized in a single cell *in vivo* with the MS2 system

Although we knew that TERRA was expressed from the telomeres in yeast and mammalian cells (P. R. Luke 2008) (Shoeftner, 2008) the transcription starting site of TERRA in budding yeast had yet not been mapped. Therefore, we inserted the MS2 stem-loop sequences very close to the telomeric repeats, to ensure we were only tagging TERRA. We did all the required experimentation to ensure that the addition of these sequences affected the telomere length no more than expected, and that it had a single integration. However, we had no evidence that the sequences were inserted after the transcription starting site for TERRA, until last year a group successfully mapped the transcription starting site of Telomer1L TERRA (Pfeiffer 2012), which allowed us to confirm that we had indeed tagged it correctly.

Apart from that we were able to demonstrate by quantitative FISH and *in vivo* experiments that TERRA was expressed predominantly as single foci in a small population of wild type cells (10-15%) and had a perinuclear localization. These results confirmed that our system did not affect TERRA expression levels and its localization in WT cells.

We think that TERRA may be able to move in various sections of the nucleus, but spends more of its time at the nuclear periphery, which we are able to easily appreciate by FISH and *in vivo* analysis. To enhance our level of localization accuracy in our *in vivo*

analysis we believe that the use of other live cell markers such as Nup49 or Nup60 (nucleoporins used as a nuclear pore live cell marker) and Nop2 (yeast nucleolar marker used in imunoflourecense, live cell imaging use hasn't yet been validated) could provide us better accuracy to measure TERRA localization and export to the cytoplasm, while allowing us to perform a more accurate cell cycle analysis (Drubin 2006).

Since the MS2 stem loop was shown to stabilize some mRNAs (Tyagi 2009), we performed IP experiments to check that the 5' end of TERRA was present as well as the 3' end of it, and we were able to find enrichment in both cases, although the enrichment in the 5' end was found to be lower, we believe this is due to primer and IP differences, and not due to stability. This was further demonstrated by the use of Rat1p temperature sensitive KO in the MS2-tagged TERRA where we saw an increase of TERRA upon depletion of Rat1p suggesting that Rat1p is still degrading TERRA in WT cells, without affecting its stability. Although we will need to perform RNA half-life studies to make sure its stability is unchanged, we believe our results provide enough evidence to prove that the MS2-GFP system can be used to tag TERRA from a single telomere without affecting its expression and localization, in WT yeast cells.

6.2 TERRA is induced in short telomeres

By being able to observe TERRA expression from a single telomere, we were able to show that only a small fraction of cells stably express TERRA from a specific telomere. Why do these few cells express TERRA from that specific telomere, compared to the majority of the cells in the population? Our results suggest that in this small population, the TERRA-expressing telomere is short, which leads to TERRA expression and accumulation.

It has been previously shown that forced transcription of TERRA from a single telomere results in its telomere shortening in yeast (Maicher 2012) (Pfeiffer 2012). Interestingly, studies in cancer cell lines which are characterized by their short telomeres show elevated TERRA levels (W. X. Deng 2012), and in different human cell lines telomere lengthening resulted in TERRA repression (Arnoult 2012). Our results show that TERRA levels are up-regulated *in cis* when telomere shortening occurs in a *tlc1*Δ strain or

in a strain containing a short inducible telomere; and telomere re-lengthening by telomerase results in a progressive decrease of TERRA levels.

These results demonstrate that rather than TERRA up-regulation being the cause of telomere shortening, as it being the result of telomere shortening in normal cellular conditions in yeast. It has been shown that the yeast telomeric-repeats DNA-binding protein Rap1 recruits inhibitory factors to telomeres, such as Sir and Rif proteins that repress TERRA expression (Iglesias et al., 2011). We can thus hypothesize that short telomeres, containing a smaller number of Rap1 binding sites, exhibit a weaker or attenuated repressive effect on TERRA expression. Similarly, telomere re-lengthening gradually reestablishes TERRA repression by restoring the missing number of telomere binding proteins. This hypothesis is supported by the fact that TERRA levels are up-regulated in *rif1*, *rif*2, and *rap1-17* mutant strains (Iglesias et al., 2011).

Our results then suggest a negative feed-back loop in TERRA regulation as the yeast telomere lengthens, similar to the one seen in mammalian cells. Therefore, TERRA expression could be used as a marker of telomere shortening in a cell population.

6.3 TERRA promotes telomerase nucleation prior to telomerase recruitment to telomeres

We show that endogenous TERRA transcripts interact with the yeast telomerase RNA *TLC1 in vivo* by immunoprecipitation experiments. It is important to note that in these experiments (Figure 3.10 and 3.11) our IP FOLD enrichment and variation between experiments (standard deviation) gave a better quality in *in vivo* IP data when endogenous TLC1 was pulled down as compared with endogenous TERRA pull down, this might be due to the expression level differences in this two RNA's where TLC1 expression is considered to have a housekeeping function in yeast being always expressed (S. a. Lange 2004), in contrast with the low level of expression we have seen in yeast TERRA's so far. Nevertheless, we were able to show that TERRA and telomerase RNA transcripts interact with each other *in vivo*.

While it is not yet clear if this interaction is direct, these results are in agreement with previous findings obtained in mammalian cells, where TERRA molecules interact with both human telomerase RNA (hTR) and human telomerase reverse transcriptase (hTERT) *in vivo* (Redon et al., 2010). In mammalian cells, TERRA mimicking oligonucleotides inhibit telomerase activity *in vitro* (Redon et al., 2010) (Schoeftner, 2008b). While these findings suggest a potential role of TERRA as a telomerase inhibitor, direct evidence of this function *in vivo* is still missing (Farnung et al., 2012) (Shoeftner, 2009).

Using three color live cell imaging we were able to visualize the nucleation of *TLC1* RNA molecules on TERRA foci in late G1/early S phase cells. These nucleation events lead to the formation of telomerase clusters or T-Recs, which have been previously described as the active form of telomerase at telomeres in S phase (Gallardo et al., 2011). Indeed, we were able to follow and find that the T-recs/TERRA foci co-localized with the TERRA telomere of origin, presumably short, during late S phase.

Our data contradict the current model of TERRA acting as a telomerase inhibitor and instead at least in yeast, it shows that TERRA acts in the recruitment of the active telomerase complex since: 1) TERRA is expressed when a telomere shortens, 2) TERRA is recruited on its telomere of origin in S phase, when telomere elongation occurs, 3) TERRA interacts with *TLC1* RNA, and this complex is recruited simultaneously and preferentially on the telomere of origin of TERRA, 4) association of TERRA with its telomere depends on factors involved in telomerase recruitment at telomeres (Mre11, Tel1 and yKu70).

These results suggest a novel function for TERRA as a scaffold for the spatial organization of telomerase molecules into a cluster or T-Recs. This scaffold-like activity of telomeric non-coding RNA is similar to what has been proposed for a growing number of long non-coding RNAs (lncRNAs) (Tattermusch 2011). Indeed, several studies have shown that lncRNAs play important roles in the recruitment of protein complexes to specific chromosome loci in order to control chromatin structure (Tsai et al., 2010; Wang and Chang, 2011) or induce the formation of nuclear bodies (Mao et al., 2010; Shevtsov and Dundr, 2011). While most of these nuclear lncRNAs act co-transcriptionally to recruit protein cofactors, TERRA acts *in trans* to assemble a telomerase cluster, but is then recruited with telomerase to its telomere of origin.

We propose a model in which a threshold of telomere erosion induces TERRA expression (Figure 6.1). Upon transcription, TERRA molecules are rapidly displaced from their telomere of origin and accumulate into a focus. In early S phase, a TERRA focus acts as a seed to nucleate the *TLC1* RNA, directly or via binding to different telomerase components, leading to the formation of a T-Rec. Later in S phase, the T-Rec is recruited to the telomere from which TERRA originates, which would then be elongated by telomerase. Thus TERRA expression might represent a signal induced by short telomeres to trigger telomerase clustering and subsequent telomere elongation.

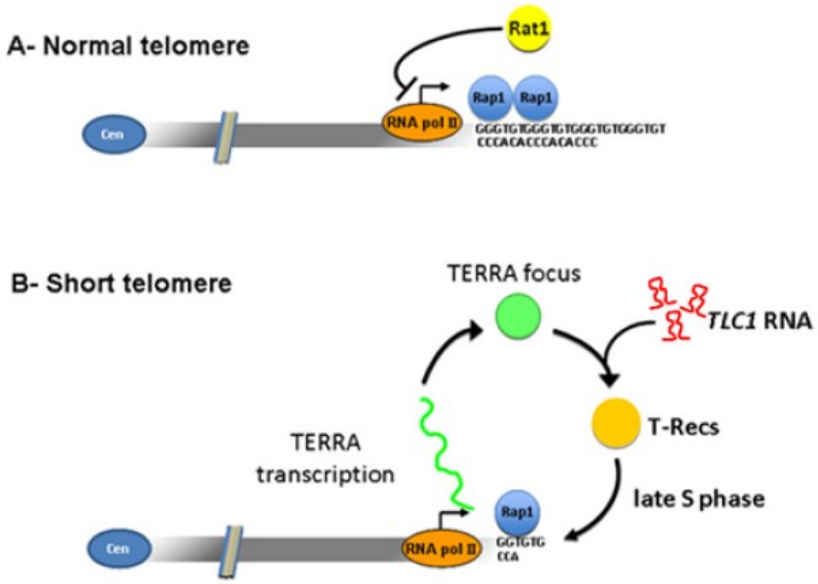

Figure 6.1 Model of yeast TERRA function in normal growth conditions. a) Normal WT yeast telomere have long telomeric repeats sequences, bound by Rap1p with the help of the Rat1 exo-nuclease negatively regulate telomeric transcription **b)** When yeast telomere length characterized by the loss of telomeric binding proteins reaches a shortened threshold, TERRA transcription get activated, TERRA molecules form into a foci that recruits telomerase RNA and nucleates its molecules into active T-recs foci in late G1/early S phase. This TERRA/T-recs complex then is recruited to the TERRA's short telomere of origin, where it is elongated by active telomerase.

6.4 TERRA levels and localization are changed during diauxic shift due to cellular stress

Our results in normal growth conditions have so far revealed a function for TERRA, which is expressed as a single perinuclear foci in a low population of WT cells, that its expression could be used as a marker of short telomeres and that it acts as a scaffold for

nucleation of telomerase RNA (TLC1) resulting in telomere elongation. Interestingly, we saw a great change in this pattern when yeast cells were subjected to other growth conditions like diauxic shift and stationary phase. Although not much is known about these late phases of yeast cell growth they are characterized by cell cycle arrest, a vast change in gene expression and cell differentiation which allows the cells to maintain viability for extended periods of time (Lui 2010). It has been shown that cells in diauxic shift and stationary phase are stressed by the lack of nutrients and by accumulation of toxic metabolites, primarily from the oxidative metabolism (Drummond 2011). These yeast cell growth stages have been proposed by some researchers as a good complex stress model, which could be used to model aging conditions in single eukaryotic cells (Galdieri 2010). Therefore studying TERRA and TLC1 in these conditions could give an insight on their regulation and function during stress, aging and diseases such as cancer.

Several cellular stresses have been described to influence TERRA levels and its localization including heat shock, DNA damage, oxidative and proliferative stress (Schoeftner, 2009). For example, TERRA levels have been found to be up-regulated in early cancer evolution in a variety of human cancer cells and replicative stress; these cells are characterized by large TERRA foci that do not co-localize with normal DNA damage response foci like γH2AX foci, promyelocytic leukemia (PML) or Cajal bodies by FISH, which suggest that TERRA RNA aggregates may form a novel nuclear body in highly proliferating mammalian cells (W. X. Deng 2012). They also propose that higher levels of TERRA result from a DNA damage response that protects telomere ends by promoting telomeric heterochromatin formation during conditions of proliferative stress (N. W. Deng 2009). Uncapping of the telomere due to oxidative stress leads to an increase in expression of TERRA that depends on epigenetic marks (Caslini 2009). Stress caused by heat-shock in mouse cell has been show to increase TERRA levels as well a number of nuclear foci per cell, interestingly TERRA levels drop back to almost normal levels once cells were shifted to normal conditions, indicating that heat shock-induced telomeric transcription is reversible and tightly regulated during stress (Shoeftner, 2008b). Interestingly in human cells, other poly-adenylated non-coding RNA transcribed from pericentric heterochromatic SatIII repeats, and NEAT also increase in response to thermal stress, and are involved in

the formation of nuclear stress bodies (Valgardsdottir 2005), and paraspeckles (Lakhotia 2012).

Although the function of TERRA in any kind of these stresses are still unknown, we can see that its induction seems to be a common factor in response to most kinds of cellular stress in human cells. Interestingly, we find a similar increase in TERRA transcription during diauxic shift conditions where the cell is undergoing a complex stress response caused by glucose starvation, DNA damage and oxidative stress (Galdieri 2010). Indeed, preliminary results in our laboratory have shown that yeast TERRA foci increase if cells are subjected to glucose starvation, and DNA damage induced by bleomycin. Intriguingly, TERRA foci localization seems to be different depending on the biological process they are undergoing, for example in cells that have undergone DNA damage and in cells with short telomeres caused by the deletion of TLC1 RNA, TERRA foci levels increase but do not show an obvious cytoplasmic localization. However, if cells are subjected to glucose starvation or diauxic shift conditions, the cytoplasmic localization of TERRA fociincreases, this might suggest two different pathway of TERRA regulation during stress in yeast: one where TERRA localization is mainly nuclear and plays a role in telomere protection in accordance to the finding in mammalian cells, and a second one with a novel cytoplasmic localization which might play a role in cell viability and survival when complex metabolic changes occur.

6.5 TERRA might be regulated by/or regulate metabolic changes in yeast

Global gene expression changes occur due to glucose limitation during diauxic shift. Interestingly, many proteins involved in metabolic change and mechanisms to maintain cell viability and survival are found in the sub-telomeric repeat areas of most yeast telomeres and are induced during different kinds of stress, as can be seen summarized in the next Table 6.1. An important fact to note is that many X core telomeres have alcohol dehydogrenase and proteins involved in metabolic changes and use of other glucose source. Meanwhile, the Y' element telomeres contain helicases which are highly expressed when

telomerase is deleted and proteins involved in survival and stress response. Therefore, sub-telomeric regions might be subjected to different transcriptional regulation depending on the kind of stress condition.

Telomere	Type	Sub-telomeric protein coding genes	Expressed/involved in
1R	X	dehydrogenase?, PHO11	phosphate starvation
1L	X	PAU8, SEO1	Permease
2R	X	COS2, MAL32, PAU24, PHO89, PCA1	anaerobic conditions/early growth phase
2L	Y	helicase?, PAU9, PCK1, SRO77, SEA4	cell wall remodelling
3R	X	AAD3, ROS1, ADH7, PAU3, GIT3	fermentation regulated by oxygen
3L	X	GEX1, VBA3, MRC1, CHA1, VAC17	oxidative stress, Sphase check point
4R	Y	YRF1-1 helicase?, PAU10, FDC1	in TLC1 KO
4L	X	COS7, MPH2, SOR2, HXT15, THI3, AAD4, LRG1	oxidative stress, mitochondria, low glucose levels, cell wall integrity
5R	Y	YER 188W, YRF1-2 helicase?, PUG1	anaerobic conditions, in UV damage
5L	Y	RMD6, DLD3	sporulation, mitochondria damage
6R	X	IRC 7, HXK1, RET2, RPN12	nitrogen limitation, non glucose carbon sources, proteasome, golgi/ER transport
6L	Y	YFL066C helicase?, COS4, DD12, SNO3, SNZ3, AAD16/6	UV and DNA damage, oxidative stress, diauxic shift/stationary phase,
7R	Y	YRF1-3, COS6, PAU12, MAL12/11/13	in TLC1 KO, maltose metabolism
7L	X	COS12, PAU11, YPS5 MNT2, ADH4	zinc absence
8R	Y	helicase?, IMD2, PHO12, YHR214C	phosphate starvation
8L	Y	COS8, ARN1/2, PAU13	unfold protein, iron uptake, ethanol shock
9R	X	PAU15, YPS6, GTT1, HYR1, IRC24, LYS1	cell wall maintenance, diauxic shift/stationary phase, DNA damage
9L	Y	YIL177C helicase?, PAU14, VTH1, IMA3	vacuole
10R	X	COS5, MPH3, SOR1, HXT16, THI11, AAD10	sorbitol metabolism,low glucose levels, thiamine systesis
10L	Y	YJL255C, PAU1, VTH2, IMA4, HXT9	alcohol fermentation, low oxygen
11R	X	GEX2, VBA5, NFT1M FLO10	oxidative stress resistance, drug resistance
11L	X	PAU16, MCH2, FRE2, COS9, SYR1	low iron levels,
12R	Y	YRF1-4/5, PAU4, YLR460C, GAB1, NBP1	in TLC1 KO, fermentation
12L	Y	YLL066C helicase?, PAU18, MHT1, MMP1	sulfur metabolism
13R	X	PAU19, ERR3, SNO4, FET4, ADH6, DIA1	glyceron metabolism, heat shock, aldehyde tolerase, invasive growth
13L	Y	COS3, YML13W dehydrogenase?, ERO1, COX14, MSC1, RCS9, ERG13	osmotic shock, DNA damage, chromatine remodeling, TOR activation
14R	X	PAU6, COS10, AILF1, HXT17	fermentation, apoptosis, raffinose and galactose media
14L	Y	YRF1-6, COS1	in TLC1 KO
15R	Y	YRF1-8, PAU21, HSP33, ERR1, FDH1	protect cell from formate
15L	X	AAD15, BDS1, PAU20, ENB1	sulfate source, low temperature, fermentation, iron depravation
16R	Y	YPR204W, ARR3, ARR1, SGE1	arsenic resistance
16L	Y	YRF1-7, PAU21, ERR2, HSP32	in TLC1 KO, heat shock

Table 6.5 Proteins express from the sub-telomeric area and their function/expression. This table comprises the sub-telomeric repeat regions as far as 20Kbp from each telomere end, with the type of telomere they are expressed from X or Y core, and the name of all the known/putative? protein coding genes in the region, as well as the summarized conditions they are expressed/involved in. There is a repetitive family of proteins expressed from the sub-telomeres like the PAUp which are members of the seripauperin family and the COSp which are members of the DUB380 family and localize in the mitochondria, these two families of proteins are expressed in different types of stress but their function is still unknown. The data was accessed and analysed from the Saccharomyces Genome Database (SGD).

So are these genes located in the sub-telomeric areas important in TERRA regulation during stress? The answer, although still unknown, might lie not in how these genes regulate TERRA expression but in the change in chromatin structure in the area. Telomeres and sub-telomeric areas of the genome are characterized by their compacted

chromatin structure which leads to low or repressed transcription of genes in those areas (Tham 2002). It has been shown that TERRA levels can get up-regulated if chromatin structures open or get relaxed near the chromosome ends, by change in their epigenetic marks (Schoeftner, 2009 and 2010). Therefore, overall activation of transcription in sub-telomeric proteins involved in stress, metabolic changes and cell survival might result in an open chromatin structure in the sub-telomeric areas where the TERRA promoter is located, which might in turn result in an induction of its transcription. The difference in transcription levels in the X' and Y' core sub-telomeric regions, might result in a different induction and properties of TERRA coming from X' and Y' core telomeres.

In other organisms open chromatin structure in the sub-telomeric areas, results in a relaxed state of the telomere uncapping it and making it accessible to telomerase or proteins involved in DNA damage response (Weuts 2012) (Jacob 2004). Therefore, a relaxed state in the sub-telomeric areas might result in telomere uncapping during diauxic-shift, that may be alleviated by the over expression of TERRA which can 'restore telomeric heterochromatin through a self-reinforcing negative feedback loop' (C. L. Deng 2010).

Most of the genes that are up regulated in the stationary phase experience increased transcription already at the diauxic shift (Galdieri 2010). Thus, lower global transcriptional and metabolic changes are observed during post-diauxic shift and stationary phase, this in conjunction with TERRA's negative feedback loop might explain the reduction in TERRA's transcription during these growth phases.

However until the regulation of TERRA during diauxic shift is understood we cannot discard a possible function of TERRA in yeast metabolism which could explain its cytoplasmic localization, since we have found TERRA up-regulation not only during diauxic shift, but when cells are shifted from carbon source media including raffinose/galactose, and galactose/glucose, which might suggest a possible role of TERRA in yeast metabolism. Indeed many transcription factors involved in the metabolic changes during these cell growth stages have binding sites close to the telomeric repeats, which might point to a specific induction of TERRA rather than TERRA being a result of chromatin structure change.

A summary of the transcription factors induced during diauxic shift that have putative binding sites close to the telomeric repeats of telomere (1/6 or R/L) can be found in Table 6.2. This list of transcription factors could be used as a starting point to solve the riddle of TERRA regulation by yeast metabolism and its possible role in it.

Trascription factor	Binding Domain	Bind Telomere	Function
CUP9	WWTRTGTCA	Tel1R	Negative regulation of oligopeptide transport
DAL80	GATAA	Tel1L, Tel1R, Tel6R, Tel6L	Negative regulator of nitrogen degradation pathways
	YGATAAG	Tel1L, Tel1R	
GAT3	RGATCTAC	Tel6R	Associated with this nitrogen control system
	RGATCYV	TEL6R, TEL6L, TEL1L	
GZF3	HGATAAS	Tel1L, Tel6R	Function requires a repressive carbon source
	GATAAG		Nitrogen catabolite repression of transcription
MSN4	AAGGGG	Tel1L, Tel1L	Induce stress related genes
NRG1	CCCT	TEL1L, TEL1R, TEL6R, TEL6L	Mediates glucose repression
	GGACCCT	Tel1L	
PHD1	CNTGCAT	Tel6L, Tel6R	Enhances pseudohyphal growth
RGM1	AGGGG	Tel1L	Impairs cell growth
ROX1	ATTGT	Tel1L, Tel6R, Tel6L, Tel1R	Repressor of hypoxic genes
XBP1	YTCGAR	Tel1L, Tel6R, Tel6L, Tel1R	Transcriptional repressor of the cyclin genes during stress
YAP6	TTANGTNA	Tel6R, Tel1L, Tel1R	Regulation of genes in carbohydrate metabolism

Table 6.5 Transcription factors induced during diauxic shit. This table comprises transcription factors that were found to play a role during diauxic shift and stationary phase (Galdieri 2010) (Rao 2011) and that have putative binding sites near the telomeric repeats of telomere 1 or 6 in both left or right arms. The binding domains, as well as known function are summarized in the table. The data was accesed and analysed from the Saccharomyces Genome Database (SGD).

6.6 TLC1 cytoplasmic localization might play a role in cell survival and viability

So far we have explored the reasons of why TERRA might be induced during diauxic shift, however TLC1 overexpression shortly after TERRA induction has yet to be described. An important characteristic of diauxic shift and stationary phase is that cells are subjected to DNA damage caused by oxidative stress, a condition similar to the one seen during cellular senesce in mammalian cells (Galdieri 2010). Oxidative stress in cells has previously been shown to cause telomere shortening and contribute to telomere uncapping, since guanine triplets found on telomeres are sensitive to reactive oxygen species (ROS) which causes single strand DNA break accumulation in the area (Kawanishi 2004). Accelerated telomere shortening can also occur in humans due to environmental influences such as smoking, obesity, or stress (Schoeftne, 2010). Humans suffering from chronic

psychological stress have significantly higher oxidative stress in the cells which results in a lower telomerase activity, and shorter telomere length leading to accelerated aging (B. L. Epel 2004); indeed, lower telomerase activity associated with oxidative stress seems to be conserved in eukaryotic cells (Passos 2007). Interestingly, we were able to find that when cells undergo a second diauxic shift there is telomere shortening characterized by the induction of telomerase. The small induction of telomerase during diauxic shift might not be due to telomere shortening, but a result of a need for higher levels of telomerase to counteract the lower telomerase activity associated with stress.

Oxidative and replicative stress can induce various types of DNA damage, including oxidized bases, single/double-strand breaks, which trigger a DNA damage response that can be repaired by normal homologus recombination means (Murnane 2010). Alternative less common pathways exist to repair DNA damage one of these pathways is the *de novo* telomere addition where the end of a broken chromosome is stabilized by telomerase-dependent addition of telomeres at non-telomeric sites, which can result in chromosomal instability leading to cancer (Pennaneach 2006). Although, none of this evidence explains why we find a cytoplasmic localization of telomerase RNA there might be cellular pressure to keep a low count of active telomerase molecules in the nucleus for telomere lengthening purposes and to avoid *de novo* telomere addition in chromosomal DNA, which could explain TLC1 cytoplasmic localization.

Preliminary results with three color live cell imaging of yeast cells expressing 10xMS2-TLC1(MS2-CFP)/12xPP7Tel6R-TERRA(PP7-GFP)/Tel6R(TetR-RFP) revealed that a few TERRA foci co-localize with its telomere of origin during early diauxic shift, no nuclear T-recs foci were seen to co-localize with telomere 6R however, we cannot discard the possibility that they might be co-localizing with other telomeres. Interestingly, during early diaxic shift we found evidence that TERRA get exported from the nucleus into the cytoplasm after co-localizing with its telomere; while in later diauxic shift we found that the majority of TERRA/*TLC1* cluster co-localize in the cytoplasm. This results shows that TERRA and TLC1 might get exported into the cytoplasm as a complex.

We have shown in logarithmic growth conditions that TERRA acts as a scaffold and helps nucleate telomerase clusters (T-recs) in G1 cells, and later in S phase they co-localize

as a complex in TERRA's telomere of origin. Therefore, the same function of TERRA acting as a scaffold for the nucleation of telomerase molecules, might be happening during diauxic shift, when the TERRA/*TLCI* cluster get exported into the cytoplasm. Further studies of the export of TERRA/TLC1 complex during diauxic shift could give further evidence toward their cytoplasmic function.

To understand the function of TERRA/TLC1 during diauxic and stationary phases of yeast cell growth, it is essential to know in which cellular cytoplasmic compartment they are localizing. The evidence behind the possibility of their localization to cytoplasmic compartments p bodies/stress granules and mitochondria will be shown next.

6.7 TERRA/TLC1 complex might localize in p bodies or stress granules during diauxic shift

During diauxic shift and stationary phase yeast cells stop dividing, change in metabolism and differentiate to allow the maintenance of cell viability during times of stress until more favourable conditions arise (Galdieri 2010). Following glucose depletion or stress, rapid inhibition of translation initiation occurs leading to the formation of cytoplasmic RNA protein granules known as P-bodies, which contain un-translated mRNAs, and proteins involved in mRNA degradation (Olszewska 2012). Following prolonged periods of stress, dynamic aggregates of RNA, translation initiation factors, and ribosome subunits appear; they are known as stress granules (Lui 2010). These two cytoplasmic compartments usually co-localize or are side by side interchanging RNAs and other components, making them important sites for decisions of mRNA fate: degradation or storage (Buchan 2008). Both P-bodies and stress granules disappear once normal or favorable growth conditions occur (Eulalio 2007).

It has been shown that several non-coding RNAs can localize to cytoplasmic or nuclear stress granules in higher eukaryotes and coordinate cellular response to stress (Lakhotia 2012) and it is known that telomerase is of prime importance for cell viability maintenance in yeast and mammalian cells (Gomez 2012). However, the strongest evidence that suggests TERRA/TLC1 complex might be localizing to p-bodies/stress

granules was found by RNA pull-down carried in our laboratory that demonstrated that during normal growth conditions TERRA can bind Lsm7p which forms part of the heteroheptameric Lsm complex, important for p-body assembly and maintenance. UPF and SMG proteins involved in nonsense-mediated mRNA decay (and found in P-bodies durring stress), are enriched at telomeres where they negatively regulate TERRA association and modulate telomerase function during normal growth conditions (Isken 2008). Finally a recent study has shown a genetic association between TLC1 and Ebs1p, which localizes to P-bodies upon glucose starvation and is involved in inhibition of translation and nonsense-mediated decay (Hu 2013). Indeed, we see motile cytoplasmic TERRA and TLC1 foci during diauxic shift and stationary phase whose numbers are decreased upon fresh glucose media addition. Therefore, the possibility of a TERRA/TLC1complex localizing to P-bodies or stress granules should be considered to further understand their function during stress and the reason behind their cytoplasmic localization.

We may then propose that during diauxic shift it would be beneficial for cells to protect valuable and limiting transcripts like TLC1 in cytoplasmic granules until better growth condition arise, to avoid TERRA`s nuclear degradation, and to sort/degrade telomerase whose activity had been compromised due to oxidative stress.

6.8 TERRA/TLC1 complex might localize to the mitochondria due to stress

Diauxic shift in yeast is characterized by the metabolic change from fermentation to respiration; this is accompanied by wide genetic reprograming which include the biosynthesis of new mitochondria to cope with its respiration needs (Kotiadis 2012). Active mitochondria are the major source of intracellular reactive oxygen species (ROS), which cause the up-regulation of antioxidant and stress defense system, conferring cells stress resistance and viability during diauxic and stationary growth (Maris 2001). It has been shown that altering the energy state in tumor cells confers apoptotic resistance and involves telomerase in a non-telomere specific manner (Bagheri 2006). Expression of genes involved in mitochondria metabolism has been reported to be dependent on telomerase in

human and yeast cells, which endow the cells with stress resistance, antioxidant production, and cell differentiation capacity (Bagheri 2006) (Nautiyal 2002). Interestingly, the human reverse transcriptase subunit of telomerase (TERT) has a mitochondrial import sequence at its N-terminus, and upon oxidative challenge it has been find to shuttle from the nucleus to the mitochondria, were its function is not clear (Martínez 2011). Indeed some groups have shown that TERT mitochondrial localization renders cells apoptotic resistant, while other groups show that this change in localization makes cells more susceptible to oxidative stress-mitochondrial DNA damage which leads to apoptosis (Passos 2007).

An interesting possibility of TERRA's role in the context of a mitochondrial localization, comes from the evidence that suggest that mammalian TERRA can be processed by dicer into TERRA like small RNAs, which is tied to epigenetic regulation of cell differentiation, pluripotency and disease (Cao, 2009) (Zhang 2009). Interestingly, in the mitochondria TERT associates with an RNA component of mitochondrial RNA called rMrP, and form a RNA-dependent RNA polymerase complex, which produces rMrP double-stranded RNAs (dsRNA), that are further processed into small interfering RNAs (siRNA) in a Dicer-dependent manner that controls the endogenous levels of rMr (Martínez 2011). The role of TERT in silencing RNA biology, and the possibility of TERRA being processed into siRNA opens a new way of regulation of gene expression by telomerase in diverse biological conditions.

In normal growth conditions, TLC1 molecules cluster in TERRA foci into T-recs which have been previously shown by our laboratory to have active telomerase comprising Est2 the telomerase reverse transcriptase in yeast (L. C. Gallardo 2011). Our results show for the first time that TLC1/TERRA foci are found in the cytoplasm in diauxic and stationary phase conditions in budding yeast cells. In mammalian cells TERT has been seen in the mitochondria of cells, however in yeast this phenotype has been yet to be proven since most analysis done up until now had relied on the deletion of TLC1, to find transcriptional profiles related to DNA damage, mitochondria metabolism and cell survival (Hu 2013) (Nautiyal 2002). Interestingly, none of these studies have reported TLC1 in any cellular compartment in the cytoplasm, since so far it is has been shown to play a uniquely nuclear role (Martínez 2011). Therefore, our system and diauxic shift conditions could help

study TLC1 and TERRA role in this phenomenon, to help solve the contradictions behind telomerase mitochondrial localization.

Until further evidence is available, we could even speculate that TLC1/TERRA foci are exported with Est2 in a complex to the mitochondria upon oxidative stress, where TERRA can then be degraded to small RNA and control gene expression during stress.

Conclusion

In these studies, we were able to gain insight into TERRA and telomerase RNA *TLC1* regulation and function by the use cytological approaches like: FISH and *in vivo* labelling of RNAs by the MS2 and PP7 system. We demonstrated that TERRA is expressed from a shortened telomere and accumulates as a single perinuclear foci, in a small percentage of logarithmic cell population. There TERRA acts as a scaffold promoting the nucleation of *TLC1* RNA molecules to form active telomerase clusters (T-Recs), which later are recruited to the short telomere from which TERRA originated, allowing the controlled elongation of specific and critically short telomeres.

Therefore, similar approaches, such as single molecule FISH analysis and live cell imaging by bacteriophage *in vivo* systems like the MS2 and PP7, should be pursued and optimized for use in different organism, and conditions. So that eventually they can be used as a high-through put technique, to allow us to gain powerful insight into the regulation of the new long-non-coding RNAs which function remains unknown to the world.

Using the same cytological approaches, we were able to find an up-regulation of TERRA, and telomerase RNA *TLC1,* accompanied by a predominant cytoplasmic localization as cell growth progresses from exponential growth to diauxic shift, and stationary phase. Although the punctual function, of the cytoplasmic TERRA/*TLC1* complex remains elusive, the results suggest that the function we found for TERRA, as a scaffold molecule to generate telomerase cluster, remains conserved during yeast cell growth phases.

Since TERRAs trascription remains conserved through nature, maybe so does its scaffold function. It will be interesting to study TERRA/*TLC1* cluster formation in mammalian cells, to understand their basic biological functions as well as in a telomere related disease context such as accelerated aging or cancer.

Afterword

… This started as a journey to uncover the mystery behind TERRA, as we searched for answers, more questions arose, and bigger mysteries to be solved, knocked on our door… Thankfully, this journey allowed us to discover the tip of the treasure waiting to be revealed. Our results in normal growth conditions give us a better understanding and a possible mechanism of action of TERRA in telomerase recruiting and telomere maintenance, which challenges the actual model of TERRA acting as telomerase inhibitor.

The cytoplasmic localization of TERRA came to all of us as a shock, but it was even more shocking to me to find that TLC1 followed the same pattern; it was a delightful discovery to my eyes, although up until now we cannot understand it, its finding will always remain in me, as the precious enigmas that make science a carrier worth living for. As once Carl Sagan said: "When you make the finding yourself - even if you're the last person on Earth to see the light - you'll never forget it. Until their unsolved mystery of TERRA/TLC1 cytoplasmic localization is uncovered their function will remain a mystery that can only be remarked by speculations. However, I believe scientific progress starts with brave ideas waiting to be proved, as once Einstein said: "To raise new questions, new possibilities, to regard old problems from a new angle, requires creative imagination and marks real advance in science".

Further studies in this area, could reveal the proteins and complexes involved in this regulation, which could serve in the understanding of telomere related diseases such as cancer and aging. Basic knowledge is of utmost importance, to later develop applied techniques to help humanity deal with these diseases. But before that is possible a need of communication between basic and applied research has to be established where publishing and money are not the driving force, but helping humanity by knowledge and its application to make this world be a better place.

It was an incredible journey full of new experiences, new on the edge technology and unraveling knowledge, which had changed its traveller; however as in every journey, travelers come and go, but as long as someone is willing to understand the mystery, the journey shall continue, fuelled by old dreams and new knowledge. As once a researcher in this field said: "The closer we get the more can be seen. This is not the end. It is not even the beginning of the end. But it is, perhaps, the end of the beginning of this journey to TERRA". (Feuerhahn 2010)

Thank you for bearing with me and letting me share this journey with you…

Bibliography

Arnoult, Van Beneden, Decottignies. "Telomere length regulates TERRA levels through increased trimethylation of telomeric H3K9 and HP1α." *Nature structural & molecular biology*, 2012: 948-956.

Arora, Brun, Azzalin. "TERRA: Long Noncoding RNA at Eukaryotic Telomeres." *Progress in Molelucalr and Subcellular Biology*, 2011: 65-94.

Ashrafi, Sinclair, Gordon, Guarente. "Passage through stationary phase advances replicative aging in Saccharomyces cerevisiae." *Proceedings of the National Academy of Sciences of the United States of America*, 1999: 9100-9105.

Azzalin, Reichenbach, Khoriauli, Giulotto, Ligner. "Telomeric Repeat–Containing RNA and RNA Surveillance Factors at Mammalian Chromosome Ends." *Science*, 2007: 798-801.

Bagheri, Nosrati, Li, Fong, Torabian, Rangel, Moore, Federman, LaPosa, Baehner, Sagebiel, Cleaver, Haqq, Debs, Blackburn, Kashani-Sabet. "Genes and pathways downstream of telomerase in melanoma metastasis." *Proceedings of the National Academy of Sciences of the United States of America*, 2006: 11306-11311.

Beery, Lin, Biddle, Francis, Blackburn, Epel. "Chronic stress elevates telomerase activity in rats." *Biology letters*, 2012: 1063-1066.

Bertrand, Chartrand, Schaefer, Shenoy, Singer, Long. "Localization of ASH1 mRNA particles in living yeast." *Molecular Cell*, 1998: 437-445.

Brauer. "Homeostatic Adjustment and Metabolic Remodeling in Glucose-limited Yeast Cultures." *Molecular Biology of the Cell*, 2005: 2503-2517.

Brevet, Marcand, Gilson. "Dynamics of telomere replication." *Biology of the Cell*, 1999: 556–556.

Buchan, Muhlrad, Parker. "P bodies promote stress granule assembly in Saccharomyces cerevisiae." *The Journal of Cell Biology*, 2008: 441-455.

Buck, Lieb. "A chromatin-mediated mechanism for specification of conditional transcription factor targets." *Nature genetics*, 2006: 1446-1451.

Campisi. "Senecent cells, tumor suppresion, and organismal aging: good citizens, bad citizens ." *Cell*, 2005: 513-522.

Cao, Li, Hiew, Brady, Liu, Dou. "Dicer independent small RNAs associate with telomeric heterochromatin." *RNA*, 2009: 1274-1281.

Cao, Li, Hiew, Brady, Liu, Dou. "Dicer independent small RNAs associate with telomeric heterochromatin." *RNA*, 2009: 1274-1281.

Caslini, Connelly, Serna, Broccoli, Hess. "MLL Associates with Telomeres and Regulates Telomeric Repeat-Containing RNA Transcription." *Molecular and Cellular Biology*, 2009: 4519-4526.

Chartrand, Gallardo and. "Telomerase biogenesis: The long road before getting to the end ." *RNA biology*, 2008: 212-215.

Clontech. *Yeast Protocol Handbook: Yeast transformation procedures.* United States: Clontech laboratories, 2009.

Collins. "Single-stranded DNA repeat synthesis by telomerase." *Current Opinion in Chemical Biology*, 2011: 643-648.

Dai, Punchihewa, Ambrus, Chen, Jones, Yang. "Structure of the intramolecular human telomeric G-quadruplex in potassium solution: a novel adenine triple formation." *Nucleic Acids Research*, 2007: 2440-2450.

de Silanes, d'Alcontres, Blasco. "TERRA transcripts are bound by a complex array of RNA-binding proteins." *Nature Communications*, 2010: 33.

Deng, Campbell, Lieberman. "TERRA, CpG methylation and telomere heterochromatin: lessons from ICF syndrome cells." *Cell Cycle*, 2010: 69-74.

Deng, Norseen, Wiedmer, Reithman, Lieberman. "TERRA RNA Binding to TRF2 Facilitates Heterochromatin Formation and ORC Recruitment at Telomeres." *Molecular Cell*, 2009: 403-413.

Deng, Wang, Xiang, Molczan, Baubet, Conejo Garcia, Xu, Lieberman, Dahmane. "Formation of telomeric repeat-containing RNA (TERRA) foci in highly proliferating mouse cerebellar neuronal progenitors and medulloblastoma." *Jornal of Cell Science*, 2012: 4383-4394.

Dionne, Wellinger. "Cell cycle-regulated generation of single-stranded G-rich DNA in the absence of telomerase." *Proceedings of the National Academy of Sciences of the United States of America*, 1996: 13902-13907.

Doheny, Mottus, Grigliatti. "Telomeric Position Effect: A Third Silencing Mechanism." *Plos One*, 2008: 3864.

Drubin, Garakani, Silver. "Motion as a phenotype: the use of live-cell imaging and machine visual screening to characterize transcription-dependent chromosome dynamics." *BMC Cell Biology*, 2006: 7-19.

Drummond, Hildyard, Firczuk, Reamtong, Li, Kannambath, Claydon, Beynon, Eyers, McCarthy. "Diauxic shift-dependent relocalization of decapping activators Dhh1 and Pat1 to polysomal complexes." *Nucleic Acids Research* (Nucleic Acids Research), 2011: 7764-7774.

Egan, Collins. "Biogenesis of telomerase ribonucleoproteins." *RNA*, 2012: 1747-1759.

Epel, Blackburn, Lin, Dhabhar, Adler, Morrow, Cawthon. "Accelerated telomere shortening in response to life stress." *Proceedings of the National Academy of Sciences of the United States of America*, 2004: 17312-17315.

Epel, Lin, Dhabhar, Wolkowitz, Puterman, Karan, Blackburn. "Dynamics of telomerase activity in response to acute psychological stress." *Brain, Behavior, and Immunity*, 2010: 531-539.

Eulalio, Behm-Ansmant, Izaurralde. "P bodies: at the crossroads of post-transcriptional pathways." *Nature reviews. Molecular cell biology*, 2007: 9-22.

Farnung, Brun, Arora, Lorenzi, Azzalin. "Telomerase Efficiently Elongates Highly Transcribing Telomeres in Human Cancer Cells." *PLoS ONE*, 2012.

Feuerhahn, Iglesias, Panza, Porro, Lingner. "TERRA biogenesis, turnover and implications for function." *FEBS Letters*, 2010: 3812-3818.

Galdieri, Mehrotra, Yu, Vancura. "Transcriptional regulation in yeast during diauxic shift and stationary phase." *Omics: a journal of integrative biology*, 2010: 629-638.

Gallardo, Chartrand. "Visualizing mRNAs in fixed and living yeast cells." *Methods in Molecular Biology* , 2011: 203-219.

Gallardo, Laterreur, Cusanelli, Ouenzar, Querido, Welligner, Chartrand. "Live cell imaging of telomerase RNA dynamics reveals cell cycle-dependent clustering of telomerase at elongating telomeres." *Cell*, 2011: 819-827.

Gallardo, Olivier, Dandjinou, Wellinger, Chartrand. "TLC1 RNA nucleo-cytoplasmic trafficking links telomerase biogenesis to its recruitment to telomeres." *EMBO*, 2008: 748-757.

Gasser, Buhler and. "Silent chromatin at the middle and ends: lessons from yeast." *EMBO*, 2009: 2146-2161.

Geli, Gilbson and. "How telomeres are replicated." *Nature Reviews* , 2007: 825-838.

Gerst, Chung, Takizawa. "In Vivo Visualization of RNA Using the U1A-Based Tagged RNA System." *In Vivo Visualization of RNA Using the U1A-Based Tagged RNA System*, 2011: 221-235.

Godlman, Spector. "Live Cell Imaging: A Laboratory Manual." *Cold Spring Harbor Press*, 2005: 602-620.

Gomez, Armando, Farina, Menna, Cerrudo, Ghiringhelli, Alonso. "Telomere structure and telomerase in health and disease." *International Journal of Oncology*, 2012: 1561-1569.

Greider, Blackburn. "Identification of a specific telomere terminal transferase activity in Tetrahymena extracts." *Cell*, 1985: 405-413.

Hocine, Raymond, Zenklusen, Chao, Singer. "Single-molecule analysis of gene expression using two-color RNA labeling in live yeast." *Nature methods*, 2013: 119-121.

Hu, Tang, Liu, Tong, Dang, Fu, Zhang, Peng, Meng, Zhou. "Telomerase-Null Survivor Screening Identifies Novel Telomere Recombination Regulators." *PLoS genetics*, 2013.

Iglesias, Redon, Pfireer, Dees, Ligner, Luke. "Subtelomeric repetitive elements determine TERRA regulation by Rap1/Rif and Rap1/Sir complexes in yeast." *EMBO Journal* , 2011: 587-593.

Isken, Maquat. "The multiple lives of NMD factors: balancing roles in gene and genome regulation." *Nature Reviews Genetics*, 2008: 699-712.

Jacob, Stout, Price. "Modulation of Telomere Length Dynamics by the Subtelomeric Region of Tetrahymena Telomeres." *Molecular Biology of the Cell*, 2004: 3719-3728.

Kaganman. "Another Handle for RNA." *Nature Methods*, 2008: 872-874.

Kawanishi, Oikawa. "Mechanism of telomere shortening by oxidative stress." *Annals of the New York Academy of Sciences*, 2004: 278-284.

Keryer-Bibens, Barreau, Osborne. "Tethering of proteins to RNAs by bacteriophage proteins." *Biology of the Cell*, 2008: 125–138.

Klis, Boorsma, De Groot. "Cell wall construction in Saccharomyces cerevisiae." *Yeast*, 2006: 185-202.

Kotiadis, Leadsham, Bastow, Gheeraert, Whybrew, Bard, Lappalainen, Gourlay. "Identification of new surfaces of cofilin that link mitochondrial function to the control of multi-drug resistance." *Journal of Cell Science*, 2012: 2288-2299.

Lai, Lee, Zhang. "Immunofluorescence protects RNA signals in simultaneous RNA-DNA FISH." *Experimental cell research*, 2013: 46-55.

Lakhotia. "Long non-coding RNAs coordinate cellular responses to stress." *Wiley Interdisciplinary Reviews: RNA*, 2012: 779–796.

Lange, de. "How Telomeres Solve the End-Protection Problem." *Science*, 2009: 948-952.

Lange, Smorgorzewska and de. "Regulation of telomerase by telomeric proteins ." *Annual Reviews in Biochemistry*, 2004: 177-208.

Larson, Singer, Zenklusen. "A Single Molecule View of Gene Expression." *Trends in Cellular Biology* , 2009: 630-637.

Larson, Zenklusen, Wu, Chao, Singer. "Real-Time Observation of Transcription Initiation and Elongation on an Endogenous Yeast Gene." *Science*, 2011: 475-478.

Lescasse, Pobiega, Callebaut, Marcand. "End-joining inhibition at telomeres requires the translocase and polySUMO-dependent ubiquitin ligase Uls1." *The EMBO Journal*, 2013: 805-815.

Levy, Allsopp, Futcher, Greider, Harley. "Telomere End-Replication Problem and Cell Aging." *Journal of Molecular Biology*, 1992: 951-960.

Lui, Campbell, Ashe. "Inhibition of translation initiation following glucose depletion in yeast facilitates a rationalization of mRNA content." *Biochemical Society Transactions*, 2010: 1131.

Luke, Lingner. "TERRA: telomeric repeat-containing RNA." *EMBO Journal*, 2009: 2503-2510.

Luke, Panza, Redon, Iglesias, Li, Lingner. "The Rat1p 50 to 30 Exonuclease Degrades Telomeric Repeat-Containing RNA and Promotes Telomere Elongation in Saccharomyces cerevisiae." *Cell*, 2008: 465-477.

Maicher, Kastner, Dees, Luke. "Deregulated telomere transcription causes replication-dependent telomere shortening and promotes cellular senescence." *Nucleic Acids Research*, 2012: 6649-6659.

Maris, Assumpção, Bonatto, Brendel, Henriques. "Diauxic shift-induced stress resistance against hydroperoxides in Saccharomyces cerevisiae is not an adaptive stress response and does not depend on functional mitochondria." *Current Genetics*, 2001: 137-149.

Martínez, Blasco. "Telomeric and extra-telomeric roles for telomerase and the telomere-binding proteins." *Nature Reviews Cancer*, 2011: 161-176.

Murnane. "Telomere loss as a mechanism for chromosome instability in human cancer." *Cancer research*, 2010: 4255-4259.

Nautiyal, DeRisi, Blackburn. "The genome-wide expression response to telomerase deletion in Saccharomyces cerevisiae." *Proceedings of the National Academy of Sciences of the United States of America*, 2002: 9316-9321.

Olszewska, Bujarski, Kurpisz. "P-bodies and their functions during mRNA cell cycle: Mini-review." *Cell Biochemistry and Function*, 2012: 177–182.

Passos, Saretzki, von Zglinicki. "DNA damage in telomeres and mitochondria during cellular senescence: is there a connection?" *Nucleic Acids Research*, 2007: 7505-7513.

Pennaneach, Putnam, Kolodner. "Chromosome healing by de novo telomere addition in Saccharomyces cerevisiae." *Molecular Microbiology*, 2006: 1357–1368.

Pfeiffer, Lingner. "TERRA promotes telomere shortening through exonuclease 1-mediated resection of chromosome ends." *PLoS genetics*, 2012.

Porro, Feuerhahn, Reichenbach, Lingner. "Molecular Dissection of Telomeric Repeat-Containing RNA Biogenesis Unveils the Presence of Distinct and Multiple Regulatory Pathways." *Molecular and Cellular Biology*, 2010: 4808-4817.

Querido, Chartrand. "Using fluorescent proteins to study mRNA trafficking in living cells." *Methods Cell Biology*, 2008: 273-292.

Rao, Pellegrini. " Regulation of the yeast metabolic cycle by transcription factors with periodic activities." *BMC Systems Biology*, 2011: 160.

Redon, Reichenbach, Lingner. "The non-coding RNA TERRA is a natural ligand and direct inhibitor of human telomerase." *Nucleic Acid Research*, 2010: 5797-5806.

Riethman. "Human Telomere Structure and Biology." *Annual Reviews*, 2008 a: 1-21.

Riethman, H. "Human subtelomeric copy number variations." *Cytogenetic and genome research*, 2008 b: 244-252.

Rodriguez, Condeelis, Singer, Dictenberg. "Imaging mRNA movement from transcription sites to translation sites." *Seminars in Cell & Developmental Biology*, 2007: 202-208.

Sandell, Gottschiling, Zakian. "Trascription of a yeast telomere alleviates etelomere position effect without affecting chromosome stability. ." *Proceeding of the National Academy of Sciences*, 1994: 12061-12065.

Schoeftner, Blasco. "A 'higher order' of telomere regulation: telomere heterochromatin and telomeric RNAs." *The EMBO journal*, 2009: 2323-2336.

Schoeftner, Blasco. "Chromatin regulation and non-coding RNAs at mammalian telomeres." *Seminars in Cell & Developmental Biology*, 2010: 186-193.

Schoeftner, Blasco. "Developmentally regulated transcription of mammalian telomeres by DNA-dependent RNA polymerase II." *Nature cell biology*, 2008: 228-236.

Shay, Bacchetti. "A survey of telomerase activity in human cancer." *European journal of cancer* , 1997: 787-791.

Shore, Bianchi and. "Early replication of short telomeres in budding yeast." *Cell*, 2007: 1051-1062.

Tattermusch, Brockdorff. "A scaffold for X chromosome inactivation." *Human genetics*, 2011: 247-253.

Teste, Duquenne, François, Parrou. "Validation of reference genes for quantitative expression analysis by real-time RT-PCR in Saccharomyces cerevisiae." *BMC Molecular Biology*, 2009: 99.

Tham, Zakian. "Transcriptional silencing at Saccharomyces telomeres: implications for other organisms." *Oncogene*, 2002: 512-521.

Trcek, Chao, Larson, Park, Zenklusen, Shenoy, Singer. "Single-mRNA counting using fluorescent in situ Single-mRNA counting using fluorescent in situ." *Nature Protrocols*, 2012: 408-419.

Tuzon, Wu, Chan, Zakian. "The Saccharomyces cerevisiae telomerase subunit Est3 binds telomeres in a cell cycle- and Est1-dependent manner and interacts directly with Est1 in vitro." *PLoS genetics*, 2011: e1002060.

Tyagi. "Imaging intracellular RNA distribution and dynamics in living cells." *Nature Methods*, 2009: 331-338.

Valgardsdottir, Chiodi, Giordano, Cobianchi, Riva, Biamonti. "Structural and functional characterization of noncoding repetitive RNAs transcribed in stressed human cells." *Molecular biology of the cell*, 2005: 2597-2604.

Verheggen. "Box C/D small nucleolar RNA trafficking involves small nucleolar RNP proteins, nucleolar factors and a novel nuclear domain." *EMBO Journal*, 2001: 5480 - 5490.

Wellinger, Ethier, Labrecque, Zakian. "Evidence for a new step in telomere maintenance." *Cell*, 1996: 423-433.

Wellinger, Zakian. "Everything you ever wanted to know about Saccharomyces cerevisiae telomeres: beginning to end." *Genetics*, 2012: 1073-1105.

Weuts, Voet, Verbeeck, Lambrechts, Wirix, Schoonjans, Danloy, Marynen, Froyen. "Telomere length homeostasis and telomere position effect on a linear human artificial chromosome are dictated by the genetic background." *Nucleic Acids Research*, 2012.

Xu, Komiyama. "Structure, function and targeting of human telomere RNA." *Methods*, 2012: 100-105.

Zhang, Ogawa, Ahn, Namekawa, Silva, Lee. "Telomeric RNAs Mark Sex Chromosomes in Stem Cells." *Genetics*, 2009: 685-698.

Zhao, Abreu, Kim, Stadler, Eskiocak, Terns, Terns, Shay, Wright. "Processive and distributive extension of human telomeres by telomerase under homeostatic and nonequilibrium conditions." *Molecular cell*, 2011: 297-307.

Zhu, Gustafsson. " Distinct differences in chromatin structure at subtelomeric X and Y' elements in budding yeast." *PLoS One*, 2009: e6363.

Annex I

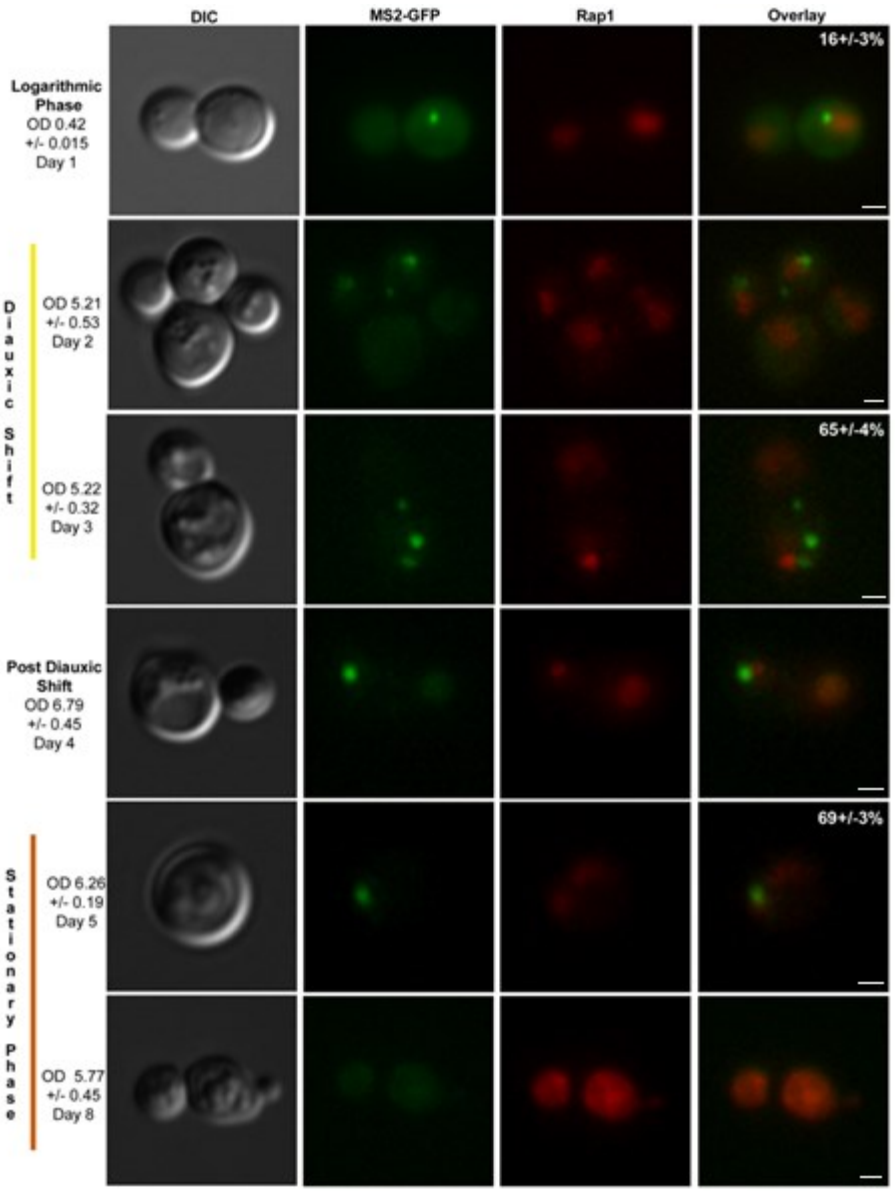

6xMS2-Tel1L TERRA time course during different yeast cell growth stages. Live cell imaging of the 6xMS2-Tel1L TERRA, revealed brighter and more numerous TERRA foci with a cytoplasmic localization during diauxic shift, post-diauxic shift and stationary phase conditions. TERRA-MS2-GFP foci are in green, mCherry-labeled telomeres are in red. Quantification of the number of cytoplasmic TERRA foci (superior-right corner of the overlay), indicates a majority of cytoplasmic TERRA foci during late cell growth stages compared to logarithmic growth; where TERRA is present as a single perinuclear foci. A minimum of 300 cells were counted in each independent experiment N=4. Scale bar: 1 μm.

Annex II

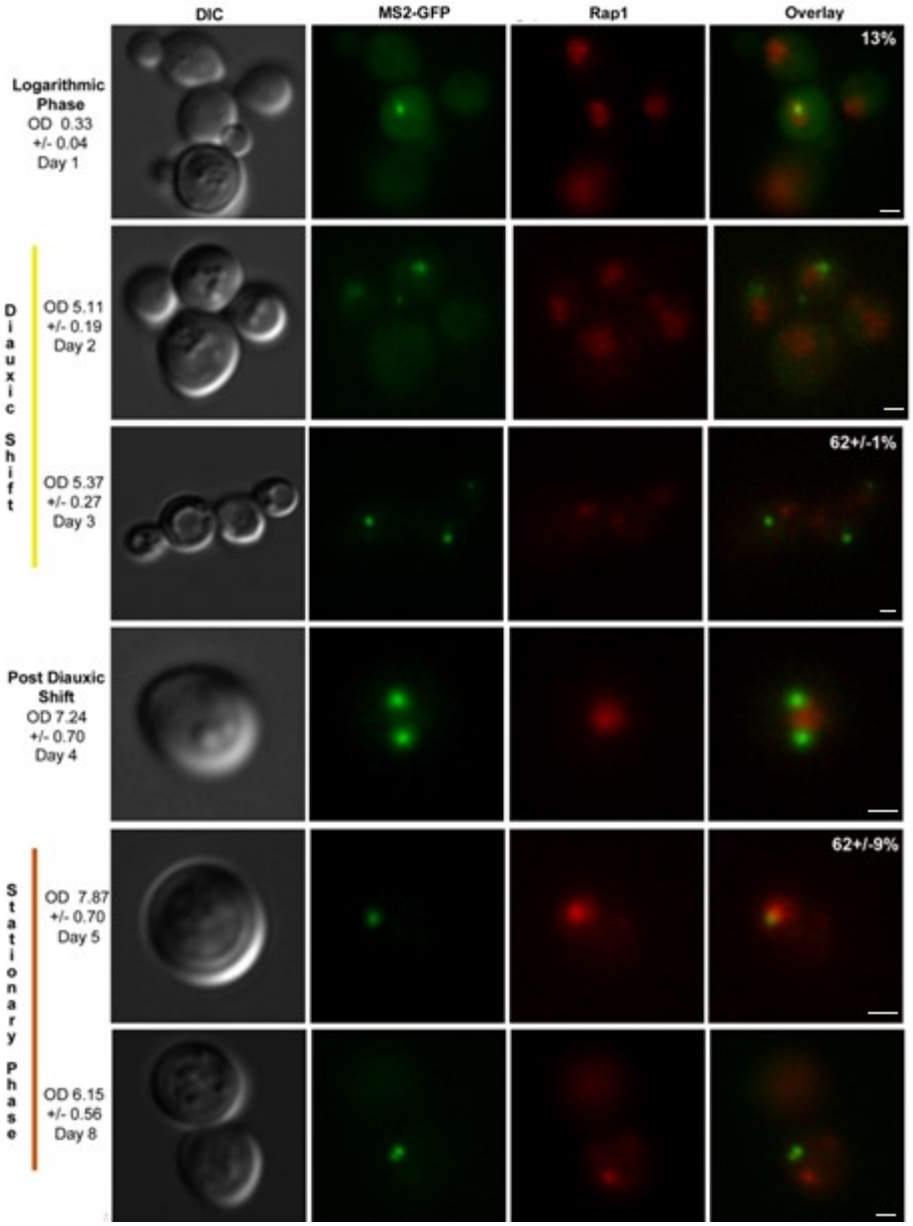

6xMS2-Tel6R TERRA time course during different yeast cell growth stages. As with Tel1L TERRA, live cell imaging of the 6xMS2-Tel6R TERRA, revealed brighter and more numerous TERRA foci with a cytoplasmic localization during diauxic shift, post-diauxic shift and stationary phase conditions. TERRA-MS2-GFP foci are in green, mCherry-labeled telomeres are in red. Quantification of the number of cytoplasmic TERRA foci (superior-right corner of the overlay), indicates a majority of cytoplasmic TERRA foci during late cell growth stages compared to logarithmic growth; where TERRA is present as a single perinuclear foci. A minimum of 300 cells were counted in each independent experiment N=4. Scale bar: 1 μm.

Annex III

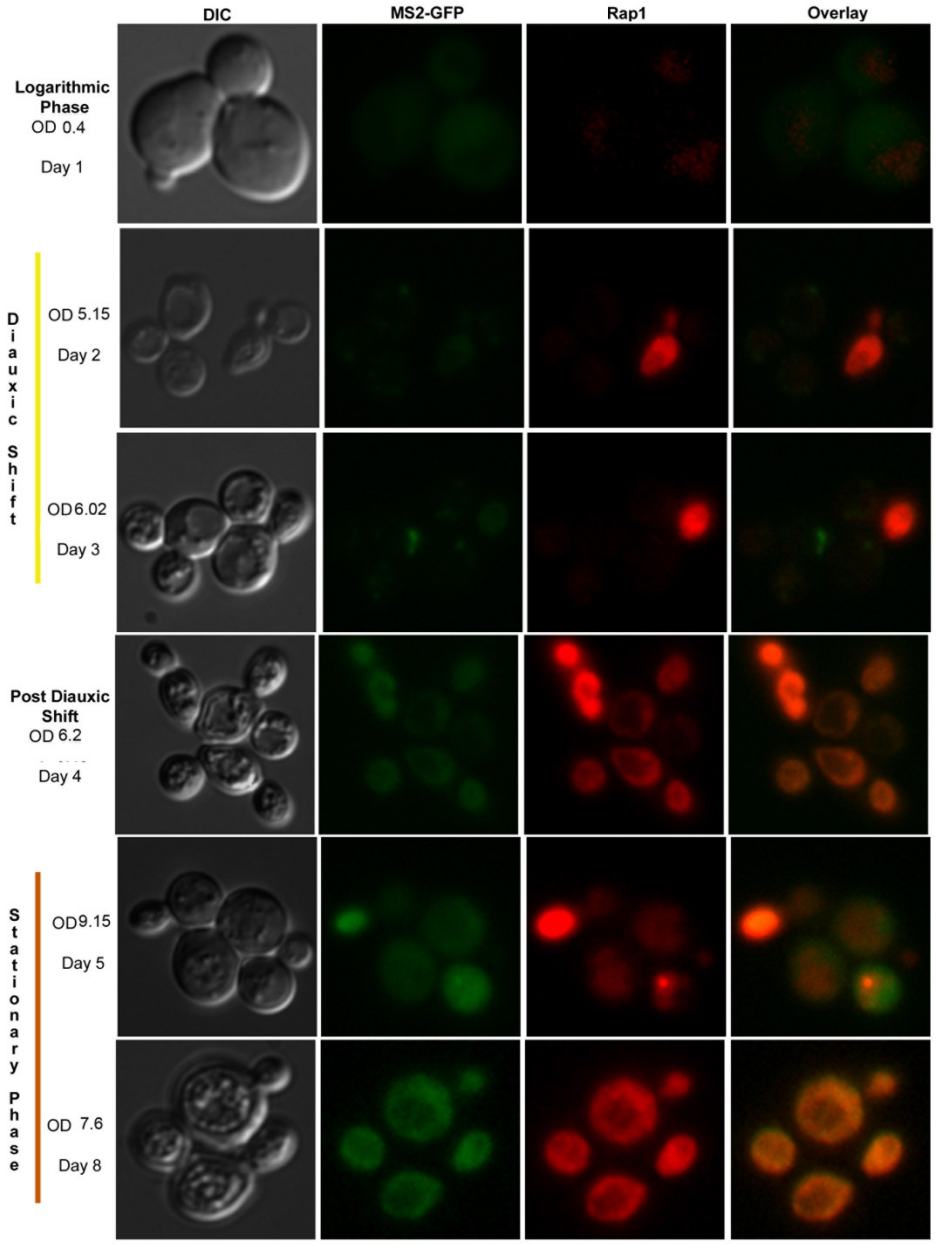

WT cell time course during different yeast cell growth stages. WT cells expressing MS2-GFP fusion protein, were use as control for GFP agglomeration although some of this foci might form during diauxic shift and stationary phase it is important to note that the brightness difference between the GFP agglomeration foci and TERRA or TLC1 foci is significant (p value =0.02), and on later stationary phase cells become auto-fluorescent as noted before.